Faculty of Electrical Engineering and Computer Science

Hochschule Zittau/Görlitz
UNIVERSITY OF APPLIED SCIENCES

Program: N2612 Electrical Engineering and Informatics

Branch: Mechatronics

DEVELOPMENT OF SIMULATION MODELS IN ENERGY TECHNOLOGY

THE THESIS DEALS WITH SIMULATION MODELS, MAPPING OF A NEW HEAT STORAGE CONCEPT, SIMULATING THE STORAGE PROCESS AND MODELING THE HEAT STORAGE.

MASTER THESIS

Grant recipients: Hochshule Zittau/Göerlitz

Author: Bc. Jan Krofta

Assessor: Prof. Dr.-Ing. Alexander Kratzsch (HS Zittau/Görlitz)

Supervisor: Dipl.-Ing. (FH) Sebastian Braun (HS Zittau/Görlitz, IPM)

Date of issue: 02/04/2013

Date of submission: 30/09/2013

Faculty of Electrical Engineering and Computer Science

Hochschule Zittau/Görlitz
UNIVERSITY OF APPLIED SCIENCES

Assignment for the master thesis

Course of studies: Mechatronics

Student's name: Jan Krofta

Subject: *Development of simulation models in energy technology*

As part of the State of Saxony funded project "Energy efficiency in thermal power plants" simulation models should be created that will allow the mapping of a new heat storage concept in power plant-cycle processes. To simulate the dynamic phenomena of the storage process, the modeling of heat storage (latent and sensible heat storage) is necessary.

Assignment:

- Survey of available literature on simulation models (model availability) of sensible and latent heat storage
- Choosing the most appropriate simulation tools (Modelica, DynaStar (Delphi), etc.)
- Development of a simulation model for heat storage (latent and sensible heat)
- Perform simulations for designing a pilot heat storage
- Documentation of results

Assessor: Prof. Dr.-Ing. Alexander Kratzsch (HS Zittau/Görlitz)
Supervisor: Dipl.-Ing. (FH) Sebastian Braun (HS Zittau/Görlitz, IPM)
Date of issue: 02/04/2013
Date of submission: 31/07/2013
Registry-Number.: MA/EMIm11 - 02/13

Assessor

Dean

Prohlášení

Byl jsem seznámen s tím, že na mou diplomovou práci se plně vztahuje zákon č. 121/2000 Sb. o právu autorském, zejména § 60 – školní dílo.

Beru na vědomí, že Technická univerzita v Liberci (TUL) nezasahuje do mých autorských práv užitím mé diplomové práce pro vnitřní potřebu TUL.

Užiji-li diplomovou práci nebo poskytnu-li licenci k jejímu využití, jsem si vědom povinnosti informovat o této skutečnosti TUL; v tomto případě má TUL právo ode mne požadovat úhradu nákladů, které vynaložila na vytvoření díla, až do jejich skutečné výše.

Diplomovou práci jsem vypracoval samostatně s použitím uvedené literatury a na základě konzultací s vedoucím bakalářské práce a konzultantem.

Datum

Podpis

Acknowledgements

I would never have been able to finish my diploma thesis without help from friends, and support from my family especially my sister. I would like to thank all the people who contributed in some way to the work described in this thesis.

I thank my academic supervisor Dipl.-Ing. Sebastian Braun for his guidance, caring, patience, and for providing a helpful atmosphere for my academic work. I have been lucky to have a supervisor who cared about my work, and who responded to my questions and queries. Thanks also belong to Prof. Kratzsch for his advice during the colloquiums. I would like to thank all the staff members at Hochschule Zittau/Görlitz who helped me in my supervisor's absence.

Furthermore, I thank the Technical University of Liberec for their support and technical advice. Thank belong Ing. Hubka Lukáš, Ph.D , who endorses my thesis at the University of Liberec.

Abstract

This work covers three topics. Firstly, it summons a survey of available literature on simulation models of sensible and latent heat storages. Secondly, it describes a developed model for sensible or latent heat storage with Matlab® simulation tool. Thirdly, it performs simulations for designing a pilot heat storage.

The development of simulation models in the field of energy technology surveys the simulation models of the sensible and latent heat storages. Thermal energy storage is a key technology in providing a balance between energy supply and demand for heating and cooling systems. Use of proper thermal energy storage systems presents a better solution for discrepancy between energy supply and demand. Heat transfer involving phase change is very important in latent heat storage applications. The numerical model and model based on number of transfer units method, proposed in this thesis, employ thermal distribution in phase change material and heat transfer fluid. The predication of temperature distribution and rate of melting or solidification is crucial in order to design latent heat storage devices. Phase change material melting time depends on not only thermal and geometric parameters, but also on the thermo-physical properties of the phase change materials.

Keywords: thermal energy storage, latent heat energy storage, sensible heat energy storage, heat transfer, simulation model, phase change material, numerical method, charging, discharging, number of transfer method, finite difference method.

Content

List of figures

List of tables

List of nomenclature

A	area	[m^2]
Cp	specific heat capacity	[J / kgK]
f	liquid fractiom	[-]
F	frozen fraction	[-]
H	latent heat	[kJ/kg]
h, U	convection heat transfer coefficient	[W/(m^2K)]
k	thermal conductivity	[W/mK]
L	length	[m]
m	mass	[kg]
m_f	mass flow rate	[kg/s]
Q	heat	[J]
r, R	radius	[m]
Ste	Stefan number	[-]
t	time	[s]
T	temperature	[°C]
ε	efficiency	[%]
ρ	density	[kg/m^3]
θ	temperature difference ($T-T_m$)	[K]

List of abbreviations

ES	Energy Storage
HTF	Heat Transfer Fluid
LHS	Latent Heat Storage
NTU	Number of Transfer Units
PCM	Phase Change Material
PDE	Partial Differential Equation
SHS	Sensible Heat Storage
TES	Thermal Energy Storage
TESD	Thermal Energy Storage Devices

1 Introduction

The main focus of this thesis about the development of simulation models in the field of energy technology is to examine in particular the simulation models of the sensible and latent heat storages. As simulation modeling is the process of creating and analyzing a digital prototypes of the particular physical models of new technological propositions to predict their performance in the real world it is an important part of the technology development. This kind of simulations can predict, analyze, understand, and avoid design errors of the proposed systems.

The purpose of my thesis is to introduce and explain the reasons for creation of the specific situational model of the particular choice. The text also introduces background knowledge and individual calculations which were used to enumerate the heat storage capacity and other potential values.

The thesis is divided in three big chapters where each introduces a specific aspect of the topic. First chapter brings the general literature review of specialized technical literature in the field of thermal energy storage technologies. Second chapter deals with the introduction of different kinds of heat storage systems with the major focus on simulation models of sensible and latent heat storages. The chapter also deals with the choice of heat storage and phase charge materials. The final, third chapter is devoted to the proposal of a particular situational models of heat storage based on the NTU method and numerical model. The content of the chapters covers the results of the executed simulation and performed calculations. The gained results are explained and documented. The content is particularly valuable as an analysis of a specific type of the tube energy storage system technology.

2 Problem Statement

Large amounts of electricity cannot be effectively stored. The only way to store electricity is to convert it to another medium or store it in the form of heat. Power systems require a large amount of heat rejection from a power cycle in a short period of time. Proposed solution is to use a latent or sensible energy storage system to absorb the rejected heat. It allows this excess of thermal energy to be collected and stored for later use. Its subsequent release to space over a longer period of time is desirable and effective as for example in case of balancing unequal energy demand between day and night times.

Due to the increased cost of the fossil fuels the alternative options for the heat recovery and waste heat storage are becoming increasingly attractive. Furthermore, a thermal energy storage can be used as a thermal management tool to achieve a better capacity factor, to avoid start-up and part load losses, and investment cost can be reduced in combination with cost intensive components.

Fossil oils, coal, and gases constitute 85 per cent of the total energy consumption. However, their stores and reserves are limited. The fossil fuels propose the increase in CO_2 emissions which cause temperature climate change. High efficiency systems offer the benefits of controlling the rate of CO_2 increase and global temperature rise. There are many reasons why heat transfer and heat exchangers play a key role in the development of sustainable energy systems as well as in the reduction of emissions and pollutants.

Energy storage mediums can be very variable and can include water or ice-slush tanks ranging from small to massive, masses of native earth or bedrock accessed with heat exchangers in clusters of small-diameter boreholes, deep acquifers contained between impermeable strata, lined pits filled with gravel, water, and/or different phase-change materials.

The main purpose of the energy storage methods are the consumptions of surplus or low-cost energy for conversion into resources such as hot/cool water which is then used for heating/cooling at other times when electricity is in higher demand or perhaps at greater cost per kilowatt hour for better balancing of power supply and demand.

Plant efficiency increases with the decrease in heat losses from the stack during the operations at higher temperature and pressures, in combined heat and power systems, and through the use of integrated energy conversion systems. In real power plants, a lot of heat is lost in the stack or at the tail end of the boiler or power plant. The characteristic efficiency of

a power plant is only about 30 per cent. By utilizing the waste heat significant gains in the thermal efficiency can be obtained, and significant increase in plant efficiency can be achieved. The extent of waste heat from a plant varies with the type of the plant. This is mainly due to certain temperature range of interest for each application. [15]

The sustainable energy development, as is generally known, can be achieved by three parallel approaches: by reducing final energy consumption, by improving overall conversion efficiency, and by making use of renewable energy sources. In these three areas, it is important to apply advanced heat transfer and heat exchanger technologies.

Electricity demand represents a significant impact to the cost of electricity. Therefore, there is a need for off peak storage. Even with all commercial off peak storage systems, there is a need to prevent an increase of energy consumption.

Thermal energy storage (TES) is a key element for effective thermal management in the sectors of heating and cooling, processing heat, and power generation. Thermal energy storage is the temporary storage or removal of heat energy for later use. Such storing is indispensable for increased utilization of renewable energy systems. The characteristic of TESs is that they are diversified with respect to temperature, power level, and heat transfer fluids. Also, each application is characterized by its specific operation parameters. This requires the understanding of a broad portfolio of storage designs, media, and methods.

The most widely used TES technologies are based on the models of shell-and-tube heat exchanger. The use of such exchangers should be considered in the optimization of heat exchanger networks. It reduces the capital cost because of its small size needed for a given duty. It also reduces the temperature driving force which reduces the entropy generation and increases the efficiency of the system. In addition, heat transfer enhancement enables heat exchangers to operate at a smaller velocity but still achieve the same or even higher heat transfer coefficients. All these advantages have made heat transfer enhancement technology attractive in the field of heat exchanger applications.

Storing the coolness or heat from the off peak period of energy system operations by using the phase change material (PCM) is a potential option for such systems. PCMs are materials in which the heat at the solid – liquid or solid – solid phase transition point is used in applications for storing large amounts of thermal energy at a certain temperature. A principle advantage of PCMs is the large energy storage density compared to sensible energy storage with rock or water. The main drawback of PCMs is the low thermal conductivity which reduces the useful amount of energy which can be stored. In a latent heat thermal

energy storage system, the heat transfer fluid (HTF) passes through an area of encapsulated PCM.

2.1 Thermodynamic Systems

A thermodynamic system is a device or combination of devices that contains a certain quantity of matter. It is important to carefully define a system under consideration and its boundaries. We can define three basic types of systems. They are as follows:

- *Closed system*. A closed thermodynamic system is defined as a system across the boundaries of which materials do not cross. It contains a fixed quantity of matter.
- *Open system*. An open thermodynamic system is defined as a system in which material crosses over the boundaries are allowed.
- *Adiabatic system*. An isolated thermodynamic system is defined as a closed system that is not affected by the surroundings. No materials such as mass, heat, or work cross its boundary. [1]

2.3 Sensible and Latent Heats

It is known that all substances can hold a certain amount of heat. This property is called the thermal capacity of substances. When a liquid is heated, its temperature rises to the boiling point, which is the highest temperature that the liquid can reach at the measured pressure. The heat absorbed by the liquid during the process of raising the temperature to its boiling point is called sensible heat. The heat required to convert a liquid to a vapor at the same temperature and pressure is called latent heat. This is a change in the enthalpy during a state change. The change of the enthalpy is in other words the amount of heat which is absorbed or rejected at constant temperature at any pressure, or the difference in enthalpies of a pure condensable fluid between its dry saturated state and its saturated liquid state at the same pressure. [29]

3 Literature Survey on Simulation Models of Sensible and Latent Heat Storages

This chapter is concerned with thermodynamic systems of temporary storage of high- or low-temperature energy for later use. These storage devices create the possibility of storing energy before its conversion to electricity. Mainly, two modes of thermal energy storages (TESs) will be discussed. These primal models of possible energy storages are a sensible heat storage (SHS) and a latent heat storage (LHS). Both these types are expected to be seen in multiple extended applications as the new energy technologies which are constantly being developed. They also form important means of offsetting the surplus between thermal energy availability and demand.

For storing sensible heat in thermal power plants the storage in concrete is an option shown in Figure 1. To demonstrate this idea *Bahl et al.* have built and tested a module in a real technology. This simulation is a first step towards the investigation of the yearly electricity yield of a thermal energy storage using concrete and thermal oil as HTF for parabolic trough power plants. It has been working for 16 months with using actual weather data. Design temperature of the test module is 400°C, length of storage concrete is 8.60 m, height / width are 1.70 m x 1.30 m and charging or discharging time is 6 hours. *Bahl's* simulation shows that parabolic trough power plants with concrete storages of the analyzed size could deliver 3,500 full load hours annually in the climate zone of southern Europe. The operation time of the plant lies at 4,550 hours annually there. The electricity generation during the storage operation is about 30 per cent over the entire year. This means that the storage realizes one third of the power plant operation. This power plant generates 175 GWh electricity in one year. The concrete storage module is principally composed of a tube register and the storage concrete. [16]

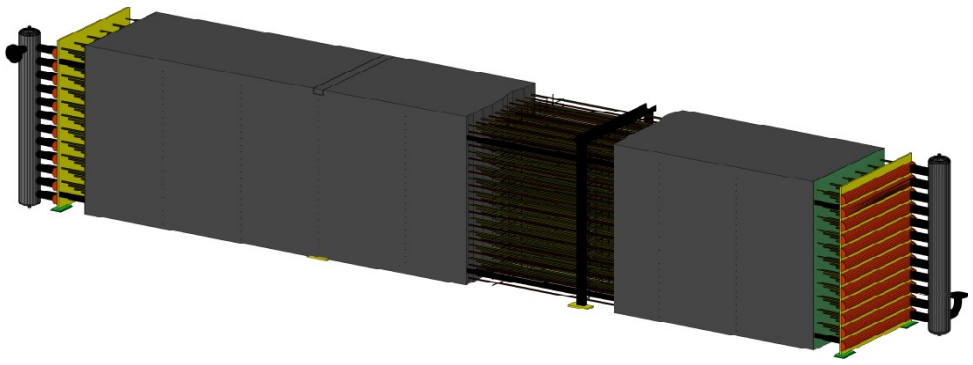

Figure 1: Storage module with visible tube register [16]

A. F. Regin et al. and *L. Xia et al.* have analyzed the performance of a packed bed LHS system shown in Figure 2. The packed bed is composed of spherical capsules or pebbles filled suitable PCM usable with water as a HTF. The phase change phenomena of PCM inside the capsules are analyzed by using enthalpy method. They solve equations numerically for both analysis such as charging and discharging processes. *Regin* and *Xia* investigate the effects of the inlet HTF temperature, mass flow rate, and phase change temperature range on the thermal performance of the capsules of various radii. [17, 18]

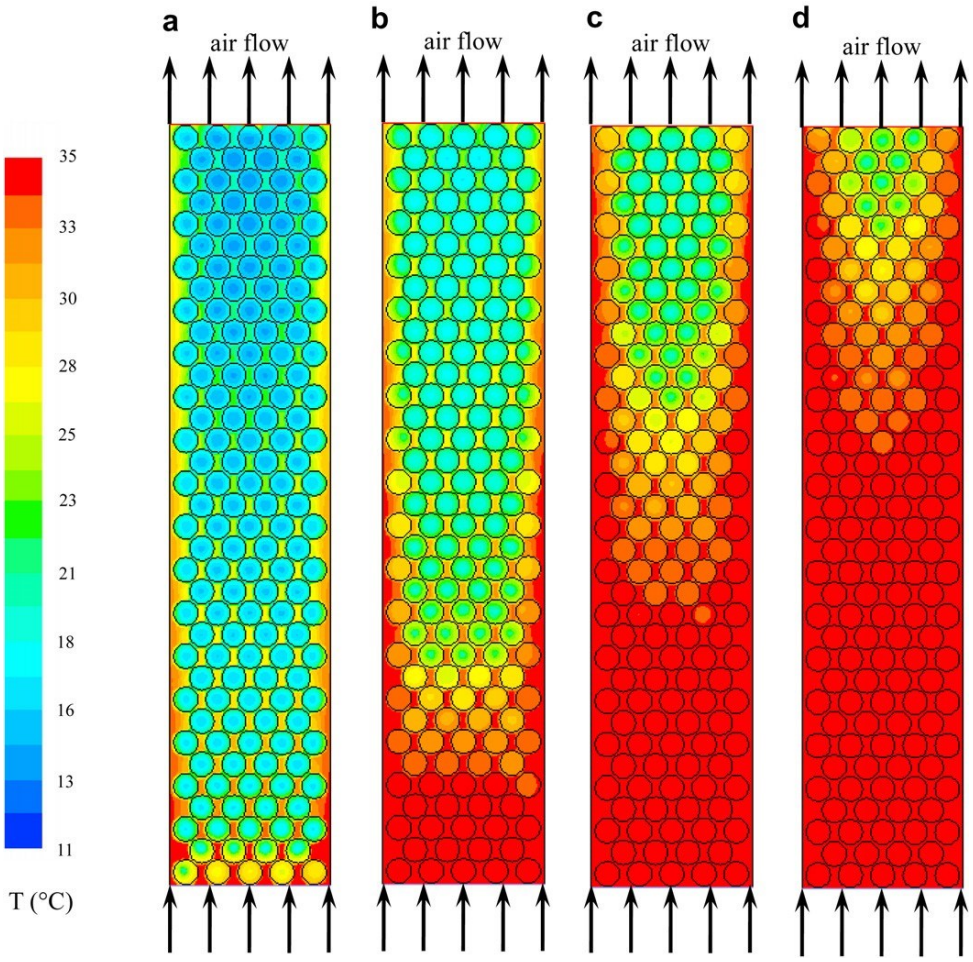

Figure 2: Packet bad SHS system during 5 hours of charging mode [18]

H. Shabgard et al. have investigated two configurations of heat pipes to serve as thermal conduits between the HTF and the PCM shown in Figure 3. The heat pipes transfer heat between the HTF and the PCM. The team developed a thermal model to investigate the effect of adding heat pipes to a high temperature LHS system. They considered charging and discharging in two storage configurations, one with the PCM contained within tubes over which the heat transfer fluid flows (Figure 3 upward), and the second with the PCM surrounding tubes that conveys the heat transfer fluid (Figure 3 downward). The influence of

the number of heat pipes, their orientation to the HTF flow direction, and the gravity vector were also investigated. [19]

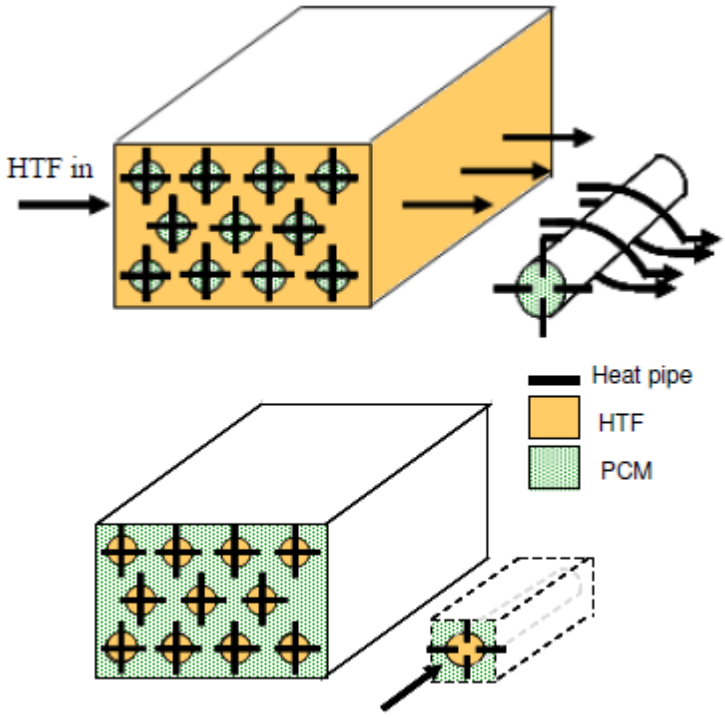

Figure 3: Upward: the PCM surrounds the HTF. Downward: the HTF passes over tubes containing PCM [19]

Jundika C. Kurnia et al. investigated various configurations TES devices, e.g., U-tube, U-tube with in-line fins, U-tube with staggered fins, and a novel festoon design as well as some different placement of different PCMs shown in Figure 4. The heat transfer between the HTF and PCM, which undergoes a cyclic melting and freezing process, was solved numerically using the computational fluid dynamic approach utilizing enthalpy-porosity formulation. The results indicate that the novel festoon design provides the highest heat transfer performance. This best performance was followed by TES with U-tube with fins. It is also found that U-tube with staggered fins performs better compared to U-tube with in-line fins. Another finding by *Kurnia* is that the implementation of multiple PCMs could enhance heat transfer performance within the TES. Different arrangement of PCMs significantly affects the heat transfer performance; placement of high melting point PCM at the inlet side during discharging improves heat transfer but it slightly underperforms during charging. [20]

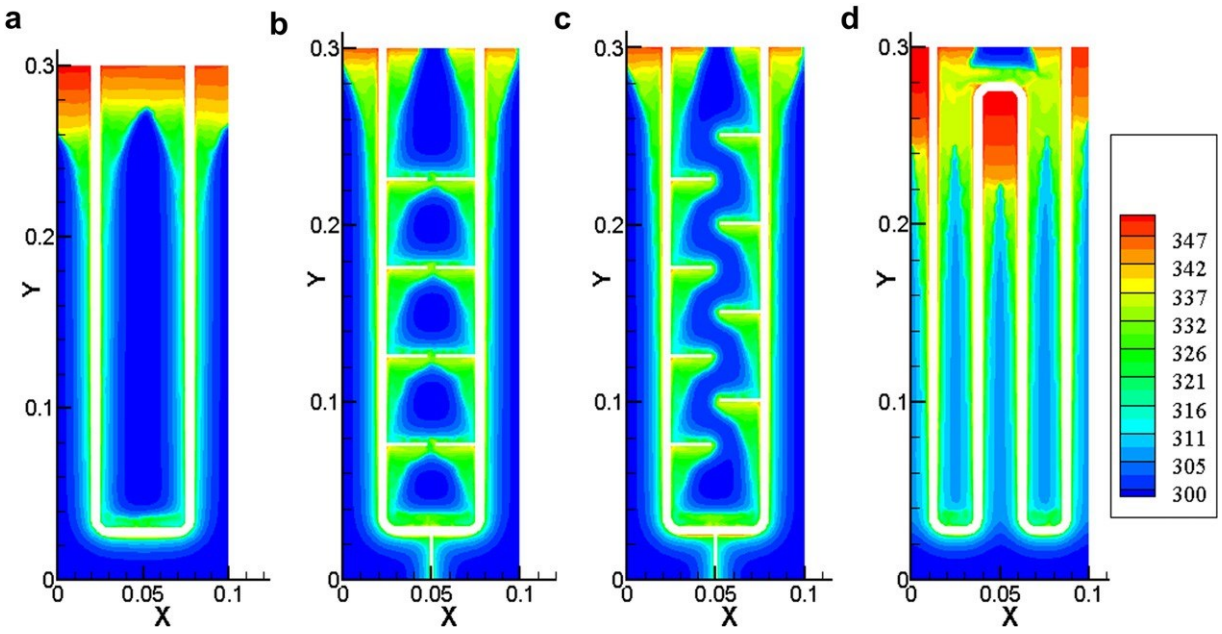

Figure 4: (a) U-tube design; (b) U-tube with inline fins; (c) U-tube with staggered fins; (d) novel festoon design during charging. [20]

H. Shabgard et al. have developed a mathematical model of shell-and-tube latent heat thermal energy storage unit of three PCMs with different melting temperatures (983 K, 823 K and 670 K) and with air based HTF on the enthalpy method shown in Figure 5. *Shabgard's* team has numerically analyzed instantaneous solid-liquid interface positions and liquid fractions of PCMs as well as the effects of inlet temperatures of the air and lengths of the shell and tube unit on melting times of PCMs. A two-dimension mathematical model using FLUENT software based on the enthalpy method was developed to predict the thermal behavior and performance shell and tube unit with three high temperature PCM1, PCM2 and PCM3. [21]

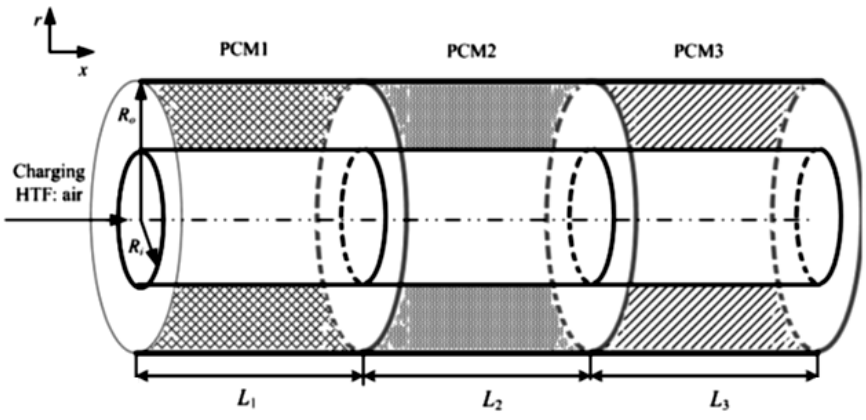

Figure 5: Shell and tube unit with three different PCMs [21]

A.H. Mosaffaa et al. have developed analytical model for the solidification process in a shell and tube finned thermal storage shown in Figure 6. Authors present comparative study

for solidification of the PCM in cylindrical shell and rectangular storages with the same volume and heat transfer surface area. The tube is composed from aluminum and PCM is $CaCl_2 \cdot 6H_2O$. Analytical solution is presented for the solidification process in a shell and tube. This analytical solution is compared to that obtained via a two dimensional numerical method based on an enthalpy formulation for prediction of the solid–liquid interface location. Their results show that the PCM solidifies more quickly in the cylindrical shell storage than in rectangular storage. The effects of air velocity and inlet air temperature on the performance of the thermal storage are analyzed. It is found that the effect of inlet air temperature is more significant than air velocity on the outlet temperature. [22]

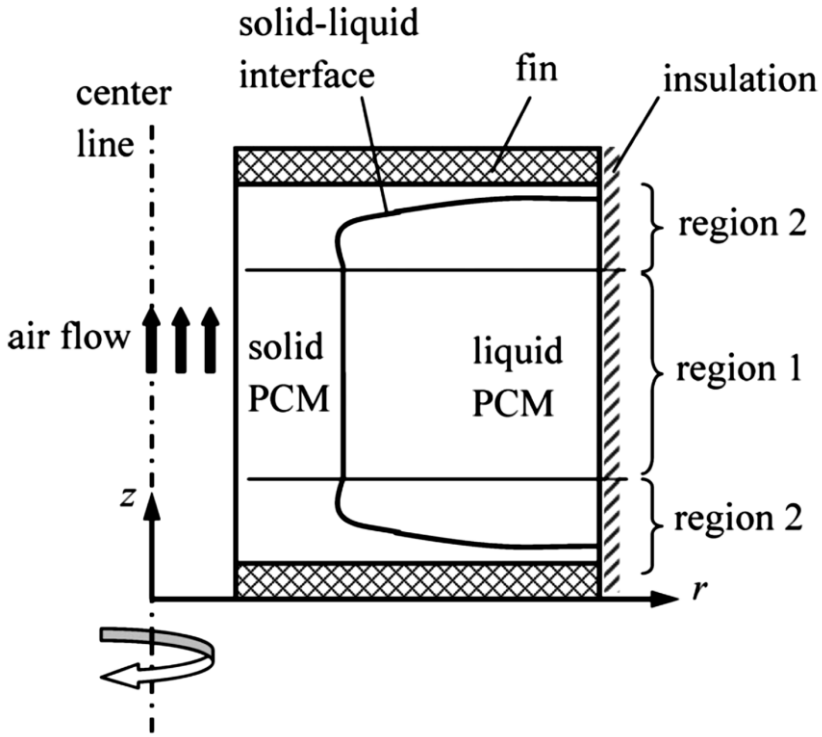

Figure 6: Shell and tube storage splitted into two region and symmetry cell [22]

Zhenyu Liu et al. have established a numerical model to predict the PCM melting process in porous media shown in Figure 7. Authors use metal foam in a shell-and-tube unit for heat transfer technique to PCM. The solid–liquid phase change phenomenon is solved with the enthalpy method. The solid–liquid interface position and the temperature distribution are predicted to describe the melting process. The physical domain includes the volume filled with a copper matrix. This matrix is saturated with the PCM RT 58. Authors compared their metal foam model with the results of the pure PCM. The phase change heat transfer can be enhanced by more than seven times. Author's study shows that the structure characteristics of

the metal foam and the HTF inlet conditions have significant influences on the storage unit performance. [23]

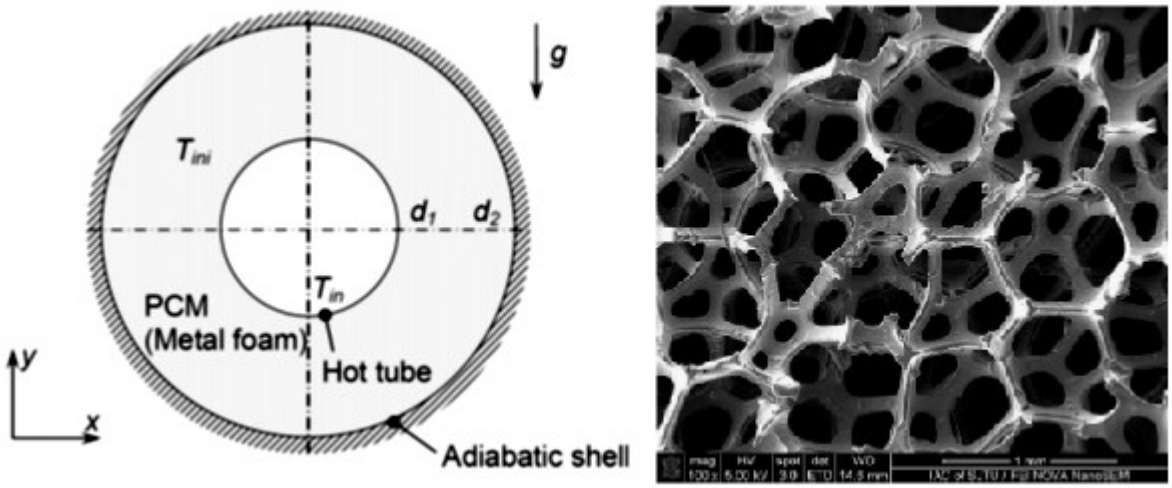

Figure 7: (a) Shell and tube unit, (b) Metal (copper) foam [23]

R. Darzi et al. investigate numerical model on melting of PCM using N-eicosane inside a cylindrical container. Authors performed numerical simulations for symmetric melting of PCM between two cylinders in concentric and eccentric arrays using the FLUENT software. Solid PCM is more melted in top region of inner cylinder. It is due to the effect of natural convection in the zone where warm liquid rises to the top region and replaces there the cooler liquid shown in Figure 8. Heat conduction occurs between hot surface of inner wall and the cold solid PCM at the bottom region. [24]

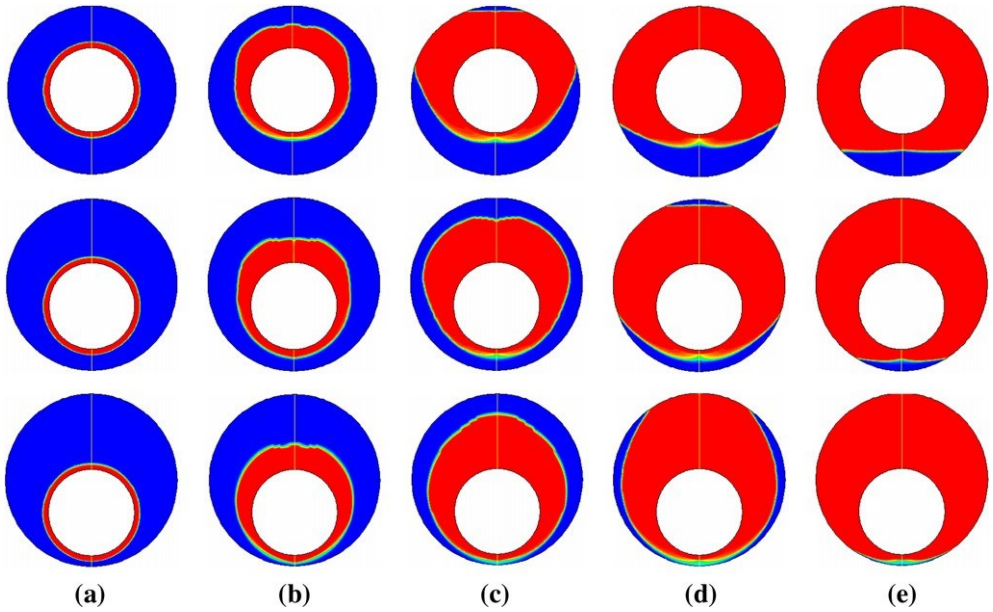

Figure 8: Computational melting phase front for different arrays

Anica Trp et al and *Hamid Ait Adine et al.* have presented an experimental and numerical two-dimensional model of transient forced convective heat transfer between the HTF and the tube wall based on the enthalpy method. Authors investigate experimentally and numerically the transient heat transfer phenomenon during melting and solidification in a shell-and-tube latent TES unit with the HTF circulating inside the tube and the PCM filling the shell side. [25, 26] *K. A. R. Ismail et al.* investigated solidification of PCM around a curved tube also in shell and tube heat exchanger. [27]

Y.B. Tao et al. have numerically carried out the effects of the non-steady-state inlet condition of HTF on the thermal performance of the PCM in shell and tube unit. Their results show that when the average HTF inlet temperature in an hour is fixed at a constant value the melting time decreases with the increase of initial inlet temperature. When the initial inlet temperature increases from 30°C to 90°C, the melting time will decrease from 42.75 min to 20.58 min. [28] This literature has been set up as a source for the section 4.6.

N. Shamsundar et al. [14] presents the results of research and development on passive latent heat storage systems. Analytical models and a computer code for simulating performance were developed by the authors. The PCM studied was a eutectic mixture of inorganic salts that fill the space outside the tubes in a shell-and-tube heat exchanger. Author's prediction of the heat transfer rates and the transient response involved the solution of a transient heat transfer problem. Heat recovery models were tested by *N. Shamsundar et al*. Authors also set up for calculating performance improvement resulting from the use of finned tubes instead of plain tubes. A simple computer program for quick calculation of design parameters for heat storage is also described by authors. This literature has been set up as a source for the section 4.2.

3.1 Thermal Energy Storage

Thermal energy may be stored by elevating or lowering of the substance temperature (i.e., by altering its sensible heat), by changing the phase of a substance (i.e., by altering its latent heat), or through a combination of the two methods.

TES is technically a temporary storage of high- or low-temperature energy for later use. Through this function it can be an important mean of offsetting the temporal difference between thermal energy availability and demand.

The technologically available ES types are applicable to electrical energy. In thermal electrical generating systems, TESs offer the possibility of storing energy before its conversion to electricity. Energy quality is measured by the temperatures of the materials entering, exiting, and stored within the storages. For this the TESs are an important considerations.

Energy demands in the industrial, utility, commercial, and residential sectors vary on a temporal (different daily, weekly, and seasonal demand) base. The use of TESs in such varied sectors requires that the various systems operate synergistically and that they are carefully matched to each specific application. Much attention has been already devoted to the use of TESs for thermal applications such as space heating, hot water heating, cooling, air conditioning and similar. A variety of new TES technologies has been developed over the past four or five decades in the top industrial countries. TESs have enormous potential for the more effective use of thermal equipment and for economical facilitation of large-scale substitutions of energy resources. However, a coordinated set of actions in several sectors of the energy system is needed for the maximum potential benefits of TESs to be realized and maximum beneficiary used. [1]

Different SHSs and LHSs for high temperature TES systems up to 100°C were identified as being commercially available. The following table summarizes the storage types, the preferred HTF, the storage medium material, and the temperature range of typical applications. Table 1 shows, that the complete temperature range from 100 to 1000°C can be covered with sensible materials.

Table 1: Available hight temperature TES

Storage type	Preferred HTF	Storage medium	Temperature range [°C]
Steam accumulator	water, steam	Water	100-300
Liquid salt storage	Liquid salt, oil	Liquid salt	150-600
Concrete storage	Oil, compressed water	Concrete	up to 500
Packed bed storage	Flue gas, air	Ceramics	up to 1300
Latent heat storage	2 phase flow, water, steam	Salt	material depending up to 1000

Energy is stored or extracted by heating or cooling a liquid or a solid, which does not change its phase during the process. As seen from the table, a variety of substances have been used in different TES systems. These include liquids like water, heat transfer oils, certain

inorganic molten salts, and solids like rocks, pebbles, and refractories. In the case of solids, the material is invariably in porous form and heat is stored or extracted by the flow of a gas or a liquid through the pores or voids.

The choice of the substance used depends largely on the temperature level of the application. Water is used for temperature below 100°C and for example refractory bricks are used for temperatures around 1000°C. [31]

3.2 Sensible Heat Storage

The SHS refers to the energy system that stores thermal energy without a phase change. It occurs by adding heat to the storage medium and increasing its temperature. Heat is added from a heat source to the liquid or solid storage medium. The thermal stratification is important for the SHS. Heating of the material that undergoes a phase change is called the LHS. The amount of energy stored in the LHS depends upon the mass and latent heat of the material. In the LHS, the storage operates isothermally at the phase change of the material. Both these types and forms of TESs are expected to be seen in extended applications as the new energy technologies are constantly being developed.

In SHS thermal energy is stored by raising the temperature of a solid or liquid. SHS system utilizes the heat capacity and the change in temperature of the material during the process of charging and discharging. The amount of heat stored depends on the specific heat of the medium, the temperature change and the amount of storage material. [2]

$$Q = \int_{T_i}^{T_f} mC_p \, dT = mC_p(T_f - T_i) \qquad 2 - 1$$

m is the mass and Cp is the specific heat at constant pressure. Ti and Tf represent the lower and upper temperature levels between which the storage operates. The difference (Ti - Tf) is referred to as the temperature swing.

SHS systems are simpler in design than LHSs. The systems are beneficial if the thermal energy of the HTF is discharged over a large temperature range. This is connected with a corresponding large temperature change of the storage medium. A slight disadvantage of the SHSs is their bigger size. For this reason, an important criterion in selecting a material for SHS is its (ρCp) value. It is desirable for the storage medium to have high specific heat

capacity, long term stability under thermal cycling, compatibility with its containment and the most important is the low cost. [30]

A second disadvantage associated with SHSs is that they cannot store or deliver energy at a constant temperature. The following Table 2 summarizes range of applications, specific heat capacity, and the volumetric heat capacity of typical sensible storage media.

Table 2: Range of application sensible storage media

Sensible storage media	Range of application [°C]	Specific heat capacity [kJ/kgK]	Volumetric heat capacity [kJ/m³K]
Liquid salt-mixtures	150-450	1,5	2450
Synthetic Oil	0-400	2,1	1800
Concrete	until 500	1	2200
Ceramics	until 1500	1,2	3000

3.2.1 Liquid Sensible Heat Storage

Because of the density differences between hot and cold fluids the liquid media maintain thermal stratification. The existence of a thermal gradient across the storage is desirable. This characteristic is used when the hot fluid is supplied to the upper part of the storage during charging, and the cold fluid is extracted from the bottom part during the storage discharging.

Storage in fresh water. Water can be used as storage and as a transport medium of energy. The water is one of the best medium to be used at temperature under 100°C. It has higher specific heat than other materials, it is cheap, and widely available.

However, due to its high vapor pressure, water requires costly insulation and pressure withstanding containment for high temperature applications. Water storage tanks are made from a wide variety of materials, like steel, aluminum, reinforced concrete and fiber glass. The tanks are insulated with glass wool, mineral wool or polyurethane. The sizes of the tanks used vary from a few hundred liters to a few thousand cubic meters.

For large scale storage applications, underground natural aquifers have been considered. Aquifers are geological formations containing ground water, offering a potential way of storing heat for long periods of time. The storage medium in aquifers consists of water

saturated gravel or sand. Large storage volumes are available, as typical aquifer sizes range from hundreds of thousands to millions of cubic meters. The attractiveness of aquifer storage is due to its low cost characteristics, its high input/output rates and its large capacity.

Storage in salty water. Molten salt is commercially used as HTF. The main advantage of its use is the low pressure of the liquid even at high temperature. Molten salt installations are operated continuously. Nitrate salts are mostly used. Well known are different binary and ternary salt mixtures, which are also used for TES for thermal power plants. Long term experience is available at several industrial manufacturers and suppliers of sub-components, melting facilities and salt producers.

Storage in other fluids. The most substitutes for water are petroleum based oils. These substitutes have lower vapor pressure than water and are capable of operating at temperatures exceeding 300°C. The oils are, however, limited to temperatures up to 350°C. Due to stability and safety reasons the mostly used fluids such as Therminol, Caloria are costly.

Next in significance is the usage of liquid metals in SHSs. However, such fluids have usually unwanted properties, which make them very narrowly focused for their application. Their properties are partly similar to water, but they also have undesirable properties such as high corrosion, difficulty in containing at high temperatures, and potential for reactivity with the container. [8]

3.2.2 Solid Sensible Heat Storage

Sensible heat storage (SHS) is the simplest form of storing thermal energy. The storage is based on the temperature change in the material. An identifying characteristic of sensible heat is the flow of heat from hot to cold by means of conduction, convection, or radiation. This type of heat storage is dependent on the temperature gradient and requires insulation to maintain the temperature gradient. The difficulties of the high vapor pressure of water and the limitations of other liquids can be avoided by storing thermal energy as sensible heat in solids. [16]

Solid materials such as rocks, metals, concrete, castable ceramic and bricks can be used. The energy can be stored at low or high temperatures, since these materials will not freeze or boil. Solids do not leak from their container. The best solid for SHSs is cast iron which exceeds the energy density level of water storage [9]. Cast iron is more expensive than

stone or brick and the payback period is much longer. Due to the low cost of pebble beds or rock piles, they are generally preferred as the storage materials.

Storage in rocks. The pebble bed or rock pile consists of a bed of loosely packed rock material. The HTF can flow through this bed. The thermal energy is stored in the packed bed by forcing heated HTF into the bed and utilized again by recirculating ambient air into the heated bed. This energy depends on the thermo physical properties of the bed material, rock size and shape, packing density, or heat transfer fluid.

Storage in metals. Most of the materials proposed for high temperature (120±1400°C) energy storages are either inorganic salts or metals. Metals such as aluminum, magnesium, and zinc are suitable examples. The use of metal media may be advantageous where high thermal conductivity is required and where cost is of secondary importance. Solid industrial wastes such as copper slag, iron slag, cast iron slag, aluminum slag, and copper chips could be used as storage materials [8].

Storage in concrete. Concrete as a material for energy storages is chosen for its low cost, availability, and easy processing. Concrete is a material with high specific heat, good mechanical properties (e.g. compressive strength), and thermal expansion coefficient near that of steel, and high mechanical resistance to cyclic thermal loading.

When concrete is heated, a number of reactions and transformations take place. These alternations influence its strength and other physical properties. Compressive strength decreases about 20 per cent at 400°C, the specific heat decreases in the range of temperature between 20 and 120°C, and the thermal conductivity decreases between 20 and 280°C [12].

Resistance of concrete to thermal cycling depends on the thermal expansion coefficients of the individual materials used in the concrete mixture in use. Steel needles and reinforcements are sometimes added to the concrete to impede cracking. Hereby the thermal conductivity is increased about 15 per cent at 100°C and 10 per cent at 250°C [12].

Table 3: Thermal capaties at 20°C of some sensible storage materials [1]

Material	Density [kg/m^3]	Specific heat capacity [J/kgK]	Volumetric heat capacity [MJ/m^{3}K]
Water	998	4182	4,17
Wood	700	2390	1,67
Brick	1800	837	1,51
Aluminium	2710	896	2,43
Steel	7840	465	3,68

3.2.3 Sensible Heat Storage System Design and Configuration

SHS made by solid materials are usually used in packed beds. Such beds require fluids to exchange the heat. For specially high temperatures concrete, or castable ceramic is being used as a suitable material to surround the tubes of the heat storages. For low temperatures water tanks are used. Because of their low cost, good thermal conductivity, and moderate specific heat concrete and cast ceramics are the most suitable and preferable.

3.2.3.1 Design Sensible Heat Storage

Multitank. Most SHS systems are design variations of a two-tank system. Multitank storage refers to the type of SHS system which uses more than two tanks.

In a two tank system, in Figure 9, each tank must have the capacity to hold all the fluid. Thus there must be twice the tankage volume to the fluid volume. In case of three tanks of equal volume, any two of the three tanks must at any given time be able to hold all the storage fluid in order to provide separation of the hot and cold storage fluid.

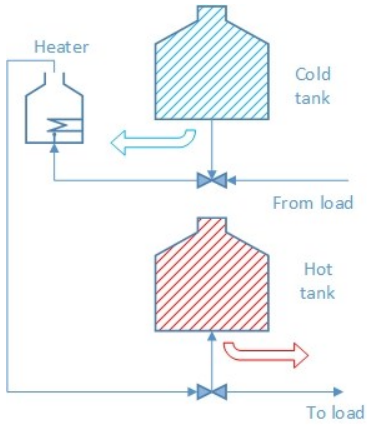

Figure 9: Two-tank sensible heat storage

Following is the description of the three-tank SHS operational cycle shown in Figure 10. At the start of the day tanks 1 and 2 are full of cold fluid and tank 3 is empty. Cold fluid is withdrawn from tank 1, heated and placed in tank 3 which was empty until now. After some time tank 3 is full of hot fluid and tank 1 is empty. Cold fluid is then withdrawn from tank 2 and after being heated, it is placed in tank 1. Tanks 1 and 3 are consequently full of the hot fluid, tank 2 is empty and the cycle of the three-tank multitank ends.

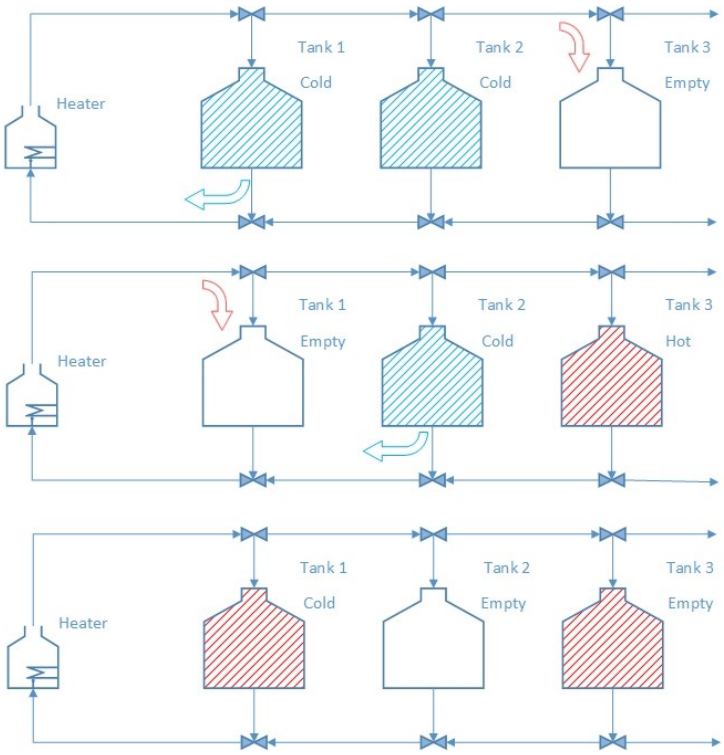

Figure 10: Multi-tank sensible heat storage

Thermocline Energy Storage. The reduction in storage tank volume is achieved when the storage tank volume equals the storage fluid volume shown in Figure 11. Thermocline system has both the hot and cold storage fluids occupying the same tank. The storage tank is full of cold fluid at the start of the operation. Cold storage fluid is withdrawn from the bottom of the storage tank and heated. The hot storage fluid is then put back into the top of the storage tank. The less dense hot storage fluid will "float" on top of the cold storage fluid. This phenomenon actually occurs quite commonly in many fluid systems ranging from the ocean to residential hot-water heaters. One of the most critical design parameters in the thermocline TES systems is proper provision for diffusion of the incoming and leaving fluids in order to minimize mixing which results in formation of vortices or jetting of the incoming fluid.

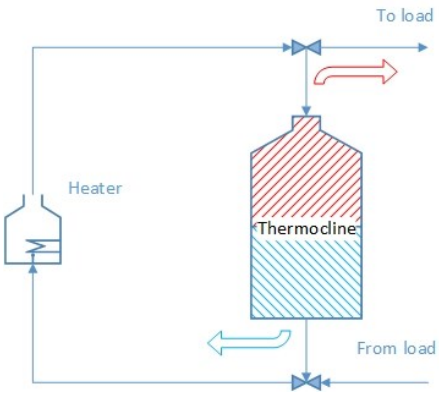

Figure 11: Thermocline Energy Storage

High-Temperature SHS. The ability to store high temperature thermal energy is limited by the availability of HTF. Fluids such as molten salts, liquid metals, and air are considered for electric power generation. However, in temperatures above 400ºC organic HTF incline to decompose thermally.

Pressurized Fluids. The use of water or steam as a storage medium reduces storage fluid costs. This advantage is significant as SHS are usually overwhelmed by the expense of the pressurized storage tank which is needed.

3.3 Latent Heat Storage

As it was previously mentioned, the LHS refers to the energy system that store thermal energy with a phase change. LHSs are based on the heat absorption or release when a storage material undergoes a phase change from solid to liquid, from liquid to gas, or vice versa. The storage capacity of the LHS systems with a PCM medium [2] is given by

$$Q = \int_{T_i}^{T_m} mC_p dT + m\Delta H + \int_{T_m}^{T_f} mC_p dT = m\left[C_{sp}(T_m - T_i) + \Delta H + C_{lp}(T_f - T_m)\right] \quad 2 - 2$$

where C_{sp} and C_{lp} represent the specific heats of the solid and liquid phases, ΔH is enthalpy and T_m is the melting point. The storage operates isothermally at the melting point of the material. If the isothermal operation at the phase change temperature is difficult, the system operates over a range of temperatures T_i to T_f that include the melting point. The sensible heat contributions, and the amount of energy stored have to be considered.

Any LHS systems must keep at least the following conditions. It has to have a suitable PCM with its melting point in the desired temperature range, suitable container compatible with the PCM, and a suitable heat exchange surface.

LHS systems have certain benefits in comparison with SHS systems. The most important advantages are surely its higher energy density per unit mass, and higher energy density per unit volume. Large amounts of heat with only small temperature changes are possible to be stored because of this high storage density. As the change of phase at a constant temperature takes some time to complete, it becomes possible to smooth temperature variations.

LHSs can be accomplished through solid-liquid, liquid-gas, solid-gas, and solid-solid phase transformations. The only two transformations of practical interest are the solid-liquid and solid-solid transitions [7]. Solid-gas and liquid-gas transition have higher latent heat of fusion but their large volume changes on phase transition are associated with containment problems. This particular problem rules out their potential utility in the TESs. The large changes in volume make the system complex and impractical.

In solid-solid transitions, heat is stored when the material is transformed from one crystalline to another. This transition has generally smaller latent heat and volume changes than the transition from solid to liquid. Solid-solid PCMs offer the advantages of less rigorous container requirements and better design flexibility [7].

Solid–liquid transformations have comparatively smaller latent heat than liquid-gas transitions. Thus this transition has proved to be economically attractive for the use in TES systems. These transformations also involve only a small change in volume (< 10 per cent).

3.3.1 Latent Heat Storage Materials

PCM are materials used for latent heat storage. As the source temperature rises, the chemical bonds within the PCMs break up as the material changes its phase from solid to liquid. The phase change is a heat-seeking, endothermic process and, therefore, the PCMs absorb heat.

Upon heat storage in PCM materials, the material begins to melt when the phase change temperature is reached. The temperature then stays constant until the melting process is finished. The heat stored during the phase change process of the material is called the latent heat.

LHS can be used in a wide temperature ranges. A large number of PCMs are known to melt with a heat of fusion in any required range. The PCM to be used in the design of the TES systems should accomplish desirable thermo physical, kinetic, and chemical properties. These properties are as follows:

Thermo-physical Properties:

- Melting temperature in the desired operating temperature range.
- High latent heat of fusion per unit volume so that the required volume of the container to store a given amount of energy is lower.
- High thermal conductivity of both solid and liquid phases to assist the charging and discharging of energy of the storage systems.
- Small volume changes on phase transformation and small vapor pressure at operating temperatures to reduce the containment problems.
- Consistent melting point of the PCM for a constant storage capacity of the material with each freezing/melting cycle.

Kinetic Properties:

- High nucleation rate to avoid super cooling of the liquid phase.
- High rate of crystal growth to enable the system meet the demands of heat recovery from the storage system.

Chemical Properties

- Chemical stability.
- Complete reversible freeze / melt cycle.
- No degradation after a large number of freeze / melt cycles.
- Non-corrosiveness to the construction materials.
- Non-toxicity, non-flammablility, and non-explosivity of the materials for increased safety. [3]

3.3.1.1 Types of Phase Change Materials

There is a large number of PCMs - organic, inorganic, and eutectic. All these material types can be identified as PCMs from the point of view of the melting temperatures and latent heats of fusion. No single material can have all the required properties for an ideal thermal storage media, and thus compromises must be done. For example one has to use an available material with preferable chemical properties and try to make up for the poor physical properties by an adequate system design. [3] The enthalpy is the preferred expression of system energy changes. Enthalpy change accounts for energy transferred to the environment at constant pressure through expansion or heating. Figure 12 shows the dependence of the

enthalpy to the temperature for different materials. Another method of allocating the LHS materials is shown in the Appendix A.

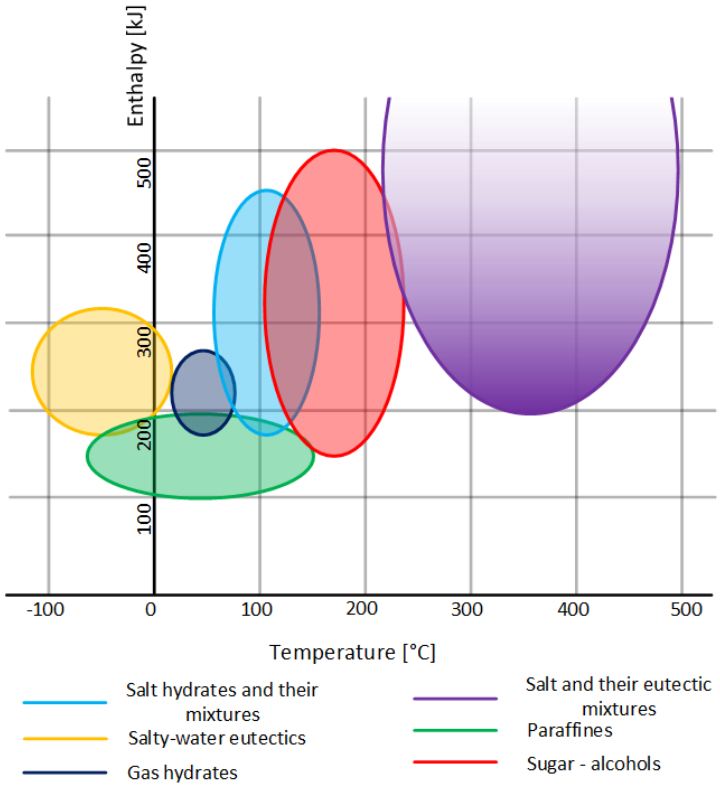

Figure 12: Types of PCM and their usage for different temperatures

Paraffin. A normal paraffin of type CnH_{2n+2} belongs to a family of saturated hydrocarbons with very similar properties. Paraffins between C_5 and C_{15} are liquids, and the rest of paraffins are waxy solids. Paraffin wax is the most-used commercial organic heat storage PCM. [4] It consists of mainly straight chain hydrocarbons that have melting temperatures ranging from 23 to 67°C [4, 5].

Advantages:

- No tendency to segregate.
- Chemical stability.
- No degradation in thermal properties.
- High heats fusion.
- Safety and non-reactiveness.
- Easy incorporation into heat storage systems.

Disadvantages:

- Low thermal conductivity in the solid state.
- High volume change between the solid and liquid stages.
- Decreased heat storage capacity in phase change.
- Flammability easily alleviated by a proper container.

Non – Paraffin. The non-paraffin organic substances are the most numerous group of the PCMs. Unlike paraffin, this group has highly varied properties. Each member of this substance family has its own unique properties. These materials are flammable and should not be exposed to excessively high temperatures or flames.

Salt Hydrates. Substances of the salt hydrate family consist of salt and water, which combine in a crystalline matrix when the material solidifies. There are many different materials, where some of them have low temperature melting ranges of 15 to 120°C [5] and other have high temperature melting ranges of 120-1000°C [10]. Salt hydrates form the most important group of PCMs on the base of its usage as PCMs.

Advantages:

- Low cost.
- Easy availability.
- Sharp melting point.
- High thermal conductivity (compared to other PCMs) which increases heat transfer in and out of the storage unit.
- High heat of fusion which decreases the needed size of the storage system.
- Lower volume change (compared to other PCMs).

Disadvantages:

- Out settlement and reduction of the active volume available for heat storage.
- Tendency to cause corrosion in metal containers.
- Under cooling phenomenon.

Fatty acids. Substances of the fatty acid family have similar characteristics as substances of paraffin. Systems, which use fatty acids to obtain melting temperatures ranging from 20–30°C, have an accuracy of 0.5°C. This desirable characteristic allows a designer to select the optimum operating temperature to obtain the maximum performance of the TES.

Fatty acids have thermally stable behavior after 1500 repeated melting / freezing cycles. Therefore, no purity guarantee can be provided. This may be the reason that the latent heats of fusion of fatty acid generally decrease with the number of thermal cycles.

Advantages

- Sharp phase transformation.
- Mild corrosiveness.

Disadvantages

- Cost (two to three times more expensive then paraffins).

Table 4: Thermal properties of latent heat storage materials [3]

Name	Material	Melting point [°C]	Density [kg/m^3]	Thermal conductivity [W/mK]	Latent heat [kJ/kg]
Glycerin	Non-parafin	17,9	1260	n.a.	198,7
Succinic anhydride	Non-paraffin	119	1104	n.a.	204
Capric acid	Fatty acid	16	901	0,149	148
Stearic acid	Fatty acid	69	848	0,172	202,5
$MgCl_2.6H_2O$	Salt hydrates	115-117	1450 (120°C)	0,570 (120°C)	165-169
Hitec XL*	Organic	140	1992	0.519	n.a.
Hitec **	Organic	142	1990	0.6	84
KNO_3-$NaNO_3$	Organic	223	1867	0.8	105
$NaNO_3$	Organic	308	2260	0.5	74
KNO_3	Organic	336	2110	0.5	266
KOH	Organic	380	2044	0.5	149.7
$AlSi_{12}$	Organic	576	2700	160	560
NaCl	Organic	802	2160	5	492
Na_2CO_3	Organic	854	2533	2	275.7
K_2CO_3	Organic	897	2290	2	235

* 48% $Ca(NO_3)_2$ 45%KNO_3 7% $NaNO_3$

** KNO_3 - $NaNO_2$ - $NaNO_3$

3.3.2 Selecting PCM to Design Thermal Energy Storage Devices

Various conventional and unconventional materials are investigated for their capability to store thermal energy. These thermal energy storage devices (TESD) are selected on the basis of some crucial physical, chemical, and economic properties. Melting point, Heat of fusion, density, heat capacity, thermal conductivity, compatibility with container, and cost of production belong to the main parameters for selection considerations. [4, 5, 10]. It is a genuine challenge to find an ultimate TESD. The overall suitability of materials to be used as TESD is governed by a multifaceted interplay between several properties of those materials.

Organic, inorganic, and hybrid materials are being used for thermal energy storage. Paraffins and fatty acids are the most preferred organics. Water and hydrated salts of alkali metals, some transition metals are popular inorganic TESDs. Salts of organic cations are characterized by wide usable temperature range, high thermal stability, high ion density and design ability. Ionic liquids mostly possess intermediate physical and chemical properties to organic and inorganic compounds. [11]

It has not been possible to gain all the desirable properties from one material substance. As we select a material with one or two favorable properties with best values, the remaining properties have to get compromised. The overall efficiency of a TESD is a result of a complex interplay between all the properties of the PCM. To overcome this difficulty, eutectics and other mixtures of fatty acids and paraffins are investigated for their ability to store thermal energy.

Melting point. The temperature (T_m) at which the first crystal of the material collapses is called the melting point. The melting point itself does not affect the energy storage capacity of a material. It is, however, vital to have the melting point of TESD within the temperature range of the targeted application. As the phase change is involved in melting, the inclusion of melting point in temperature range of application can permit the use of phase change as an on-off switch. Phase change starts and stops the flow of materials which in turn can connect and disconnect the thermal circuit and offer a smooth path for heat transfer.

Within inorganic TESDs the under cooling is a clearly visible phenomenon. Melting of a solid is usually very quick but the solidification of molten materials requires relatively longer time and reduced temperatures. Due to this, a difficulty in rapid disconnecting of the thermal circuits arises. Hence, materials with low under cooling properties are preferred TESDs.

Heat of Fusion. Heat of fusion (ΔH), or latent heat of fusion is a very important property useful in selecting a suitable TESD. It refers to the amount of thermal energy that must be absorbed or evolved by the material in order to change its phase from solid to liquid or vice versa. Large values of heat of fusion leads to more efficient TESDs.

Heat Capacity. Heat capacity (C_p) refers to the amount of energy per molecule which a compound can store before the increase in its temperature. This energy is generally stored in translational, vibrational, and rotational modes. Materials with greater atom numbers are expected to have higher heat capacity.

Thermal Conductivity. Thermal conductivity (k) measures the ability of a material to conduct heat. Greater values of k imply more efficient heat transfer. It forms a property of materials which needs to be optimized. Thermal conductivity is a phase dependent property. Thus it is important to know the values of *k* in both the solid and molten phases. It has been observed that most of molten materials exhibit much higher values of thermal conductivity as compared to that in their solid states. Higher values of thermal conductivity in molten state can facilitate an efficient heat transfer and smooth operation of the thermal circuits in TESD.

Density. Density (ρ) of a material is a property of materials that refers to its mass per unit volume. Materials with higher density occupy less space which in turn increases the energy storage capacity. Materials with high density thus, obviously, possess higher energy storage capacity. However, many of such TESD materials show a significant decrease in density in their molten states. This is due to the expansion of their volume. If the TESD is placed in a sealed container in its solid phase, empty space equivalent to its volume expansion must be kept in the container. Taking in consideration this property, materials with high density but very small change in density at the phase change temperatures are attractive TESDs.

Other properties. In addition to the above mentioned properties, material compatibility with container, thermal stability, inflammability, and economic factors play additional vital roles in determining the right PCM for TESs. [11]

3.3.3 Latent Heat Storage System Design and Configuration

Different heat transfer applications require different types of hardware and different configurations of heat transfer equipment. Some have been already described in Section 2.

Several models of LHS systems have been developed already. Well-known are mainly the three modes of cylindrical PCM containers shown in Figure 13. The first model represents a device where the PCM fills the shell and the heat transfer fluid flows through a single tube. Second model shows a device where the PCM fills the tube and the HTF flows parallel to the tube. Such examples of the pipe models have a low heat loss to the surrounding area. The third cylinder model is the combination of shell and tube system. Heat transfer in such model system has advantage due to its effect of multiple convective heat transfers compared to a single conductive heat transfer in the pipe model.

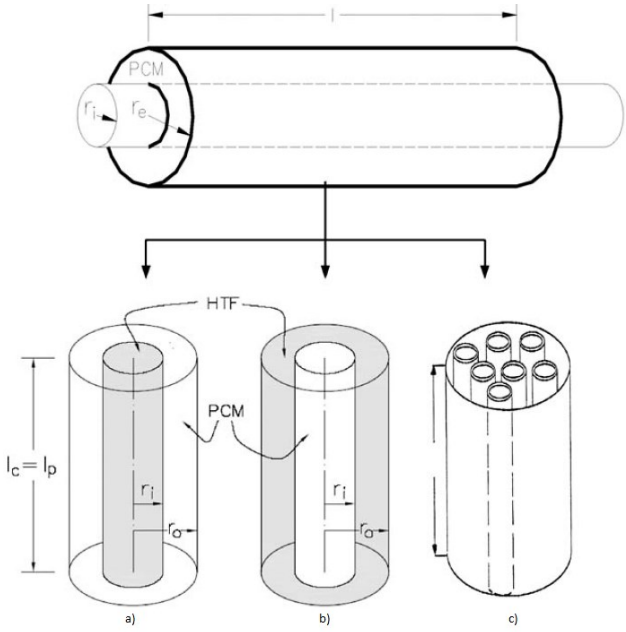

Figure 13: Tube geometry and configuration (a) Pipe model (b) Cylinder model (c) Shell and tube model [13]

In a cylindrical container configuration of the HTFs two flow directions exist shown in figure 14. They occur during charging and discharging of the PCMs. The first flow can be labeled as a parallel flow where cold and hot HTF flows in one direction. The second flow is called a counter-current flow where cold and hot HTF enters in the opposite ends of the tube. Two flow directions exist the parallel flow increases energy charge or discharge more than the counter-current flow. The counter-current flow for charge or discharge process produces super cooling of the PCM in the inlet region of cold fluid. [13]

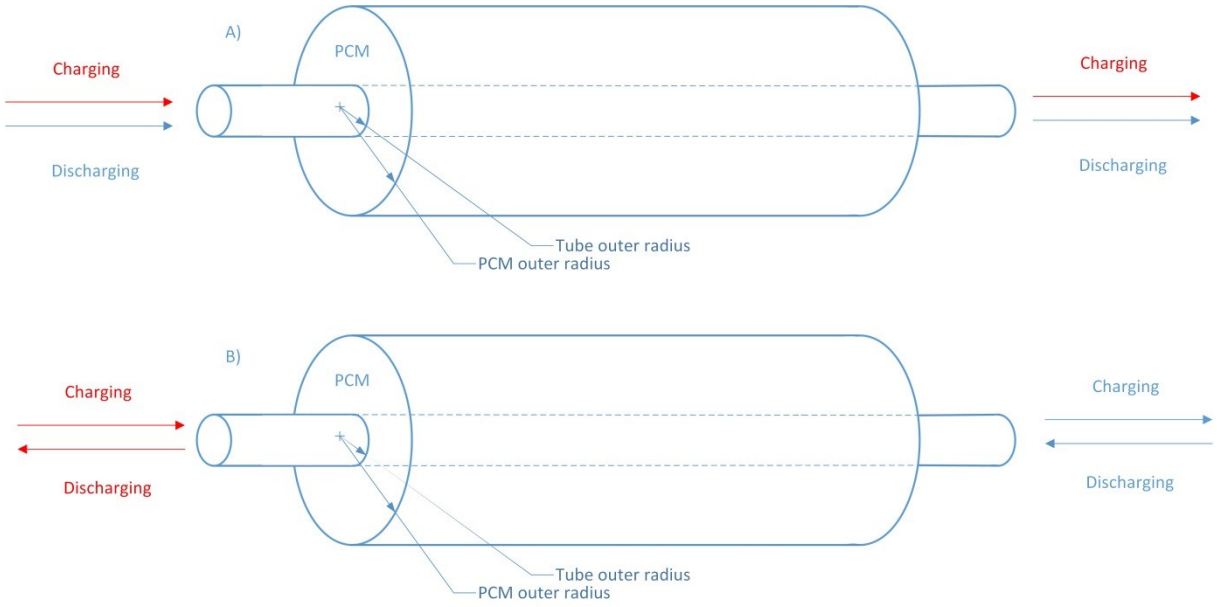

Figure 14: A) Parallel HTF flow B) Counter-current HTF flow

A double-pipe heat exchanger consists of two concentric pipes of different diameters which are shown in Figure 15. One fluid in a double-pipe heat exchanger flows through the smaller pipe while the other fluid flows through the annular space between the two pipes. Double-pipe is subdivided also in two groups parallel-flow and counter-current.

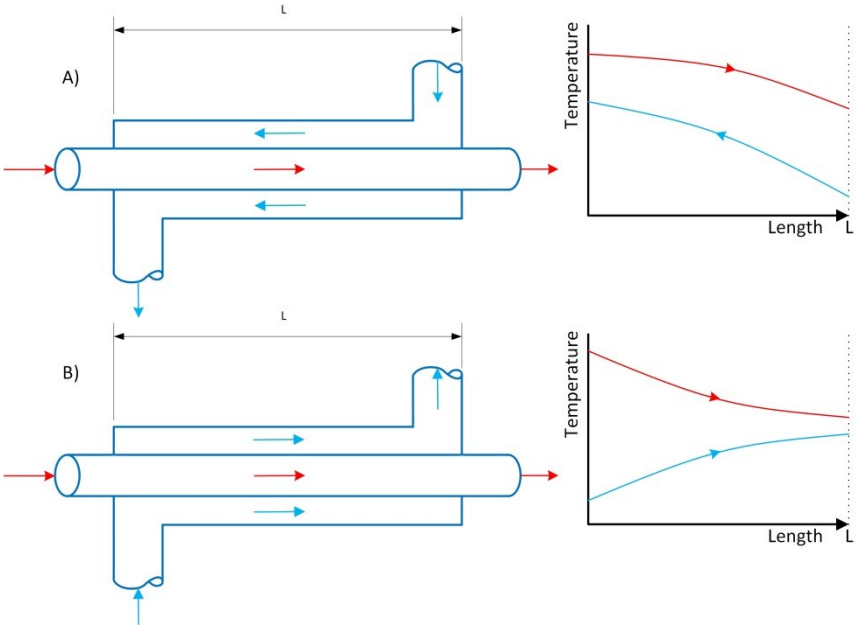

Figure 15: Double-pipe heat exchanger A) counter-current B) parallel-flow

4 Design of Heat Storage

Several facts have to be considered when deciding on the type and the design of any thermal storage system. A key issue in the design of a TES system is its thermal capacity. However, selection of the appropriate system depends on many cost-benefit considerations, technical, and environmental criteria. The cost of the TES systems depends mainly on the following items: the storage material itself, the heat exchanger for charging and discharging the system, and on the cost of the space and enclosure for the TES (commonly of its tank(s)). All the following technical and technological criteria have to be considered when deciding on the type and design of thermal storage. [32]

From the technical point of view, the most important requirements are:

- High energy density in the storage material (storage capacity).
- Good heat transfer between HTF and storage medium (efficiency).
- Mechanical and chemical stability of storage material (must support several charging/discharging cycles).
- Compatibility between HTF, heat exchanger, and storage medium (safety).
- Complete reversibility of a numerous charging/ discharging cycles (lifetime durability).
- Low thermal losses.
- Easy controllability.

From the point of view of design technology the most important requirement criteria are:

- Operation strategy.
- Maximum load.
- Temperature and specific enthalpy drop in load.
- Integration into the power plant.

4.1 Storage Classification

High temperature storage concepts in power plants can be classified as active or passive systems. An active storage system is mainly characterized by forced convection heat transfer into the storage material. The storage medium itself circulates through a heat exchanger. This system uses one or two tanks as the storage for media. Active systems are subdivided into direct and indirect systems. In a direct system, the heat transfer fluid serves

also as the storage medium. In an indirect system, a second medium is used for storing the heat.

Passive storage systems are generally dual medium storage systems. The HTF in them passes through the storage only for charging and discharging of the solid material. The HTF carries energy received from the energy source to the storage medium during charging, and receives energy from the storage when discharging. The main disadvantage of this kind of system is the HTF temperature which decreases during discharging as the storage material cools down. Other unfavorable problem is that the heat transfer is quite low, and there is usually no direct contact between the HTF and the storage material. [12]

4.2 Number of Transfer Units Design Method

Number of transfer units (NTU) is a method which was developed to simplify the calculations of heat exchanger design (Figure 16) problems. The method is applicable to shell and tube heat exchangers of any given tube size and spacing length. The method accounts for time-dependent flow-rate and inlet temperature of the tube side fluid. The storage code returns the outlet temperature of the fluid, the instantaneous heat transfer rate, and effectiveness. HTF enters the tube at a temperature which is specified. It delivers or takes heat to/from the latent heat storage material. This heat flow causes the storage material to begin melt or solidify on the outside of the tube. It also causes the temperature of HTF to rise or decrease. An analytical solution to this problem would be very desirable. Such solution would help in understanding the interplay of various parameters and in making efficient calculations without having to resort to long numerical simulations.

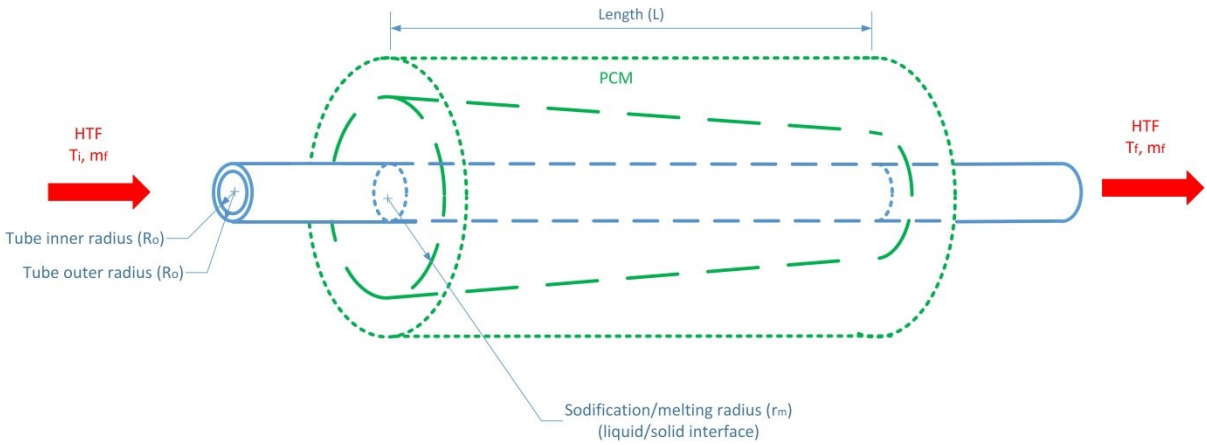

Figure 16: Tube heat exchanger design: tube, PCM and solidification/melting radius

The NTU method is also used in the model developed by Shamsundar et al. [14]. Their model is the base of the TES model proposed by me. Modifications made to the source model are due to the luck of consideration of the thermal resistance of the tube. To obtain a solution a few simplifying assumptions are made:

- The heat storage substance is completely liquid when the heat recovery phase begins in the discharging process and completely solid in the charging process.
- The initial superheat/supercool in the liquid/solid is negligible compared to the latent heat of fusion.
- Melting/freezing takes place with a smooth interface between solid and liquid and vice versa, with cavities in the frozen zone or the tube itself.
- The tube has a length much longer than its diameter. Axial conduction in the frozen layer and in the HTF can be ignored.
- The melting/freezing rate is slow enough that the temperature distribution in the melted/freeze zone can be approximated as being quasi-steady.
- The residence time of the HTF in the tube is very small compared to the typical melting time.
- The convective heat transfer in the tube is fully developed and uniform over the tube.
- The flow rate of the HTF is assumed to be steady.

4.2.1 Heat Transfer

Heat transfer (Q) is classified into various mechanisms, such as thermal conduction, thermal convection, thermal radiation, and transfer of energy by phase changes. It is the direct microscopic exchange of kinetic energy of particles through the boundary between two systems. When an object is at a different temperature from another body or its surroundings, heat flows so that the body and the surroundings reach the same temperature. At this point they are in thermal equilibrium. Such spontaneous heat transfer always occurs from a region of high temperature to another region of lower temperature.

In solid wall the variation of temperature with the time and position is represented by the one dimensional Fourier equation:

$$\frac{\partial T}{\partial \mathrm{t}} = kA\frac{\partial^2 T}{\partial x^2} \qquad 3 - 1$$

where T is the temperature, t is the time, k is the thermal conductivity, A is the area of surface, and, finally, x is the position.

Only the steady state, no change with the time at any point within the medium, condition will be of concern, in which case the partial integral of previous equation 3 - 1.

The rate of heat conduction through a medium in a specified direction (x-direction) is expressed by Fourier's law of heat conduction for one-dimensional heat conduction as:

$$Q = -kA\frac{dT}{dx} \qquad 3 - 3$$

Heat is conducted in the direction of decreasing temperature, and thus the temperature gradient is negative when heat is conducted in the positive x-direction.

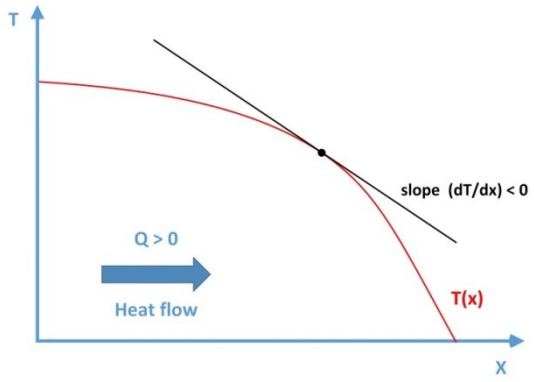

Figure 17: Fourier's law of heat conduction - temperature gradient

The heat flows from the inside to the outside the area changes constantly. Accordingly the equivalent of equation 3 - 3 becomes, for a cylinder of length (L):

$$Q = -2\pi rkL\frac{dT}{dr} \qquad 3 - 4$$

of which the integral is:

$$Q = 2\pi kL\frac{T_1 - T_2}{\ln\left(\frac{r_2}{r_1}\right)} \qquad 3 - 5$$

Heat transfer in PCMs. Because the tube has a length much longer than its diameter, the axial conduction in the frozen/melted layer and in the HTF can be ignored. The heat

conduction in the solid is purely radial. The heat transfer rate per unit length is given by the following formula:

$$Q = 2\pi k_{PCM} \frac{T_m - T_w}{\ln\left(\frac{r_m}{R_0}\right)} \qquad 3 - 6$$

where Q is the heat of conduction per unit length in the PCM, k_{PCM} represents the thermal conductivity of the PCM, T_m is the melting point of the PCM, T_w represents the wall temperature of the tube exchanger, r_m is the radius of the solidified PCM, the function of time and X, and finally, R_o is the outer radius of the tube exchanger.

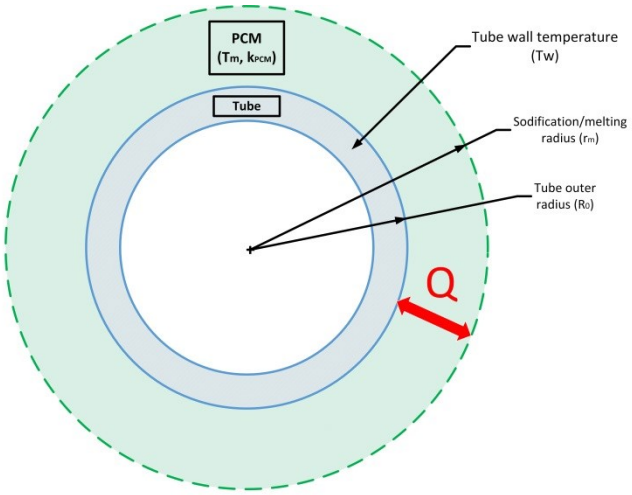

Figure 18: Heat transfer in PCM

Convection heat transfer between a surface and fluid. Convection heat transfer (Q) between a surface and fluid is governed by the Newton‘s law of cooling. It is the transfer of heat from wall tube to the movement of HTF. The heat must flow into HTF by convention. The rate of loss of heat by a body is directly proportional to the temperature difference between HTF and the wall of the tube. The greater the difference in temperature between the system and surrounding is, the more quickly the body temperature changes. The convection heat transfer can be calculated by the following formula:

$$Q = 2\pi R_i \frac{T_w - T_F}{\frac{1}{h} + \frac{R_i}{k_w} \ln\left(\frac{R_0}{R_i}\right)} \qquad 3 - 7$$

where k_w stands for the tube wall thermal conductivity, T_F represents the outflow temperature, T_w is the wall temperature of the tube exchanger, R_i is the tube inner radius, R_o represents the tube outer radius, and h stands for the convection heat transfer coefficient.

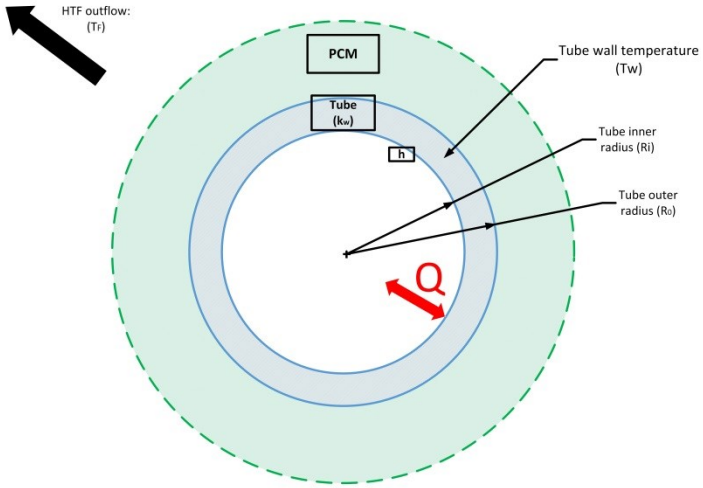

Figure 19: Convection heat transfer between a surface and fluid

Energy release from/to PCM. This released energy (Q) is heat transfer rate lost/increase of the PCM. This heat is equal to the heat transfer gained in the wall tube. The heat reduces/increases the temperature of the HTF. Energy released from PCM is given by the following equation:

$$Q = \frac{\partial(\pi(r_m^2 - R_0^2)\delta_{PCM}H)}{\partial t} \qquad 3 - 8$$

where r_m is the radius of the solidified PCM, function of time and position, R_o is outer radius of the tube exchanger, H is the latent heat of fusion, ρ_{PCM} is the density of the material, and finally, t is time.

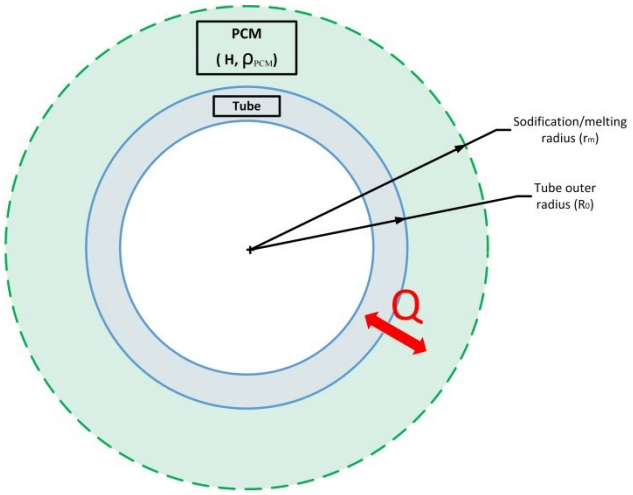

Figure 20: Energy release from/to PCM

Temperature of the HTF. The temperature of HTF is caused to increase/decrease by the heat conduction of PCM. It can be expressed by following equation:

$$Q = m_f C_p \frac{\partial T_F}{\partial x} \qquad 3 - 9$$

where Q is the heat transfer rate in the HTF, m_f is the mass flow rate, C_p is the specific heat capacity of HTF, $\frac{\partial T_f}{\partial X}$ is the change of HTF temperature as a function of axial distance along the tube heat exchanger.

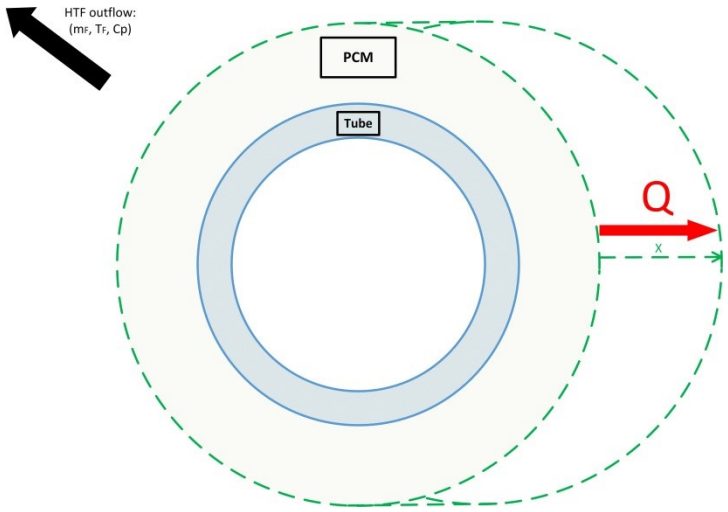

Figure 21: Temperature of the HTF

4.2.2 Nondimensional Variables

Nondimensional variables can recover characteristic properties of a system. The basic principal is the removal of units from an equation involving physical quantities by a suitable substitution of variables. It is especially useful for systems that can be described by differential equations.

Frozen fraction. The most important nondimensional variable for calculation of the effectiveness of the heat transfer between HTF and PCM is the frozen fraction (*F*). It is described by the following equation:

$$F = \frac{r_m^2}{R_0^2} - 1 \qquad 3 - 10$$

where r_m is the solidification/melting radius and Ro is the outer radius of the tube. The area of the frozen/melted region in the radial plane is divided by the area of cross-section of the tube.

Fourier number. The Fourier number (F_N) is a dimensionless number used in the study of unsteady-state heat transfer. It is equal to the product of the thermal conductivity and time, divided by the product of the density, the specific heat at a constant pressure, and the distance from the midpoint of the body through which heat is passing to the surface.

$$F_N = \frac{k_m}{R_0^2 C_p \rho} \cdot t \qquad 3 - 11$$

Stefan number. The Stefan number (*Ste)* is used for calculations of the rate of phase change. It is defined as the ratio of sensible heat to latent heat. Its solution represents the properties of the medium for each phase which are infinitesimally thin.

$$Ste = \frac{c_p(T_m - T_f)}{H} \qquad 3 - 12$$

Nondimensional time. The properties of solid and liquid phase of PCM remain constant with respect to temperature. The nondimensional time variable (τ) can be calculated as a product of Fourier and Stefan numbers:

$$\tau = \frac{k_m}{R_0^2 H \rho} \int_0^t \left(T_m - T_f\right) dt \qquad 3 - 13$$

Nondimensional variables proposed by Shamsundar [14]. To simplify more difficult calculations Shamsundar proposes yet another three important variables:

- *Nondimensional heat flow*. The nondimensional heat flow ($\dot{Q}$) which is defined as follows:

$$\dot{Q} = \frac{Q}{2\pi R_i h\left(T_m - T_f\right)} \qquad 3 - 14$$

- *Number of transfer units*. The number of transfer units (*NTU)*is defined as follows:

$$NTU = \frac{2\pi R_i x U}{m_f C_p} \qquad 3 - 15$$

- Heat exchanger effectiveness. The heat exchanger effectiveness (ε) is defined as follows:

$$\varepsilon = \frac{T_f - T_i}{T_m - T_i} = 1 - \frac{F}{F_0} \qquad 3 - 16$$

where F_0 is frozen fraction at the beginning of the tube (x=0).

Biot number. Biot number determines whether or not the temperatures inside the material will vary significantly in space from a thermal gradient applied to its surface. Biot number determines how fast heat transfers through the material. In calculations the number is set as a variable α which is half of reversed value of Biot number.

$$Bi = \frac{hR_i}{k}$$

$$\alpha_{PCM} = \frac{k_{PCM}}{2hR_i} \qquad \alpha_w = \frac{k_w}{2hR_i} \qquad 3 - 17$$

where h is convention heat transfer coefficient of HTF and k_{PCM} is the conductivity of the of the used material.

4.3 Results of Number of Transfer Unit Method

This chapter brings only the results of calculations where certain modifications have been done to the model designed by Shamsundar et al. The step by step description on how the final equations have been achieved is brought in Appendix B. I decided to use Matlab® for the calculations. Matlab® is a numerical computing environment, which uses scripts. An *.m file, or script file, is a simple text file where commands are placed. Calculation of the NTU method is performed by Matlab® with file "*NTU_Method.m*" and it is stated in Appendix D. Also, additional two auxiliary functions appear in the appendix attachments. These are "*NTU_Determination_F.m*" in Appendix E and "*NTU_Determination_e.m*" in Appendix F.

4.3.1 Process of Calculation

For the calculation of the heat transfer the following steps have to be performed. For the specific of HTF inlet temperature T_0, τ is calculated as a function of time from the equation:

$$\tau = \frac{k_m(T_m - T_f)t}{R_0^2 H \rho} \qquad 3 - 18$$

NTU values of each position, which need to be investigated in the analysis of the system, are calculated from the definition of 3 - 15. Time and position variables are calculated for each specific system.

In the following equation variables *α, τ, k* (thermal conductivity) and *R* (radius ratio) are known, the only unknown variable is F_0 which is calculated as a root of the equation. The root is calculated by m-function "*NTU_Determination_F.m*".

$$0 = \frac{1}{4}\left((1 + F_0)\ln(1 + F_0) - F_0\right) + \frac{F_0}{\alpha_{PCM}} + \frac{F_0}{2\alpha_w \alpha_{PCM}}\ln(R) - \tau \qquad 3 - 19$$

Next step in the calculation process is to determine the effectiveness which is the function of NTU and F_0. Effectiveness is determined as a root from the following equation:

$$0 = -NTU_x + \ln(1 - \varepsilon) + \frac{1}{2\alpha_w}\ln(R)\ln(1 - \varepsilon) + \frac{1}{4\alpha_{PCM}}(G(F_0) - G(F_0 - \varepsilon F_0)) \qquad 3 - 20$$

The root of the effectiveness is calculated by Matlab® m-function "*NTU_Determination_e.m*". The temperature of each position of NTU distance is calculated from the following equation:

$$T_F = \varepsilon\,(T_m - T_i) + T_i \qquad 3 - 21$$

4.3.2 Results of Number of Transfer Unit Method – Discharging Process

Corresponding values of the time and the NTU_X variables by their definitions are calculated using definitions 3 - 18 and 3 - 15. Then the root of equation 3 - 19 for F_0 is found. By using this F_0 in equation 3 - 20 we calculate instantaneous value of the effectiveness. Then the instantaneous fluid outlet temperature from the definition of the effectiveness is calculated. All numerical calculations for charging process are expressed in Appendix G. As a PCM KNO_3-$NaNO_3$ (50-50) and as a HTF water was chosen. Next parameters are as follows: length of the tube is 2000 mm, inner radius is 17 mm, and outer radius is 20 mm.

In the discharging process energy is transferred from PCM to HTF. The PCM changes phase from liquid to solid (solidification process). Inlet temperature was set at 190°C. At time t=0h the outlet temperature of HTF was 218.084°C and after 12 hours outlet temperature decreased to 214.920°C.

Temperature variation depending on the length of the tube is shown in Figure 22 as well as seen in Figure 24 where effectiveness variation represented is. In this image temperatures in times from 0h to 12h are shown. During the discharge process at time t = 0h the temperature of HTF rises faster than at t = 12h.

Figure 23 represents solidification process during 12 hours of the discharging process. At the beginning of the tube the solidification radius is greater than in the end of the tube. Small differences in solidification radius are caused by a poor conductivity of the PCM. The proposed ideal design should be based on proper distance between the tubes so that the PCM during charging/discharging process is completely charged/discharged. Each system should have its unique design to achieve best results for the particular application.

Figure 25 represents the outflow temperature during 12 hours of discharging process at different inlet temperatures. The more the input temperature approaches the melting temperature of the PCM (220°C) the smaller the temperature difference after 12 hours is. If the inlet temperature is 210°C, than, after 12 hours of the discharging it is almost the same as the output temperature at the beginning at t=0. However, if the inlet temperature was only 110°C the outlet temperature dropped from 213°C at t = 0 to 168°C at t=12h. The more the inlet temperature approaches the melting temperature the lower the effect of the discharge process is.

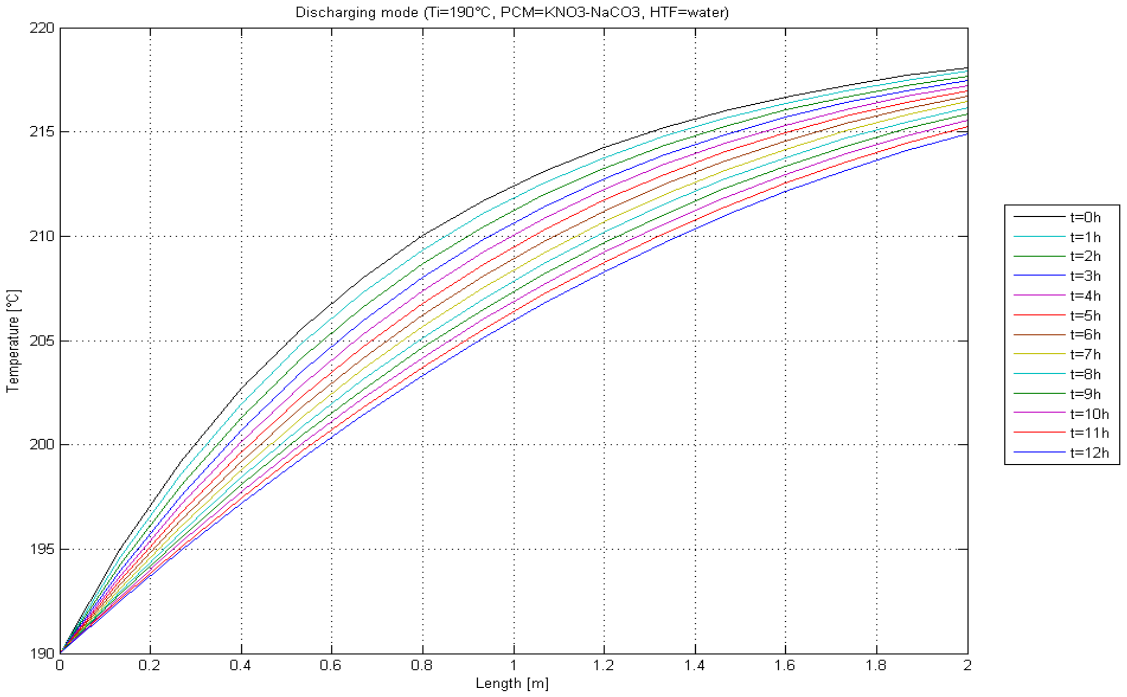

Figure 22: Discharging mode; inflow temperature 190°C during the 12 hours of discharging LHS system

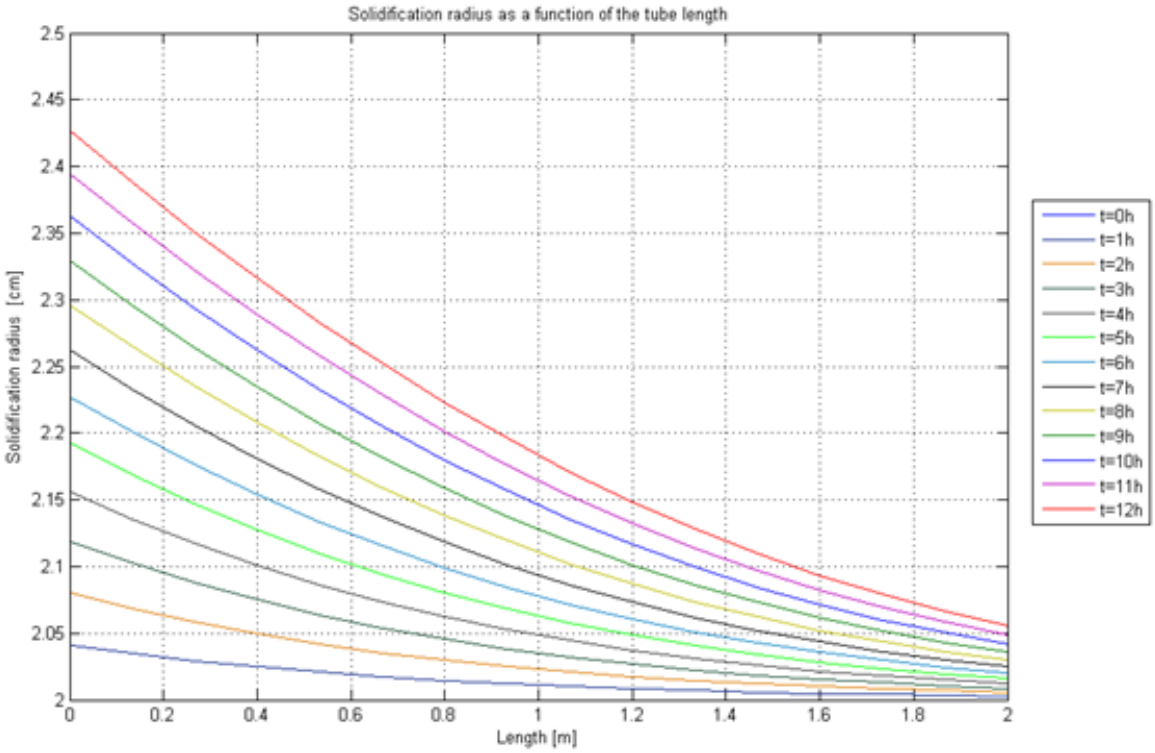

Figure 23: Discharging mode; solidification radius in certain positions

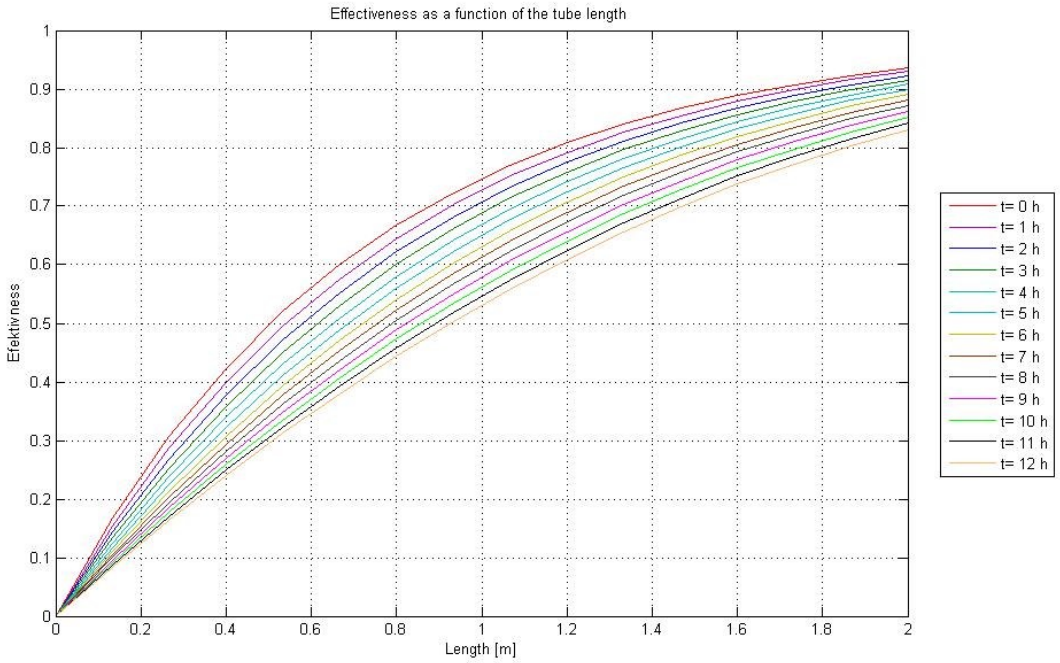

Figure 24: Discharging mode; effectiveness in certain positions

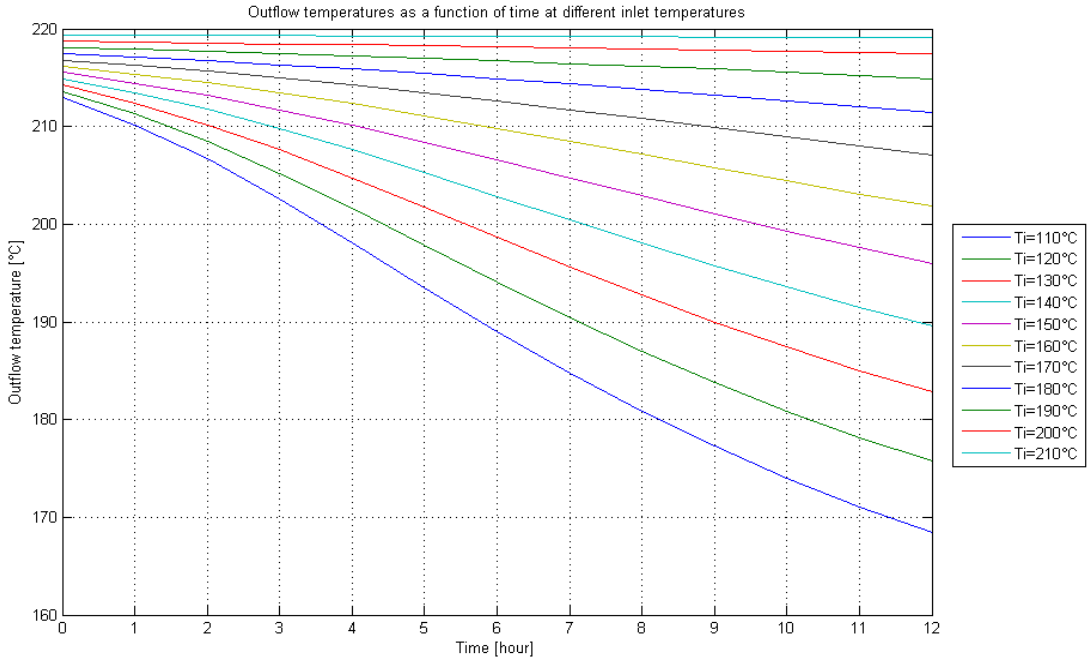

Figure 25: Discharging mode; outlet temperature as a function of time at different inlet temperatures

4.3.3 Results of Number of Transfer Unit Method – Charging Process

The calculation procedure for the charging process is the same as for the discharging process which is described in the previous chapter. Also as in the discharge process, the same PCM, HTF, and tube parameters are used. Energy transfers from HTF to PCM in the charge process. PCM changes phase from solid to liquid (melting). The inlet temperature of HTF is higher than the outlet temperature. All numerical calculations are in Appendix H.

The inlet temperature was set at 250°C as shown in Figure 26. At time t=0h the outlet temperature of HTF was 221.916°C and after 12 hours the outlet temperature increased to 225.920°C.

Temperature variation depending on the length of the tube is shown in Figure 26 as well as seen in Figure 28 where effectiveness variation represented is. In this image a temperature in times from 0h to 12h is shown. During the charging process at time t=0h the temperature HTF declined faster than at t=12h.

Figure 27 represents the melting process during 12 hours of charging. At the beginning of the tube the melting radius is greater than in the end of the tube. Small differences in melting radius are caused by a poor conductivity of the PCM.

Figure 29 represents the outflow temperatures during 12 hours of the charging process at different inlet temperatures. The more the input temperature approaches the melting temperature of the PCM (220°C) the smaller the temperature difference after 12 hours is. If the inlet temperature is 230°C, than, after 12 hours of the discharging it is almost the same as the output temperature at the beginning at t=0h. However, if the inlet temperature was 320°C the outlet temperature increased from 226°C at t=0h to 264°C at t=12h. The more the inlet temperature approaches the melting temperature the lower the effect of the discharge process is.

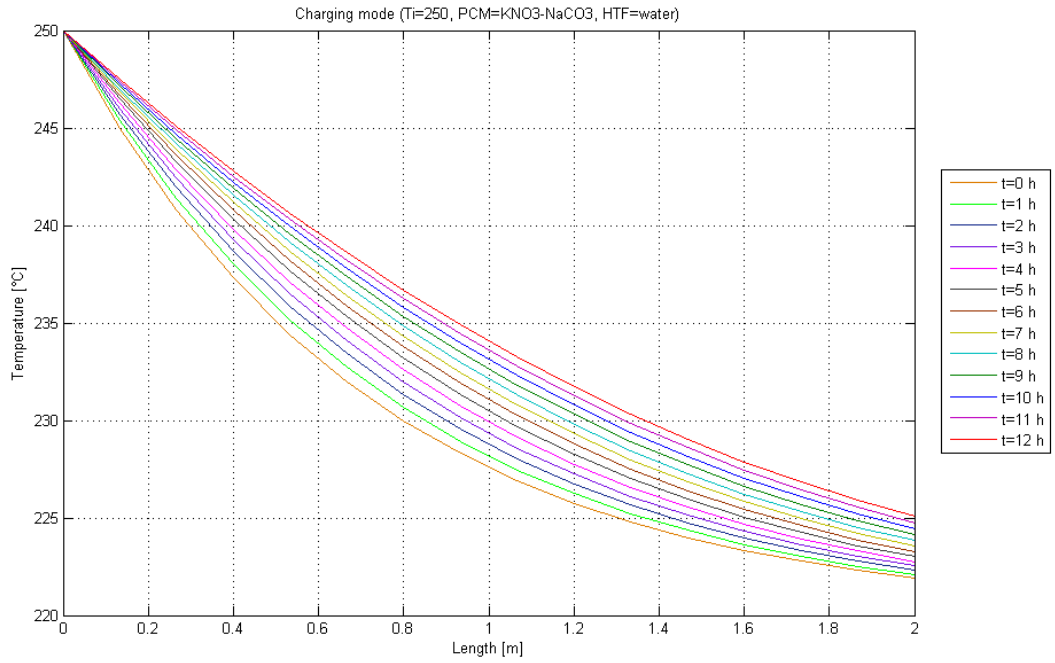

Figure 26: Charging mode; inflow temperature 250°C during the 12 hours of charging LHS system

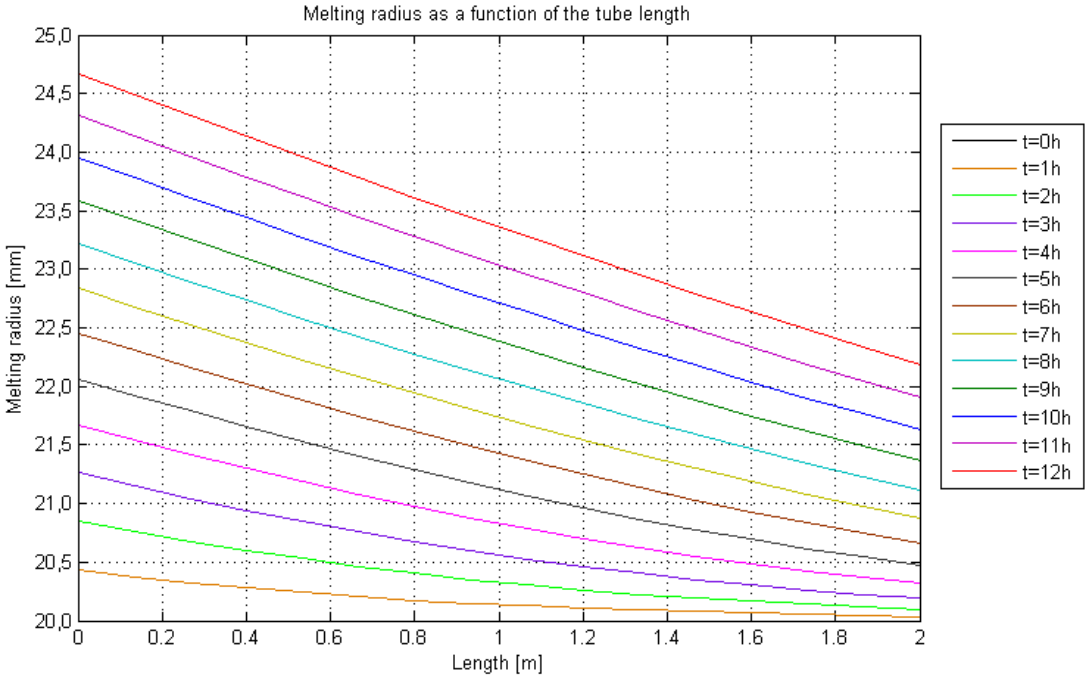

Figure 27: Charging mode; melting radius in certain positions

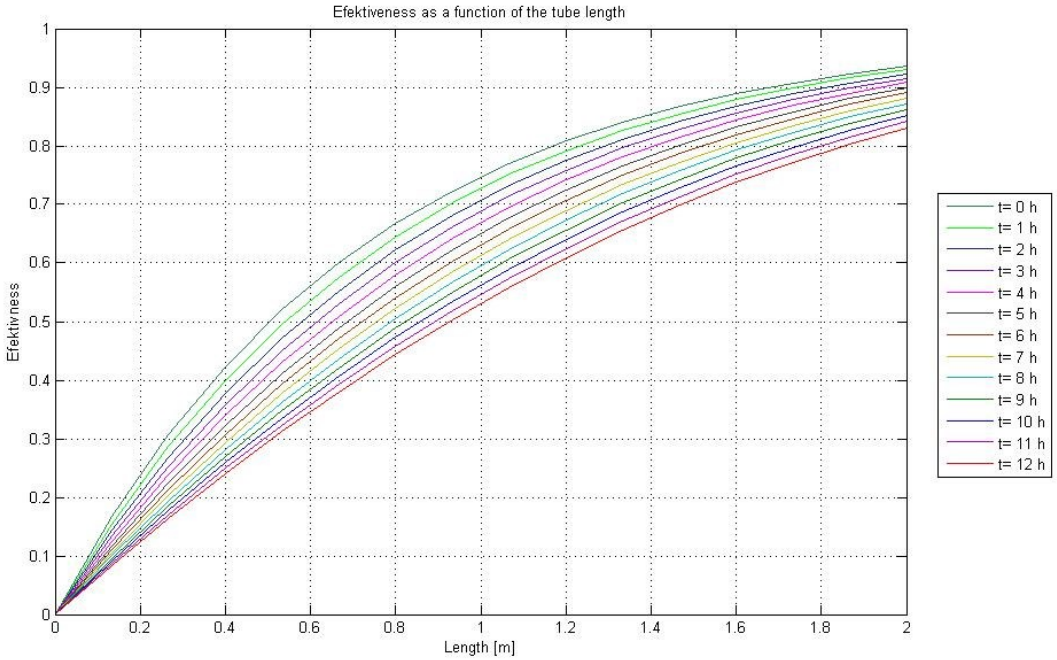

Figure 28: Charging mode; Effectiveness in certain positions

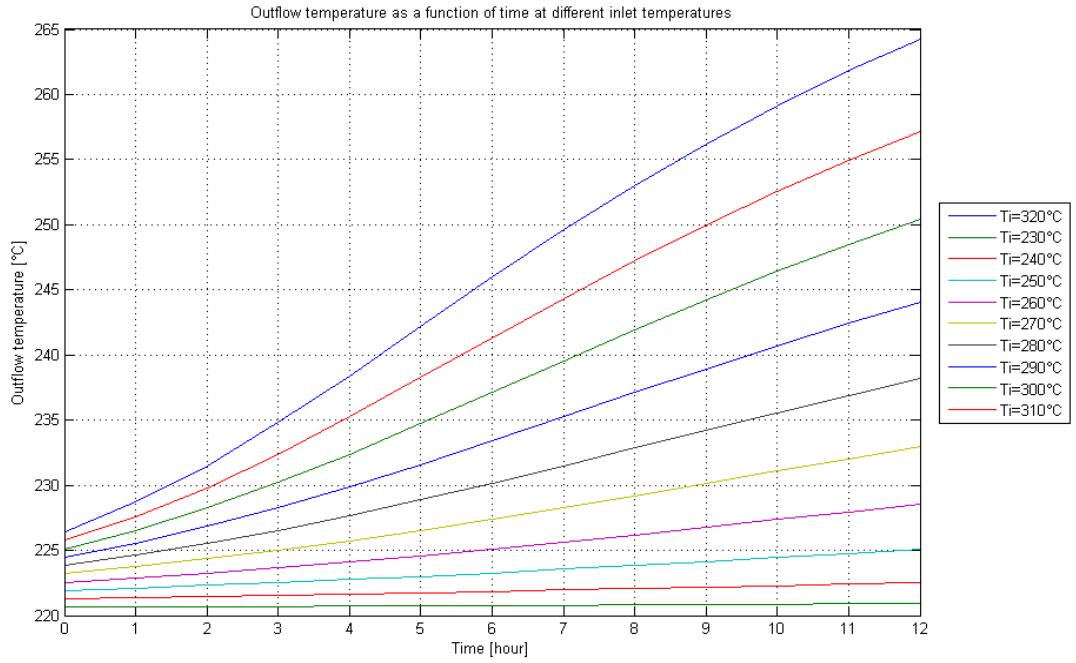

Figure 29: Charging mode; outlet temperature as a function of time at different inlet temperatures

4.3.4 Results of Number of Transfer Unit Method – Influence of Some Parameters

This chapter will described the influence of some parameters after 2 hours of discharging process to the resulting temperatures. The assumptions mentioned in chapter 3.2 effect the results. The influences of thermal conductivity, specific heat of PCM, and melting point on the output temperature are described here. All other system parameters always remain constant except for the particular impact of output parameters investigated.

Thermal conductivity. Thermal conductivity is the property of the particular material to conduct heat. Heat transfer occurs at a higher rate across materials of high thermal conductivity than across materials of low thermal conductivity. Thermal conductivity of KNO_3-$NaNO_3$ (50-50) is 0.56 $Wm^{-1}K^{-1}$. By reducing the heat conductivity to k=0.01 $Wm^{-1}K^{-1}$ the HTF temperature has increased. Similarly, if we increase the heat conductivity to k=1 $Wm^{-1}K^{-1}$ HTF the temperature will decrease, how is seen in the Figure 30.

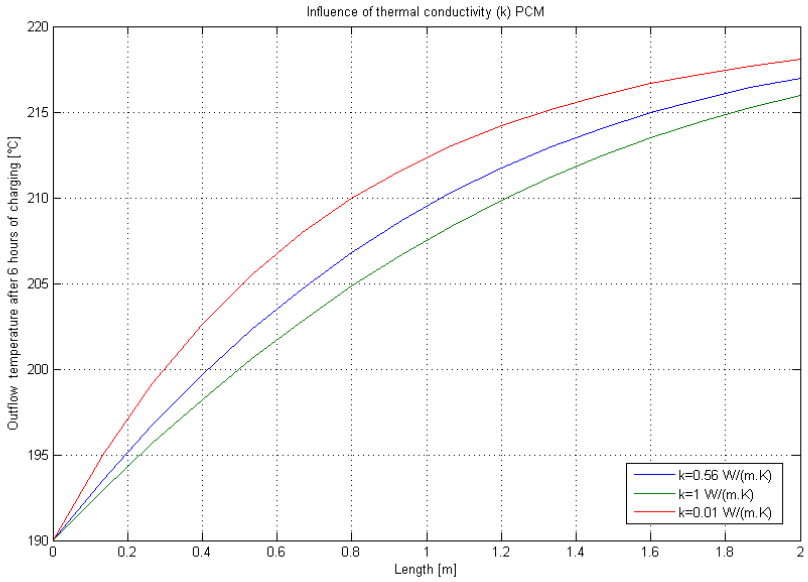

Figure 30: Influence of thermal conductivity

Specific heat of PCM. Specific heat is the heat capacity per unit mass of a particular material. It is the ratio of the amount of heat energy transferred to a PCM resulting in increase in temperature of the PCM. Specific heat of KNO_3-$NaNO_3$ (50-50) is C_p=1350 $J.kg^{-1}K^{-1}$. If the specific heat increases by 250 $J.kg^{-1}K^{-1}$ to C_p = 1600 $J.kg^{-1}K^{-1}$ the difference to the original value is small. But, if specific heat of the 250 $J.kg^{-1}K^{-1}$ is decreased,

the temperature in the HTF will rise even faster, how is seen in the Figure 31. A higher temperature than the original value of the specific heat will be at the output of the tube.

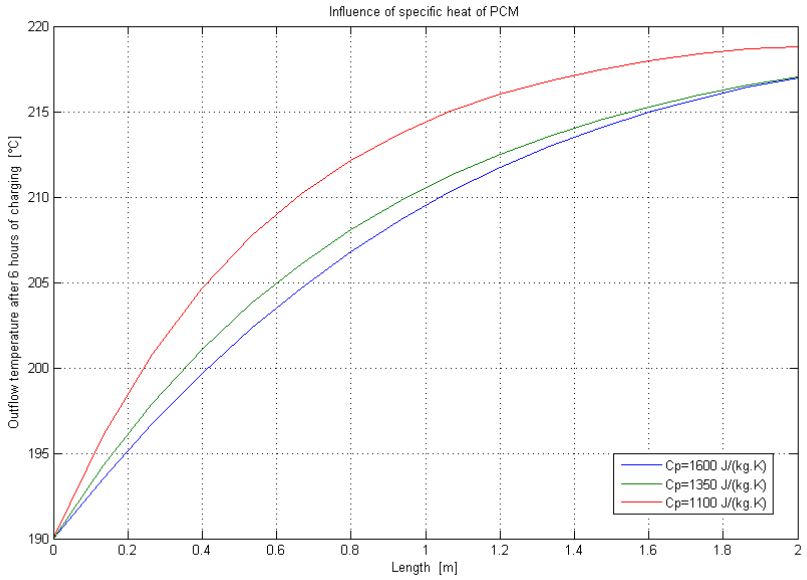

Figure 31: Influence of specific heat

Melting point. The melting point of a solid PCM is the temperature at which it changes state from solid to liquid at atmospheric pressure. Melting point has the biggest influence on the temperature of HTF. Melting point of KNO_3-$NaNO_3$ (50-50) is 220°C. At time t = 0 during the discharging process, when the entire volume of the PCM is in the liquid state, the temperature of PCM has major effect on the temperature of outflowing HTF from the tube.

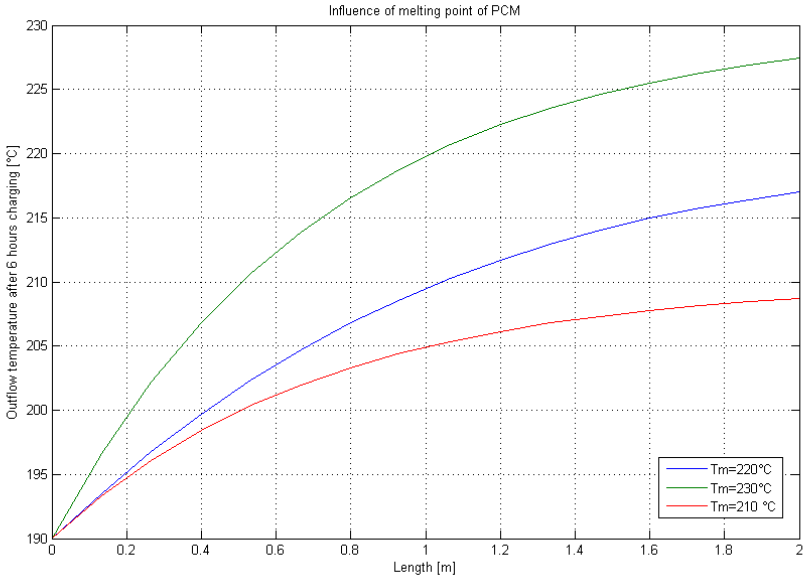

Figure 32: Influence of melting point

4.4 Numerical Methods

The difficulties of predicting the behavior of LHS systems is very difficult. The main problems include primarily non-linear nature at moving interface and the two phases have different thermo-physical properties. This problem was described in 1989 by Stefan [38]. The different classes of solution available for Stefan problem are analytical and numerical. Many approximate analytical techniques such as the heat balance integral, variation technique, isothermal migration, source and sink method and periodic solution were developed. A common drawback of these approximate techniques is limited to one-dimensional analysis and they become complicated when multidimensional solution is required. Numerical methods such as finite difference and finite element are the most powerful in solving the Stefan problem. Using the time variant mesh approach offers good accuracy but is limited. The fixed mesh approach is much simpler in practical application.

The method to solve the moving boundary problem is enthalpy formulation. The enthalpy method is used in a particular way so that the only unknown variable is the temperature of the phase change material and the solidification/melting occurs at a uniform temperature. Enthalpy method treats the enthalpy as a temperature dependent variable and constructs the latent heat flow through the volume integration with the use of the enthalpy of the system.

4.5 Finite Difference Method

Numerical model is another way to investigate the behavior of LHS systems. Numerical model of LHS is expressed by Partial differential equation (PDE). To solve the numerical model of TES is necessary to solve PDE. PDE expresses the relationship between the function of several variables and its partial derivatives. Partial differential equations and their systems are mathematical models of many technical problems. For some simple tasks you can find the exact solution in the form of infinite series. However the vast majority of tasks are able to solve only approximately or numerically. Stationary tasks are time independent, non-stationary tasks are time dependent. The unambiguous solution is not enough to determine the actual PDE equations, it is also necessary to enter a non-stationary boundary conditions and the task initial conditions. Fundamental to the development of a numerical method is the idea of discretization.

An analytical solution to a partial differential equation gives us the value as a function of the independent variables. The numerical solution, on the other hand, aims to provide us with values of at a discrete number of points in the domain. The conversion of a differential equation into a set of discrete algebraic equations requires the discretization of space. This is accomplished by means of mesh generation. Mesh generation divides the domain of interest into elements or cells, and associates with each element or cell one or more discrete values. It is these values we wish to compute.

Several numerical methods are available for converting equations to a set of discrete algebraic equations as these methods are: Finite element method, Finite volume method and Finite difference method. For numerical calculations for the TES model has been chosen the Finite element method because of this method is easy to understand and to implement [37]. Finite difference method is the method, which approximates the derivatives in the governing differential equation using Taylor series expansions. The derivatives of the partial differential equation are approximated by linear combinations of function values at the structured grid points. Taylor series approximates the value of the function that has a derivative at a given point, using a polynomial whose coefficients depend on the derivative of the function at this point.

The simplest way to approximate the numerical derivatives is linear interpolation, which uses past, current and future data shown in Figure 33.

Forward difference. Consider a linear interpolation between the current data value (x_0, u_0) and the future data value (x_{+1}, u_{+1}). The slope of the secant line between these two points approximates the derivative by the forward difference:

$$\frac{\partial u}{\partial x} \approx \frac{u_{i+1} - u_i}{\Delta x} = \frac{\phi_3 - \phi_2}{\Delta x} \qquad 3 - 22$$

Forward difference predicts the value of u_{i+1} from the derivative $u'(x_0)$ and from the value u_0. If the data values are equally spaced with the step size Δx, the truncation error of the forward difference approximation has the order of $O(\Delta x)$.

Backward difference. Consider a linear interpolation between the current data value and the past data value (x_{-1},u_{-1}). The slope of the secant line between these two points approximates the derivative by the backward difference:

$$\frac{\partial u}{\partial x} \approx \frac{u_i - u_{i-1}}{\Delta x} = \frac{\phi_2 - \phi_1}{\Delta x} \qquad 3 - 23$$

Backward differences are useful for approximating the derivatives if data in the future are not yet available. If the data values are equally spaced with the step size Δx, the truncation error of the backward difference approximation has the order of $O(\Delta x)$.

Central difference. Finally, consider a linear interpolation between the past data value and the future data value. The slope of the secant line between these two points approximates the derivative by the central difference:

$$\frac{\partial u}{\partial x} \approx \frac{u_{i+1} - u_{i-1}}{2\Delta x} = \frac{\phi_3 - \phi_1}{2\Delta x} \qquad 3 - 24$$

If the data values are equally spaced, the central difference is an average of the forward and backward differences. The truncation error of the central difference approximation is order of $O(\Delta x^2)$, where Δx is the step size. It is clear that the central difference gives a much more accurate approximation of the derivative compared to the forward and backward differences. Central differences are useful in solving partial differential equations.

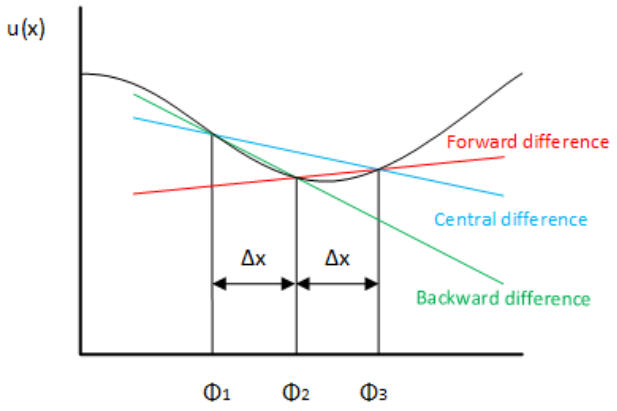

Figure 33: Different geometric interpretations of the first-order finite difference approximation

4.6 Numerical Model on Thermal Energy Storage

In the model described in section 3.2 have been used to simplify the calculations many assumptions and were made a weak solution for given problem. These assumptions simplify the laws of physics acting on the system. It is crucial to have a clear picture of exactly which phenomena are taken into account and which are not, because a model can at best be as good as its underlying physical assumptions. Because of these assumptions, it was decided to create a new model describing the same system but much more in-depth physical properties. However, all completely assumptions cannot be avoided. In this numerical model described in this section, based on studies of *Y.B. Tao at al.* [28] and *H. A. Adine et al.* [33] are taken into account the following assumptions are adopted:

- The axial heat conduction and viscous dissipation in the HTF is negligible. The flow of HTF is treated as one dimensional fluid flow. The phase change material region is treated as an axisymmetric model.
- The effect of natural convection of PCM during melting is negligible.
- Constant pressure
- Physical aspects of the tube are negligible.

For the purpose of this work let the physical aspects of the tube were neglected. However, although many authors in the literature survey supposed so, the inner and outer of the tube's material properties in the heat transfer analysis between materials have been proved are not negligible in the dynamics. In governing of the equations another dynamic equation for the tube should be added where the capacity carries major influence on time constant. This capacity has the dominant influence in transient analysis.

The effect of temperature change to heat capacity, thermal conductivity, density in isothermal phase change problem involves sudden changes. *F. Samara et al.* [36] introduce method Modified Volume Force which investigate material properties changes in PCM. Modified Volume Force is robust and uses smoother functions. This method goes deeper in the mathematical formulation of the functions required to account for phase change, but still represents the PCM as a liquid regardless of its temperature. Gaussian function, D(T), is used to account for the latent heat over a melting temperature range ΔT. This function has a value of zero everywhere except over the interval $(T_m - \Delta T)$ to $(T_m + \Delta T)$ centered at T_m. Most importantly, its integral is equal to 1, so by multiplying D(T) by H, the energy balance is ensure for a simulation that starts at a temperature lower than $(T_m - \Delta T)$ and ends above

(T_m+ΔT). Functions D(T) and B(T) are auxiliary functions to determine physical aspect of the PCM such as density, thermal conductivity and capacity. The D(T) function is presented:

$$D(T) = \frac{e^{\frac{-T(T-T_m)^2}{\Delta T^2}}}{\sqrt{\pi \Delta T^2}} \qquad 3 - 25$$

To account for the change in specific heat between the solid and the liquid phase of the PCM, a simple piecewise function B(T) is created as follows:

$$B(T) = \begin{cases} 0\,; & T < (T_m - \Delta T) \\ \dfrac{T - T_m + \Delta T}{2\Delta T}\,; & (T_m - \Delta T) < T < (T_m + \Delta T) \\ 1\,; & T > (T_m + \Delta T) \end{cases} \qquad 3 - 26$$

B(T) is equal to zero for temperature lower than the melting point, and is equal to 1 after melting. It increases linearly from 0 to 1 over the melting temperature range ΔT as show in Figure 34. The following equations then define the density, conductivity and capacity of the PCM:

$$\rho(T) = \rho_s + (\rho_l - \rho_s)\, B(T) \qquad 3 - 27$$

$$k(T) = k_s + (k_l - k_s)\, B(T) \qquad 3 - 28$$

$$C_p(T) = C_{p_s} + \left(C_{p_l} - C_{p_s}\right) B(T) + HD(T) \qquad 3 - 29$$

where ρ is density, k is thermal conductivity, Cp is specific heat capacity and finally H is latent heat. Subscript represented by l is for liquid and s for solid phase. [35]

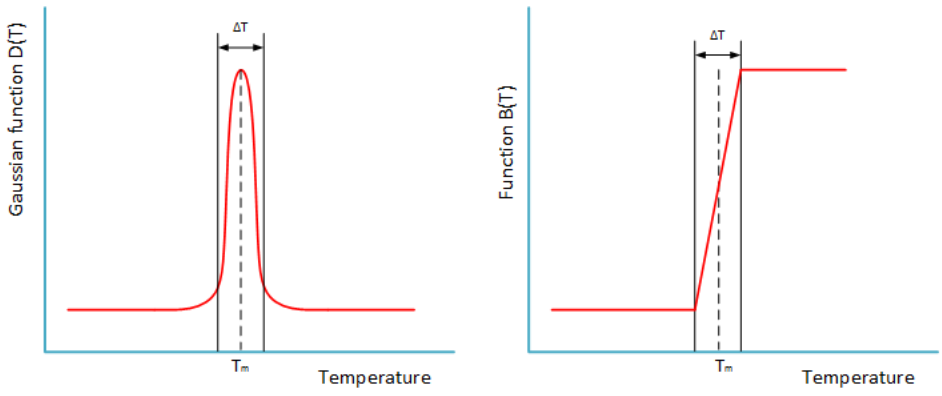

Figure 34: Auxilliary functions to define the density, conductivity and capacity of the PCM

The enthalpy method is adopted to deal with the moving boundary problem in solid–liquid phase change process. The corresponding governing equations are shown as follows two chapters.

Enthalpy method has following advantages:

- The governing equations are similar to the single phase equation.
- There is no condition to be satisfied at the solid–liquid interface as it automatically obeys the interface condition.
- The enthalpy formulation allows a mushy zone between the two phases. Phase change problems are solved by finite difference or finite element methods.
- Method does not require explicit treatment of the moving boundary.
- The enthalpy formulation belongs to fixed-domain method for solving the Stefan problem.

4.6.1 Governing Equation for the HTF

The following equations are arrived by establishing energy balances at the respective regions of HTF. The equation for the incompressible liquid is given by the following equation:

$$\frac{\partial \Theta_f}{\partial t} = -A\frac{\partial \Theta_f}{\partial x} - B(\Theta_f - \Theta^*)$$

$$A = \frac{m_f}{\rho_f \pi R_i^2}$$

$$B = \frac{2h}{\rho_f Cp_f R_i} \qquad 3 - 30$$

$$\Theta_f = T - T_m$$

$$\Theta^* = T(x, r = R_i, t) - T_m$$

where θ_f is relative temperature of HTF, θ^* relative temperature last time layer value, t is time, x is axial coordinate, m_f is mass flow rate of the HTF, ρ_f is density of HTF, R_i is inner radius

of the tube, h is heat transfer coefficient, Cp_f is specific heat of HTF, T is temperature of HTF and finally T_m is melting point temperature.

Using the backward finite difference method for the development of equation 3 - 24, we have:

$$\Theta_i^{n+1} = \Delta t \left(-A \frac{\Theta_i^n - \Theta_{i-1}^n}{\Delta x} - B(\Theta_{f_i}^n - \Theta^{*n}_i) \right) + \Theta_i^n \qquad 3 - 31$$

where the subscript i represents the location of the element in the finite difference mesh and $n+1$, the instant in that the nodal temperature is being calculated.

4.6.2 Governing Equation for the PCM

Consider a thin cylindrical shell element of thickness Δr and width Δx in a long cylinder. Assume the density of the cylinder is ρ, the specific heat is C, and the length is L. The area of the cylinder normal to the direction of heat transfer at any location is $A = 2\pi rL$ where r is the value of the radius at that location. Heat transfer area A depends on r and thus it varies with location. An energy balance in two dimensions on this thin cylindrical shell element during a small time interval Δt with considering the natural heat transfer by convection can be expressed as:

$$\begin{pmatrix} Rate\ of\ change \\ of\ the\ energy \\ content\ of\ the \\ element \end{pmatrix} = \begin{pmatrix} Rate\ of\ heat \\ conduction \\ at\ r\ and\ x \end{pmatrix} - \begin{pmatrix} Rate\ of\ heat \\ conduction \\ at\ r + \Delta r \\ and\ x + \Delta x \end{pmatrix} + \begin{pmatrix} Rate\ of\ heat \\ generation\ inside \\ the\ element \end{pmatrix}$$

or

$$\frac{\Delta E_{element}}{\Delta t} = Q_r + Q_x - Q_{r+\Delta r} - Q_{x+\Delta x} + Q_{gen} \qquad 3 - 32$$

The change in the energy content of the element and the rate of heat generation within the element can be expressed as:

$$\begin{aligned} \Delta E_{element} = E_{t+\Delta t} - E_t &= mc(\theta_{t+\Delta t} - \theta_t) \\ &= \rho c A \Delta r \Delta x (\theta_{t+\Delta t} - \theta_t) \end{aligned} \qquad 3 - 33$$

Now dividing the 3 - 32 equation above by AΔrΔx gives:

$$\frac{\rho c(\theta_{t+\Delta t}-\theta_t)}{\Delta t}=\frac{1}{A}\left(\frac{1}{\Delta \mathrm{x}}\,\frac{Q_r-Q_{r+\Delta r}}{\Delta r}+\frac{1}{\Delta \mathrm{r}}\,\frac{Q_x-Q_{x+\Delta x}}{\Delta \mathrm{x}}\right)+Q_{gen} \qquad 3 - 34$$

Taking the limit as Δx → 0, Δr → 0 and Δt → 0 yields

$$\rho c\frac{\partial \theta}{\partial t}=\frac{1}{A}\left(\frac{\partial}{\partial r}\left(kA\frac{\partial \Theta}{\partial r}\right)+\frac{\partial}{\partial x}\left(kA\frac{\partial \Theta}{\partial x}\right)\right)+Q_{gen} \qquad 3 - 35$$

since, from the definition of the derivative and Fourier's law of heat conduction

$$\lim_{\Delta \mathrm{r}\to 0}\frac{Q_r-Q_{r+\Delta r}}{\Delta r}=\frac{\partial Q}{\partial r}=\frac{\partial}{\partial r}\left(-kA\frac{\partial \Theta}{\partial r}\right) \qquad 3 - 36$$

$$\lim_{\Delta \mathrm{x}\to 0}\frac{Q_x-Q_{x+\Delta x}}{\Delta x}=\frac{\partial Q}{\partial x}=\frac{\partial}{\partial x}\left(-kA\frac{\partial \Theta}{\partial x}\right) \qquad 3 - 37$$

The term of the heat generation of energy Q_{gen} is [33,34]:

$$Q_{gen}=\rho_p \Delta H\frac{\partial f}{\partial t} \qquad 3 - 38$$

where ΔH is the latent heat of fusion, ρ_p is the cell density and finally ∂f is the fraction of solid formed during the phase transformation. Noting that the heat transfer area in this case is A= 2πrL, the two-dimensional transient heat conduction with natural heat transfer equation in a cylinder becomes:

$$\rho_p C_p\frac{\partial \Theta}{\partial t}=\frac{\partial}{\partial x}\left(k_p\frac{\partial \Theta}{\partial x}\right)+\frac{1}{r}\frac{\partial}{\partial r}\left(rk_p\frac{\partial \Theta}{\partial r}\right)+\rho_p \Delta H\frac{\partial f}{\partial t} \qquad 3 - 39$$

$$\Theta=\mathrm{T}-T_m$$

where θ is melting fraction, ρ_p is density of PCM, C_p is specific heat of PCM, r is radial coordinate, k_p is thermal conductivity of PCM and finally f is liquid fraction of melt.

The latent heat evolution was taken into account by using Scheil's equation until the remaining liquid reached the eutectic composition. The liquid fraction is estimated as [34]:

$$f = 0; \qquad \Theta < 0$$

$$0 < f < 1; \quad \Theta = 0$$

$$f = 1; \qquad \Theta > 0$$

By simplifying equation 3 - 39 we have:

$$\rho_p C_p \frac{\partial \Theta}{\partial t} = \frac{\partial}{\partial x}\left(k_p \frac{\partial \Theta}{\partial x}\right) + \frac{1}{r}\frac{\partial}{\partial r}\left(r k_p \frac{\partial \Theta}{\partial r}\right) + \rho_p \Delta H \frac{\partial f}{\partial \Theta}\frac{\partial \Theta}{\partial t} \qquad 3 - 40$$

Expanding the partial derivatives in relation to the radius and considering the material as isotropic, rearranging previous equation 3 - 40, it follows that:

$$\rho_p \left(C_p - \Delta H \frac{\partial f}{\partial \Theta}\right)\frac{\partial \Theta}{\partial t} = k_p \left(\frac{\partial^2 \Theta}{\partial r^2} + \frac{1}{r}\frac{\partial \Theta}{\partial r} + \frac{\partial^2 \Theta}{\partial x^2} + \frac{\partial \Theta}{\partial x}\right) \qquad 3 - 41$$

where

$$\gamma = C_p - \Delta H \frac{\partial f}{\partial \Theta} \qquad 3 - 42$$

and the cylindrical coordinates equation is reduced to:

$$\frac{\partial \Theta}{\partial t} = \frac{k_p}{\rho_p \gamma}\left(\frac{\partial^2 \Theta}{\partial r^2} + \frac{1}{r}\frac{\partial \Theta}{\partial r} + \frac{\partial^2 \Theta}{\partial x^2} + \frac{\partial \Theta}{\partial x}\right) \qquad 3 - 43$$

Using the backward finite difference method for the development of equation 3 - 39, we have:

$$\Theta_{i,j}^{n+1} = \frac{k_p \Delta t}{\rho_{i,j}\, \gamma_{i,j}}\left(\frac{\Theta_{i,j-1}^n - 2\Theta_{i,j}^n + \Theta_{i,j+1}^n}{\Delta r^2} + \frac{1}{r}\left(\frac{\Theta_{i,j}^n - \Theta_{i,j-1}^n}{\Delta \mathrm{r}}\right) + \frac{\Theta_{i-1,j}^n - 2\Theta_{i,j}^n + \Theta_{i+1,j}^n}{\Delta x^2} + \frac{\Theta_{i,j}^n - \Theta_{i-1,j}^n}{\Delta \mathrm{x}}\right) + \theta_{i,j}^n \qquad 3 - 44$$

where the subscript *i* and *j* represent the location of the element in the finite difference mesh and *n+1*, the instant in that the nodal temperature is being calculated.

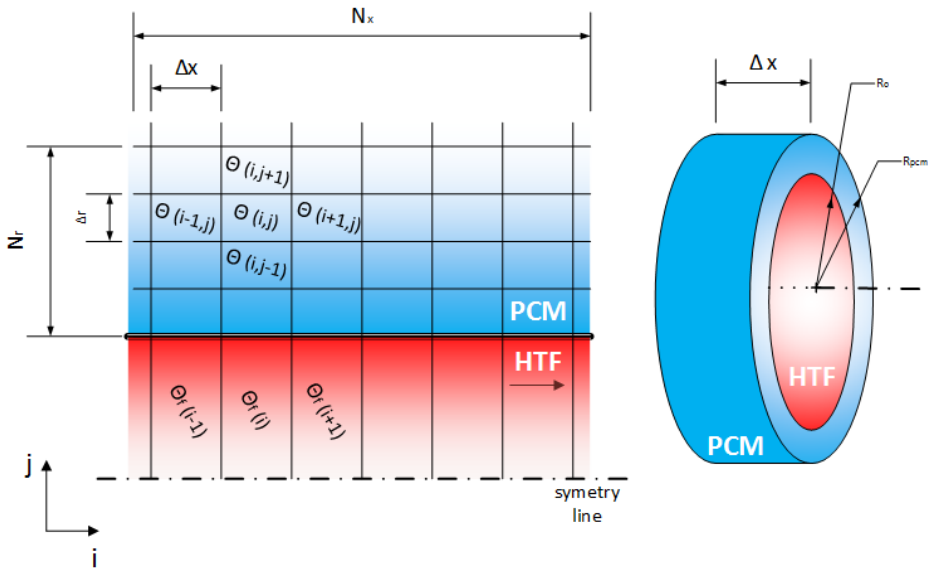

Figure 35: Cylindrical control mesh elements

4.6.3 The Initial and Boundary Conditions

To determine the temperature distribution in a medium, it is necessary to solve the appropriate form of the heat equation. The solution depends on the physical conditions existing at the boundaries of the medium. Because the heat equation (3-43) is second order in the spatial coordinates, two boundary conditions must be expressed for each coordinate to describe the system. Because the equation is first order in time, and thus the initial condition cannot involve any derivatives, only one condition, termed the initial condition, must be specified. The heat conduction equation is second order in space coordinates, and thus a boundary condition may involve first derivatives at the boundaries as well as specified values of temperature.

The conditions are specified at the coordinates *x* and *r* for a two-dimensional system. The first kind condition corresponds to a situation for which the surface is maintained at a fixed temperature. It is commonly named a Dirichlet condition. The second kind condition corresponds to the existence of a fixed or constant heat flux at the surface. This heat flux is related to the temperature gradient at the surface by Fourier's Law. It is named as Neumann condition. A special case of this condition corresponds to the perfectly insulated, or adiabatic, surface (3-47 and 3-49). The boundary condition of the third kind corresponds to the existence of convection heating at the surface and is obtained from the surface energy balance (3-48 and 3-51). The initial and boundary conditions were taken over from *Y.B. Tao at al.* [28] and *H. A. Adine et al.* [33].

The initial conditions for HTF:

$$\Theta_f(x, t = 0) = T_i - T_m \qquad 3 - 45$$

The initial conditions for PCM:

$$\Theta(x, r, t = 0) = T_i - T_m \qquad 3 - 46$$

where Ti is initial state temperature.

The boundary conditions for PCM:

Inlet and outlet insulated boundaries:

$$\frac{\partial \Theta(\mathrm{x} = 0, \mathrm{r}, \mathrm{t})}{\partial x} = \frac{\partial \Theta(\mathrm{x} = \mathrm{L}, \mathrm{r}, \mathrm{t})}{\partial x} = 0 \qquad 3 - 47$$

Inner surface convection boundary condition:

$$\begin{pmatrix} Heat\ conduction \\ at\ the\ surface \\ in\ a\ selected\ direction \end{pmatrix} = \begin{pmatrix} Heat\ convention \\ at\ the\ surface\ in \\ the\ same\ direction \end{pmatrix} \qquad 3 - 48$$

$$-k_p \frac{\partial \Theta(\mathrm{x}, \mathrm{r} = R_i, \mathrm{t})}{\partial r} = U(\Theta_f(x, t) - \Theta(x, r = R_i, t))$$

where U is the convection heat transfer coefficient.

Outer surface insulated boundary:

$$\frac{\partial \Theta(\mathrm{x}, \mathrm{r} = R_{PCM}, \mathrm{t})}{\partial r} = 0 \qquad 3 - 49$$

The boundary conditions for HTF:

Inlet boundary:

$$\Theta_f(x = 0, r, t) = \Theta_{f,in} = f(t) \qquad 3 - 50$$

Outer surface convection boundary condition:

$$-k_p \frac{\partial \Theta(\mathrm{x}, \mathrm{r} = R_i, \mathrm{t})}{\partial r} = U(\Theta_f(x, t) - \Theta(x, r = R_i, t)) \qquad 3 - 51$$

4.7 Results of Numerical Model of Thermal Energy Storage

The results of the numerical model for two dimensional mathematical model of a shell-and-tube heat exchanger described in section 3.6 will be presented here. The numerical analysis of thermal behavior during charging and discharging of the LHS system have been performed.

4.7.1 Process of Calculation

The heat transfer between the HTF and the PCM surface is by convection where the heat transfer coefficient is constant and equal to U. There is internal energy generation and the heat transfer in the PCM is controlled by pure conduction and pure PCM. For the calculation of the numerical method, which is a system of PDE with moving boundary conditions, a distinct target computer code was written by the author. A program was established again in Matlab® and the simulation code was developed to predict the behavior of LHS system with non-isothermal phase transition of PCM. The program solves discretized PDE for PCM and HTF to predict the temperature distribution and rate of melting or solidification in PCM. This program "*Numerical_method.m*" is attached in Appendix I with using auxiliary function "*Material_properties.m*", which determines physical aspect such as density, thermal capacity, and conductivity from input temperature as is described in section 4.6. This function is attached in Appendix J. Flow diagram of the code is attached in Appendix K. The computational domain in two dimensions has been discretized using backward finite differences of uniform size and constant time steps. The grid size used in this study was of 20 axial x 20 radial with time steps of 1s each. This grid's layout with marked boundary conditions and computation domain is shown in Figure 36.

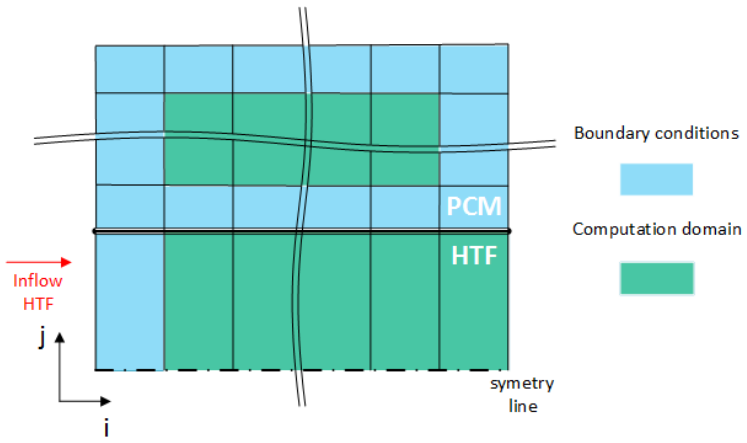

Figure 36: Two domensional computation domain

A series of numerical calculations have been done to analyze transient heat transfer during the melting and solidification process of the KNO_3 - $NaNO_3$ (50-50). Temperature changes of the HTF and the PCM storage unit can be seen in more details on the contours that represent different temperature distributions. The length for the computation domain (L) is 2m, the inner radius of tube (Ri) is 20mm, inner radius for shell side (R_{PCM}) is 30mm. The thickness of the tube wall is neglected. In order to simplify the physical and mathematical model the following assumptions are adopted. The axial heat conduction and viscous dissipation in the HTF is negligible. The flow of HTF is treated as one dimensional fluid flow. The phase change material region is treated as an axisymmetric model [28] and the effect of natural convection of PCM during melting/solidification is also negligible.

4.7.1 Results of Numerical Model of Thermal Energy Storage – Discharging Process

Solidification process delivers energy from PCM to HTF. Thermal energy stored in PCM is released to HTF. The discharging of the LHS unit during the solidification of the PCM initially in the liquid phase at temperature 240°C has been observed. KNO3 - NaNO3 was chosen as a PCM for assessing of the thermal behavior. The thermo-physical properties of PCM are stated in Table 4.

The temperatures used in this numerical model are established as differences between the temperatures of PCM or HTF and the melting point of the particular PCM. The inlet temperature initially set at 190°C thus corresponds to θ=-33K in Figure 41 due to the principle of temperature differences. In the Figures 37-40 the temperature range between -7.5K to 7.5K represents mushy phase of the PCM. In graphics it is symbolized by the divisional area of white line or line array.

The initial attempt was to make the two used methods, the NTU and the method applied in numerical model, comparable. However, this attempt failed due to the insulated boundary conditions, which influenced the results of the numerical model very significantly. As a result of the exposure of the insulated boundaries the outflow temperature has always been θ=0K thus incomparable to the results gained by the NTU method. The insulated boundary conditions are represented in equations 3-47 – 3-49 by *Y.B. Tao at al.* [28] and *H. A. Adine et al.* [33].

Figures 37 to 40 represent solidification process of the discharging PCM. At the beginning of the tube the HTF forms the PCM into a thorn shape profile. The shape of the thorn remains stable thought time, but as Figure 40 shows the profile increases its sink. The sequence of the above mentioned figures illustrates the change of PCM as it transfers energy into HTF. Visually we can notice this change through the graphical demonstration as a flattening effect of the shape of the particular PCM. In theory it means that the temperature of PCM decreases. Time span necessary for conversion from the initial conditions into the stable state is surprisingly brisk - approximately 900s. The tube's material properties in the heat transfer analysis between materials have been proved are not negligible in the dynamics. In governing of the equations another dynamic equation for the tube should be added where the capacity carries major influence on time constant. This capacity has the dominant influence in transient analysis.

The total exhaustion of energy from PCM to HTF is disabled by the insulated boundary conditions.

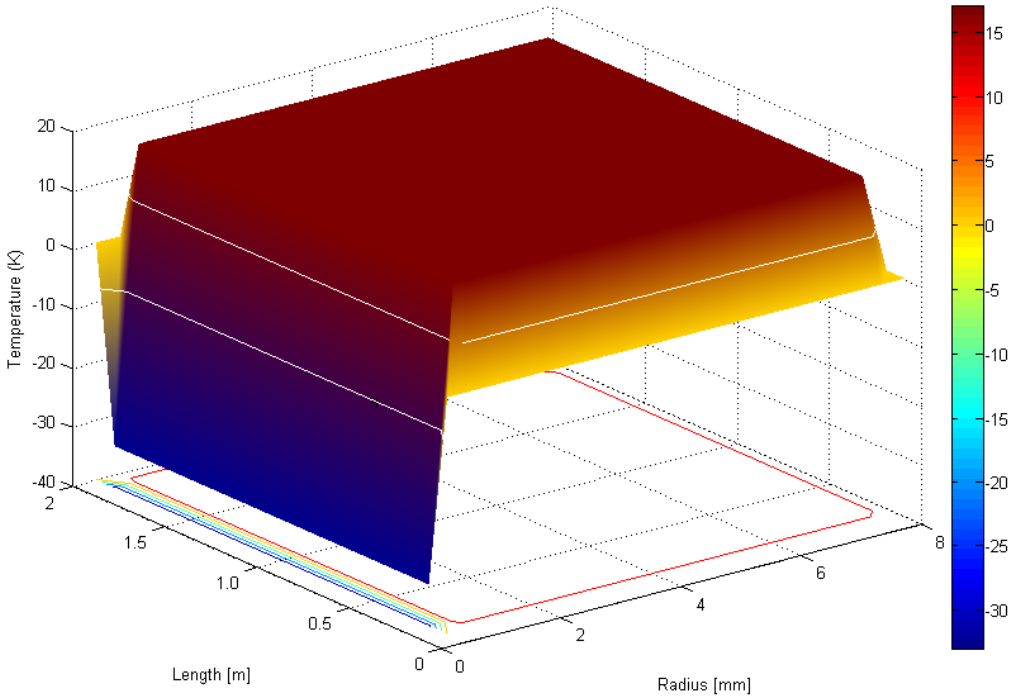

Figure 37: Discharging process of numerical model in initial coditions

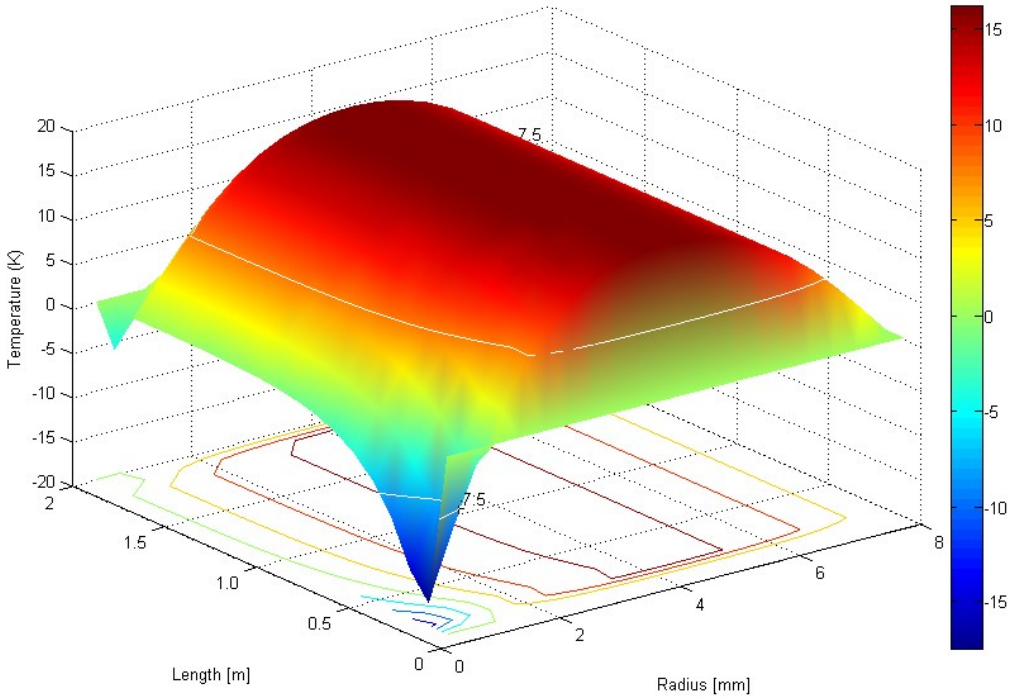

Figure 38: Discharging process of numerical model after 100 seconds

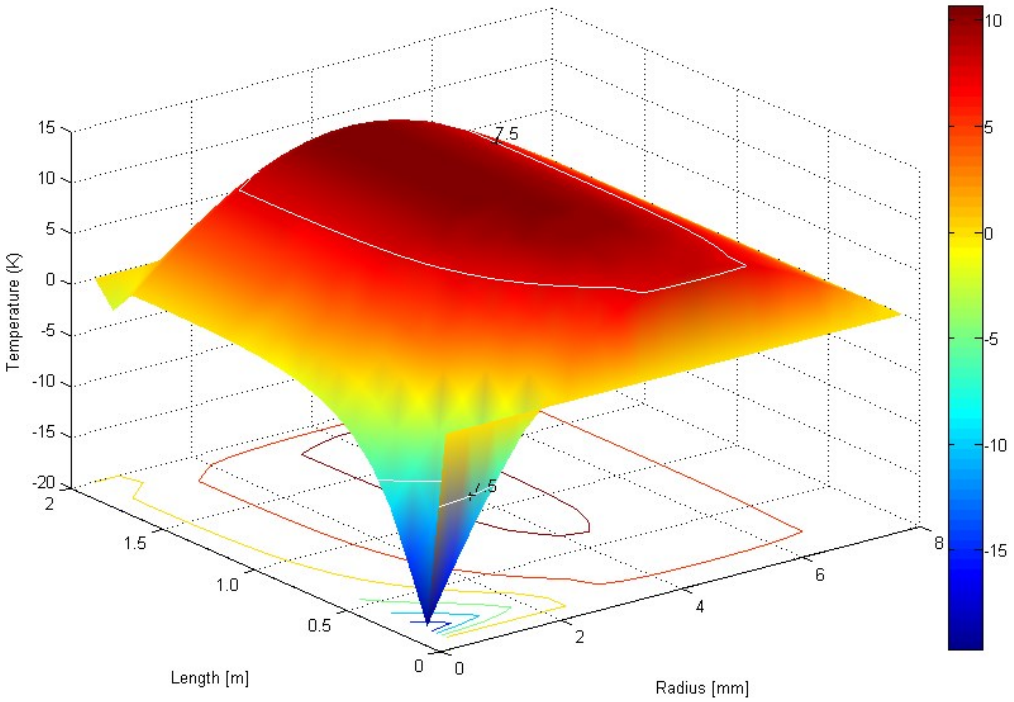

Figure 39: Discharging process of numerical model after 300 seconds

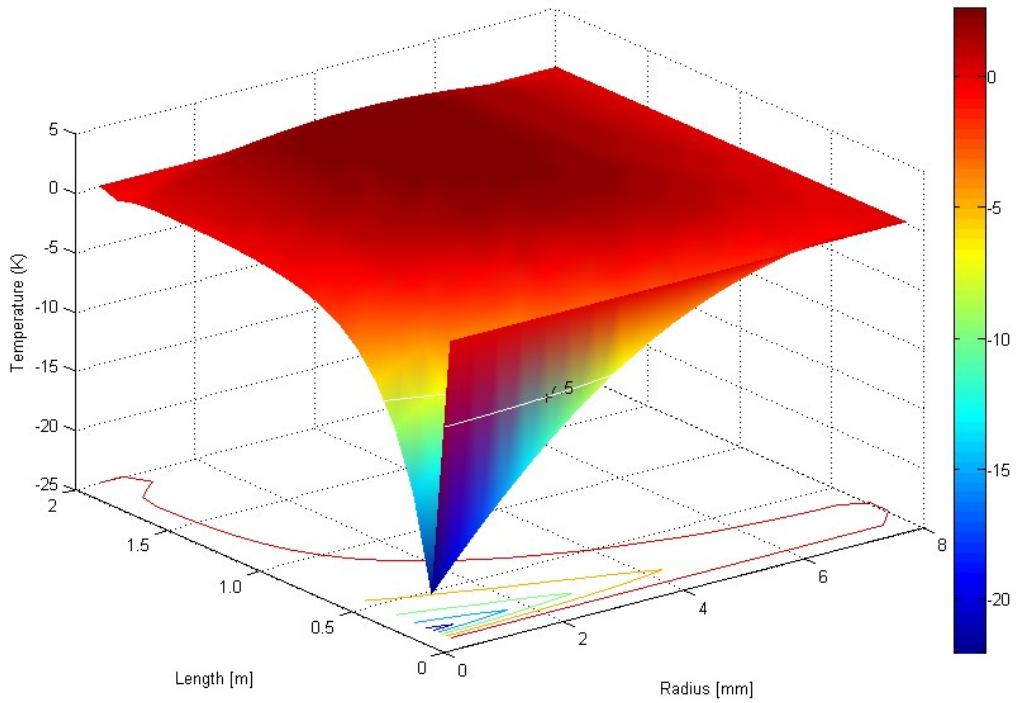

Figure 40: Discharging process of numerical model in steady-state

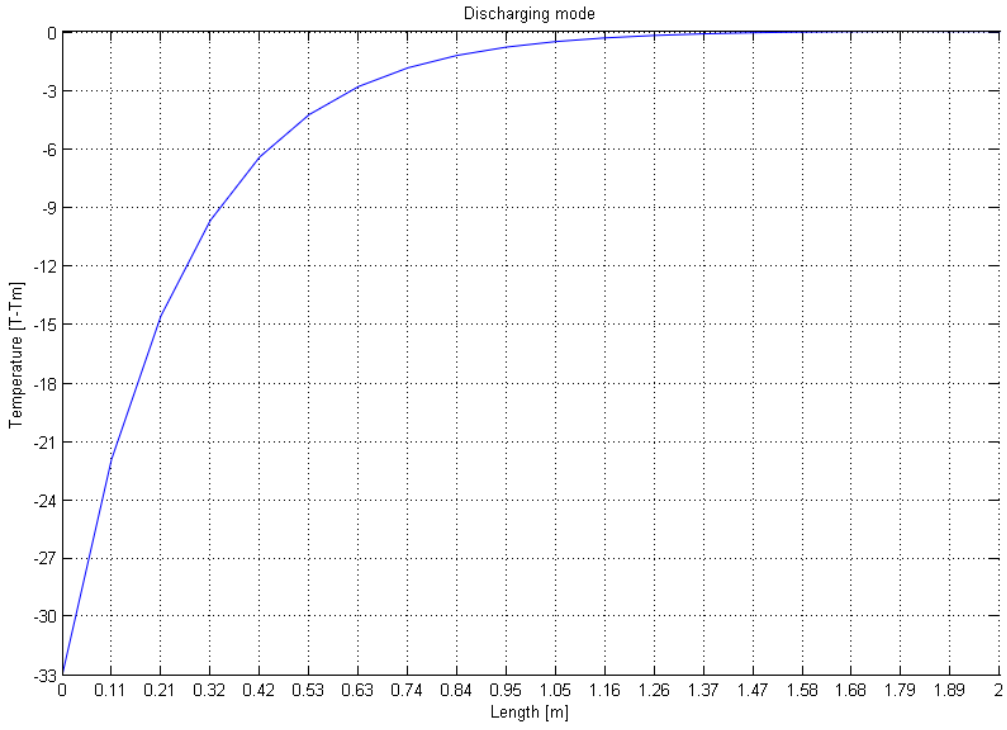

Figure 41: Disharging process of numerical model. HTF temperature depending on the length of the tube.

4.7.2 Results of Numerical Model of Thermal Energy Storage – Charging Process

Water, as a HTF, flows by forced convection through the inner tube and transfers the heat to PCM. Melting of the PCM, KNO_3 - $NaNO_3$ (50-50), represents the storing of energy. The KNO_3 - $NaNO_3$ was initially in the solid phase at the temperature of 200°C.

Again, the temperatures used in this numerical model are established as differences between the temperatures of PCM or HTF and the melting point of the particular PCM. The inlet temperature initially set at 250°C thus corresponds to θ=27K in Figure 46 due to the principle of temperature differences. In the Figures 42-45 the temperature range between -7.5K to 7.5K represents mushy phase of the PCM. In graphics it is symbolized by the divisional area of white line or line array.

Through the exposure of the insulated boundaries the outflow temperature has always been θ=0K thus incomparable to the results gained by the NTU method. These insulated boundary conditions influence the results of the numerical model dramatically.

Figures 42 to 45 represent melting process of the charging PCM. At the beginning of the tube the HTF forms the PCM into a thorn shape profile. The shape of the thorn remains stable thought time, and as opposite to the solidification process it does not increase the profile in its sink. The sequence of the above mentioned figures illustrates the change of HTF as it transfers energy into PCM. Visually we can notice this change through the graphical demonstration as a flattening effect of the shape of the particular PCM. In theory it means that the temperature of PCM increases. Time span necessary for conversion from the initial conditions into the stable state is surprisingly brisk - approximately 900s. The total exhaustion of energy from HTF to PCM is disabled by the insulated boundary conditions.

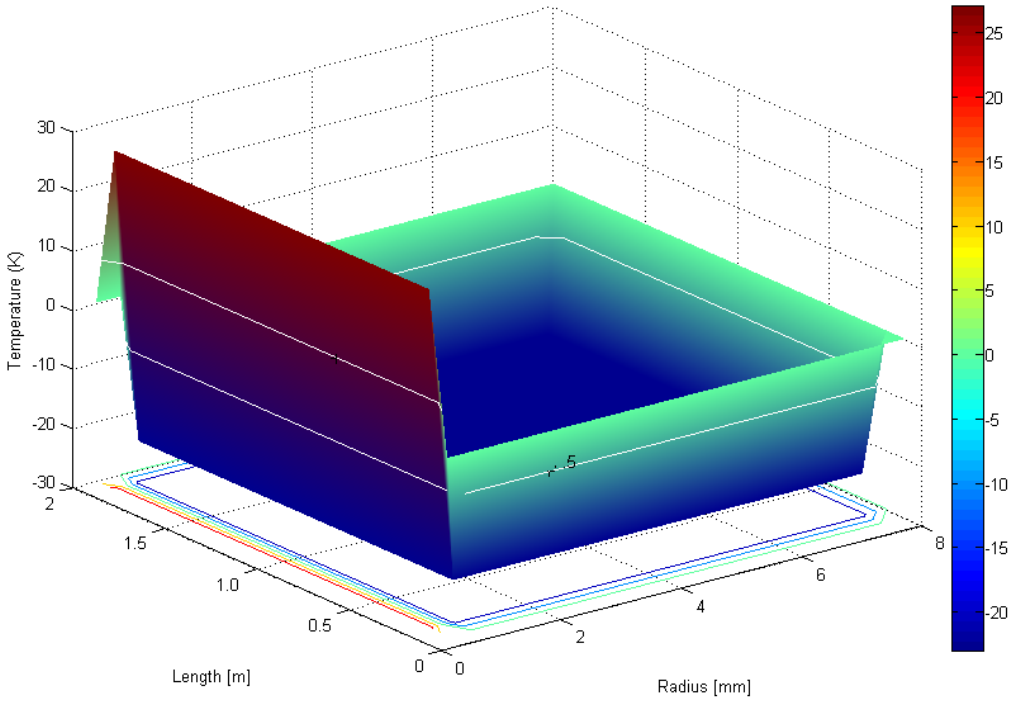

Figure 42: Charging process of numerical model in initial coditions

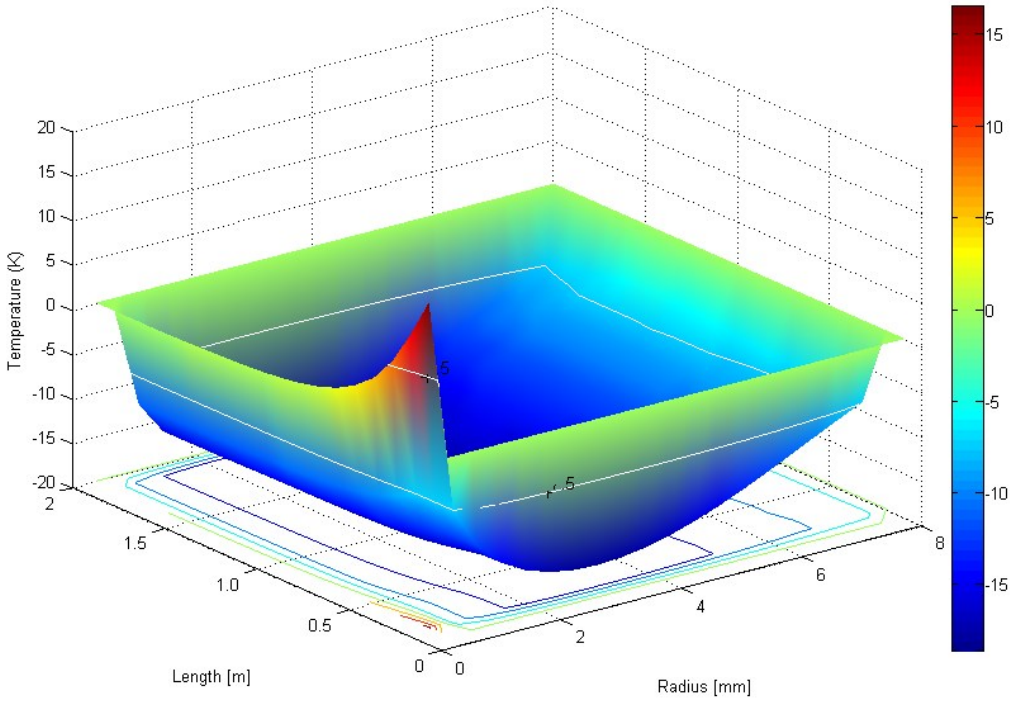

Figure 43: Charging process of numerical model after 100 seconds

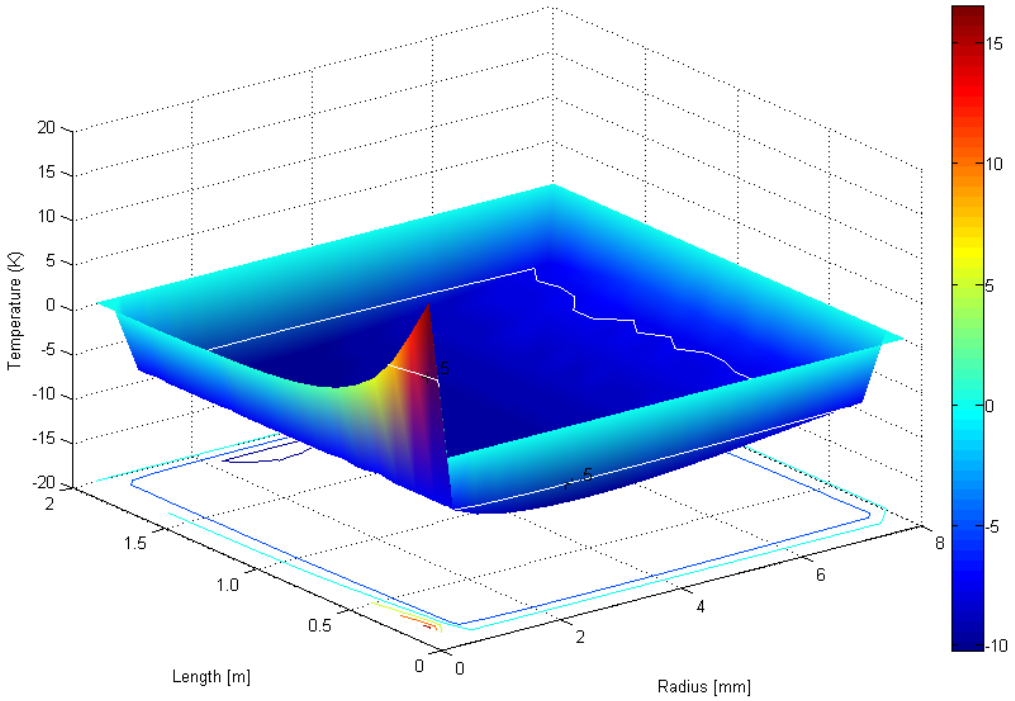

Figure 44: Charging process of numerical model after 300 seconds

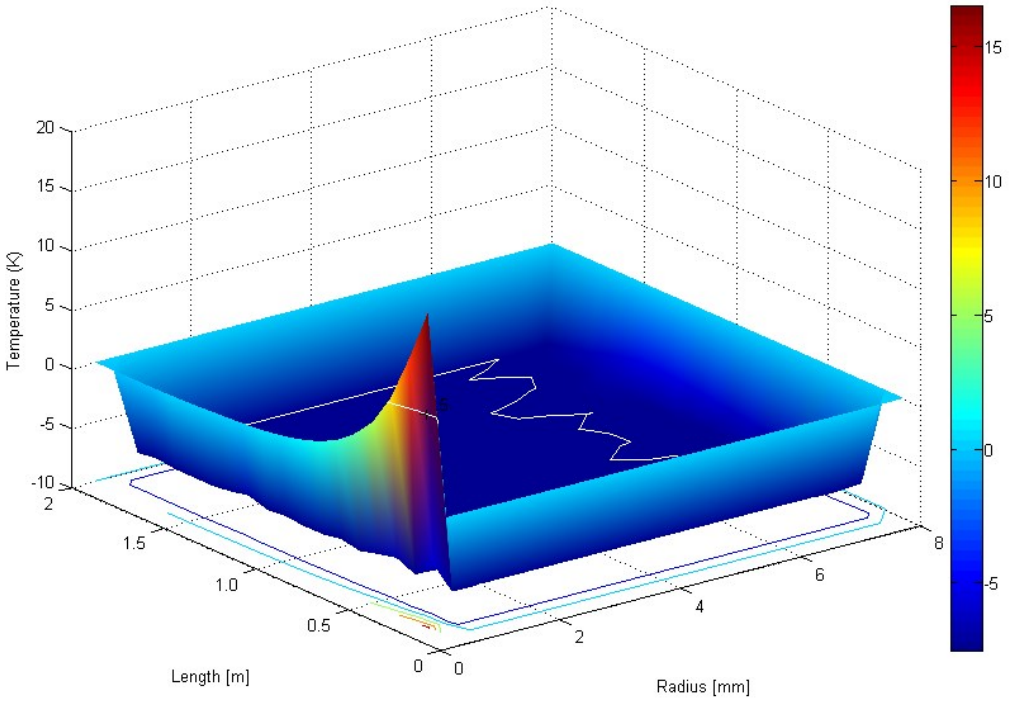

Figure 45: Charging process of numerical model in steady-state

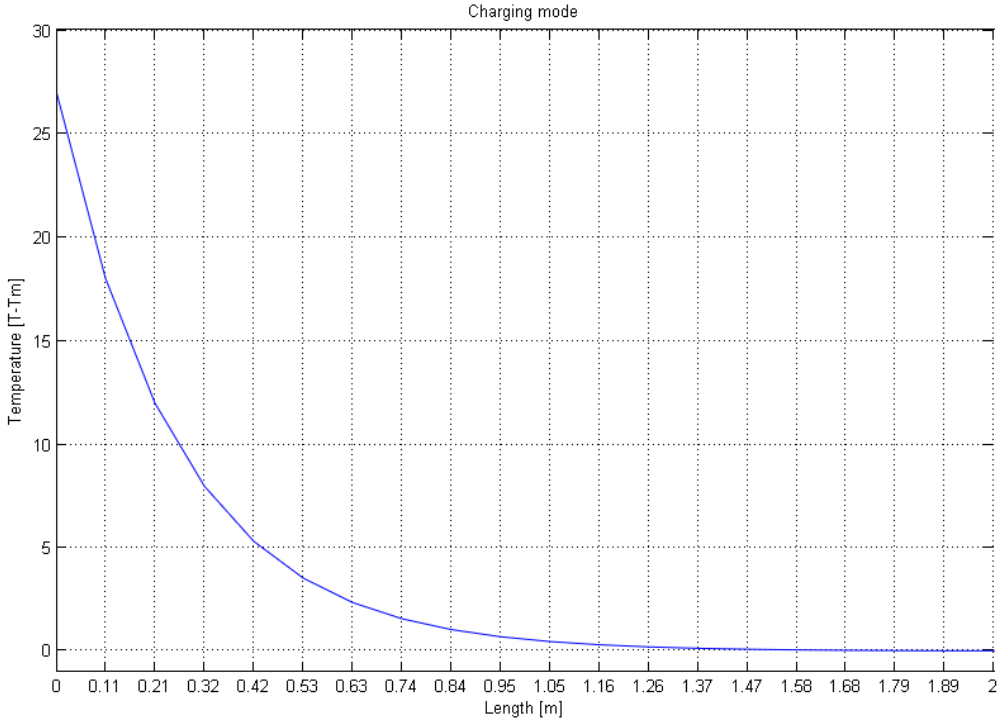

Figure 46: Charging process of numerical model. HTF temperature depending on the length of the tube.

5 Conclusion and recommendations

Most fossil fuel, solar, geothermal and thermal power plants conversion systems need thermal storage due to the energy generation which is unstable and discontinuous with different conditions such as heating value, weather and seasons. In order to ensure the continuity and stability of the energy system so it operates with high efficiency, TES unit is a necessary component. TES is a key technology in providing balance between energy supply and demand for the heating and cooling systems. The use of proper thermal energy storage systems presents a better solution for discrepancy between energy supply and demand. In both sensible and latent heat storage systems, by shifting the load from limited and expensive time period to a wide and cheaper time periods, has several economic and environmental advantages. These can be favorably achieved by TES devices.

LHS has become attractive because of the ability of storing a large amount of energy in small volumes. LHS may be a part of bigger system which manages temperature distributions. But some difficulties occur in designing such systems. Selection of the PCM and HTF materials, selection of the tank, the container's geometry and shape, economic benefits, and the actual price of PCM as well as HTF mediums have impact on the final system's design. My work attempts to find the most suitable PCM for various purposes. Attempt to grasp a suitable heat exchanger with multiple ways to enhance the heat transfer and provide the various designs to store the heat using PCM was intended.

The best option for storing energy is by the PCM as latent heat. The heat is absorbed during the melting of the PCM and retrieved during the solidification of the PCM. Two models have been developed based on different methods. Employed methods are a Number of Transfer Unit Method and Enthalpy Method using finite differences.

The objectives of this work were threefold. Firstly, a survey of available literature on simulation models of sensible and latent heat storage was summed. Secondly, a model for sensible or latent heat storage with appropriate simulation tool was developed. Thirdly, simulations for designing pilot heat storage were performed. All outlined objectives from the beginning this thesis have been reached and fulfilled.

Numerical model, created in this thesis, has more options to simulate other influences which can effect the system. In a further study investigation of the influence of non-steady state inlet temperature, effects of different materials, and physical properties of PCM, HTF, PCM spacing, where the shell space is filled with two PCMs with different melting temperatures, different temperature distribution in the PCM initial conditions can be carried.

However, the issue is whether to have such a detailed model in the situation where only some parameters are important to us. In the case of this study the only and most important parameter was the outflow temperature of HTF.

References

[1] I. Dincer, M.A. Rosen, (2002); Thermal energy storage, Systems and Applications, John Wiley & Sons, Chichester (England).

[2] Lane GA. (1983); Solar heat storage—latent heat materials, vol. I. Boca Raton, FL: CRC Press, Inc.

[3] S.D. Sharma, Kazunobu Sagara, (2005); Latent heat storage materials and systems: A review, Taylor & Francis Inc.

[4] Lane, G. A. (1983); Solar Heat Storage: Latent Heat Materials, Vol. I. Boca Raton, Florida: CRC Press.

[5] Abhat, A. (1983); Low temperature latent heat thermal energy storage: heat storage materials. Solar Energy.

[6] Hiran, S., Suwondo, A., Mansoori, G. (1994); Characterization of alkanes and paraffin waxes for application as phase change energy storage medium. Energy

[7] Wang, X., Lu, E., Lin, W., Liu, T., Shi, Z., Tang, R., Wang, C. (2000); Heat storage performance of the binary systems neopentyl glycol/pentaerythritol and neopentyl glycol/trihydroxy menthylaminomethane as solid phase change materials. Energy Conservation and Management

[8] Hasnain, S. M.; (1998); Review on sustainable thermal energy storage technologies, part I: Heat storage materials and techniques

[9] Hasnain, S. M., (1995); Energy Research Institute DR&D Project Proposal, KACST, Riyadh, Saudi Arabia.

[10] Kenisarin, Murat M.; (2009); High-temperature phase change materials for thermal energy storage

[11] Vasishta D. Bhatt, Kuldip Gohil, Arunabh Mishra1; International Journal of ChemTech Research (2010). Thermal Energy Storage Capacity of some Phase changing Materials and Ionic Liquids

[12] Antoni Gil, Marc Medrano, Ingrid Martorell, Ana Lázaro, Pablo Dolado, Belén Zalba, Luisa F. Cabeza; (2010); State of the art on high temperature thermal energy storage for power generation. Part 1 — Concepts, materials and modellization.

[13] Agyenim F., Hewitt N., Eames P., Smyth M.,(2009); A review of materials, heat transfer and phase change problem formulation for latent heat thermal energy storage systems.

[14] N. Shamsundar, E. Stein, E. Rooz, E. Bascaran, and T.C. Lee; (1992); Design and Simulation of Latent Heat Storage Units, Final Report.

[15] A.K. Gupta; Advanced technologies for clean and efficient energy conversion in power systems; (2008); Department of Mechanical Engineering, University of Maryland.

[16] Carsten Bahl, Doerte Laing, Matthias Hempel, Andreas Stückle; (2006); Concrete thermal energy storage for solar thermal power plants and industrial process heat; German Aerospace Center (DLR), Institute of Technical Thermodynamics.

[17] A. Felix Regin, S.C. Solanki, J.S. Saini; (2008); An analysis of a packed bed latent heat thermal energy storage system using PCM capsules: Numerical investigation.

[18] L. Xia, P. Zhang, R.Z. Wang; (2009); Numerical heat transfer analysis of the packed bed latent heat storage system based on an effective packed bed model.

[19] H. Shabgard, T.L. Bergman, N. Sharifi, A. Faghri; (2010); High temperature latent heat thermal energy storage using heat pipes; International Journal of Heat and Mass Transfer, Vol. 53, pp. 2979-2988.

[20] Jundika C. Kurnia, Agus P. Sasmito, Sachin V. Jangam, Arun S. Mujumdar; (2013); Improved design for heat transfer performance of a novel phase change material (PCM) thermal energy storage (TES).

[21] Y.Q. Li a, Y.L. He, H.J. Song b, C. Xuc, W.W. Wang; (2012); Numerical analysis and parameters optimization of shell-and-tube heat storage unit using three phase change materials.

[22] A.H. Mosaffaa, F. Talati, H. Basirat Tabrizib, M.A. Rosenc; (2011); Analytical modeling of PCM solidification in a shell and tube finned thermal storage for air conditioning systems

[23] Zhenyu Liu, Yuanpeng Yao, Huiying Wu; (2012); Numerical modeling for solid–liquid phase change phenomena in porous media: Shell-and-tube type latent heat thermal energy storage.

[24] AhmadAli Rabienataj Darzi, Mousa Farhadi, Kurosh Sedighi; (2012); Numerical study of melting inside concentric and eccentric horizontal annulus.

[25] Anica Trp; (2005); An experimental and numerical investigation of heat transfer during technical grade paraffin melting and solidification in a shell-and-tube latent thermal energy storage unit.

[26] Hamid Ait Adine, Hamid El Qarnia; (2008); Numerical analysis of the thermal behavior of a shell-and-tube heat storage unit using phase change materials.

[27] K. A. R. Ismail, L. M. de Sousa Filho, F. A. M. Lino; (2011); Solidification of PCM around a curved tube.

[28] Y.B. Tao, Y.L. He (2011); Numerical study on thermal energy storage performance of phase change material under non-steady-state inlet boundary.

[29] I. Dincer, M.Kanoglu (2010); Refrigeration Systems and Applications, John Wiley & Sons, Chichester (England).

[30] Babay S., Bouguettaia H., Bechki D., Boughali S., Bouchekima B. and Mahcene H.; (2000); Review on Thermal Energy Storage Systems.

[31] A.A. Adeyanju and K. Manohar; (2009); Comparison of Thermal Energy Storage Techniques; Journal of Engineering and Applied Sciences.

[32] Pilkington Solar International GmbH, Muhlengasse 7 D-50667, Cologne, Germany; authors are unknown; (2000); Survey of Thermal Storage for Parabolic Trough Power Plants.

[33] H. A. Adine, H. El Qarnia; (2008); Numerical analysis of the thermal behaviour of a shell-and-tube heat storage unit using phase change materials.

[34] A. Fardi Ilkhchy, N. Varahraam, P. Davami; (2011); Evaluation of Pressure Effect on Heat Transfer Coefficient at the Metal- Mold Interface for Casting of a356 al Alloy.

[35] M. Muhieddine, ´E. Canot, R. March; (2010); Various Approaches for Solving Problems in Heat Conduction with Phase Change.

[36] F. Samara, D. Groulx, P. H. Biwole; (2012); Natural Convection Driven Melting of Phase Change Material: Comparison of Two Methods.

[37] J. Y. Murthy, S.R. Mathur; (1998); Numerical Methods in Heat, Mass, and Momentum Transfer; School of Mechanical Engineering Purdue University.

[38] J. Stefan; (1989) Über einige Probleme der Theorie der Wärmeleitung, S. B. Wein, Acad. Mat. Natur.

Appendix A

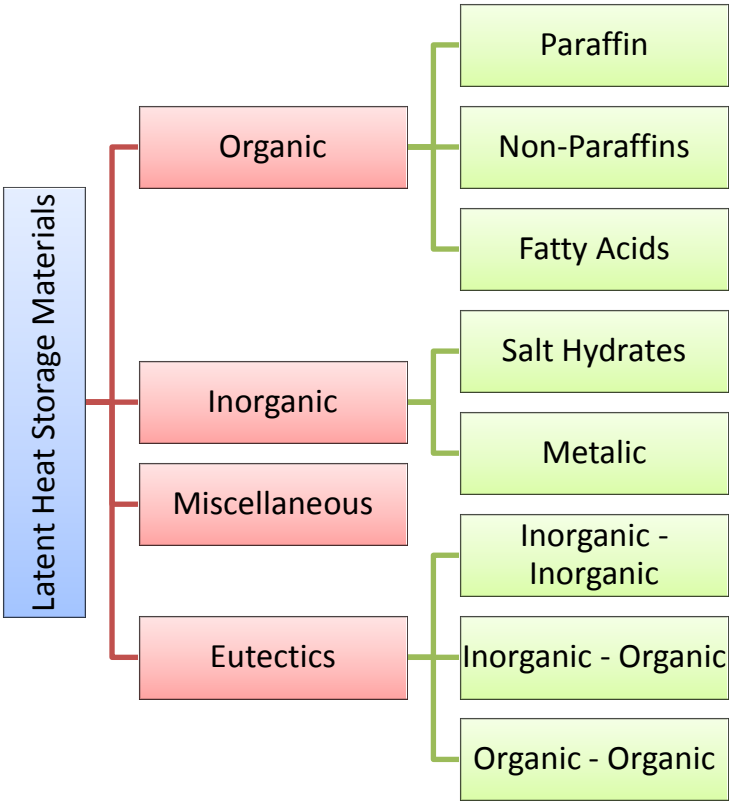
Latent Heat Storage Materials
Organic
Paraffin
Non-Paraffins
Fatty Acids
Inorganic
Salt Hydrates
Metalic
Miscellaneous
Eutectics
Inorganic - Inorganic
Inorganic - Organic
Organic - Organic

Appendix B

The mathematical model of tube LHS unit is developed and described in Appendix A.

Tube wall temperature is expressed from equation 3-6:

$$T_W = T_m - \frac{Q\ ln\frac{r_m}{R_0}}{2\pi k_{PCM}} \qquad \text{A - 1}$$

The same variable can be expressed from equation 3-7:

$$T_W = T_F + \frac{Q}{2\pi R_i}\left(\frac{1}{h} + \frac{R_i}{k_w}\ln\left(\frac{R_0}{R_i}\right)\right) \qquad \text{A - 2}$$

Tube wall temperatures from equations A.1 and A.2 are equal. Convective heat transfer from HTF through the wall tube to the PCM is expressed in equation A.3. This process is reciprocal.

$$Q = \frac{2\pi R_i(T_m - T_F)}{\frac{hR_i}{k_{PCM}}\ln\left(\frac{r_m}{R_0}\right) + 1 + \frac{R_i h}{k_w}\ln(R)} \qquad \text{A - 3}$$

where R is radius ratio $R = \frac{R_0}{R_i}$. The heat transfer with simplification and nondimensionalization is given through the equation A.3:

$$\dot{Q} = \frac{1}{\frac{1}{4\alpha_{PCM}}\ln(\mathrm{F}+1) + 1 + \frac{1}{2\alpha_w}\ln(R)} \qquad \text{A - 4}$$

After simplification of the 3-9 equation heat transfer to the HTF rises/decreases the temperature of the fluid according to the equation:

$$\dot{Q} = \frac{\partial \ln \mathrm{F}}{\partial\ NTU} \qquad \text{A - 5}$$

Subsequently simplification of the 3-8 energy release from the PCM equals to:

$$\dot{Q} = \alpha_{PCM}\frac{\partial\ F}{\partial\ \tau} \qquad \text{A - 6}$$

From this point on it should be considered that:

$$\frac{1}{\frac{1}{\alpha_{PCM}}\ln(\mathrm{F}+1)+1+\frac{1}{2\alpha_w}\ln(R)} = \frac{\partial \ln(T_m - T_F)}{\partial\, NTU} = \alpha_{PCM}\frac{\partial\, F}{\partial\, \tau} \qquad \text{A - 7}$$

Heat transfer = *Energy release* = *HTF*

from HTF to PCM *from PCM* *rice/decrease*

As a result the following operation is to achieve the formulation of the NTU which equals the second and the third equations from A.7:

$$\frac{\partial \ln F}{\partial\, NTU} = \alpha_{PCM}\frac{\partial\, F}{\partial\, \tau} \quad \Rightarrow \quad \frac{\partial\, \tau}{\partial\, F} = \alpha_{PCM}\,\frac{\partial\, NTU}{\partial \ln(T_m - T_F)} \qquad \text{A - 8}$$

The first and the third equation from A.7 are equal. They can be also expressed as:

$$\frac{1}{4\alpha_{PCM}}\ln(\mathrm{F}+1)+1+\frac{1}{2\alpha_w}\ln(R) = \frac{1}{\alpha_{PCM}}\frac{\partial\, \tau}{\partial\, F} \qquad \text{A - 9}$$

Consequently $\frac{\partial\, \tau}{\partial\, F}$ from A.8 is substituted in the equation A.9:

$$\frac{1}{4\alpha_{PCM}}\ln(\mathrm{F}+1)+1+\frac{1}{2\alpha_w}\ln(R) = \frac{\partial\, NTU}{\partial \ln F} \qquad \text{A - 10}$$

In the following step the equation is extended by $(\partial \ln F)$

$$\left(\frac{1}{4\alpha_{PCM}}\ln(\mathrm{F}+1)+1+\frac{1}{2\alpha_w}\ln(R)\right)\partial \ln F = \partial\, NTU \qquad \text{A - 11}$$

Later the equation A.11 is integrated:

$$\int_{F}^{F_0}\frac{1}{4\alpha_{PCM}}\ln(\mathrm{F}+1)+1+\frac{1}{2\alpha_w}\ln(R)\;\partial \ln F = NTU \qquad \text{A - 12}$$

Finally as a result the following equation is gained:

$$NTU = \ln\left(\frac{F_0}{F}\right) + \frac{1}{2\alpha_w}\ln(R)\ln\left(\frac{F_0}{F}\right) + \frac{1}{4\alpha_{PCM}}(G(F_0) - G(F)) \qquad \text{A - 13}$$

G(F) is an auxiliary function. To calculate G(F) Shamsundar et al. have developed an approximation because no exact analytical representation exists.

$$G(F) = \frac{\ln(1+F)(1+\frac{17}{450}[\ln(1+F)]^2)}{1+\frac{[\ln(1+F)]^2}{100}} + \frac{[\ln(1+F)]^2}{4} \qquad \text{A - 14}$$

Following steps are for calculation of the frozen fraction (F). It will be shown how it changes along the axial distance. Frozen fraction is the area of the frozen region in the radial plane divided by the area of cross-section of the tube. F_0 is the fraction at the inlet tube.

$$F = \frac{r_m^2}{R_0^2} - 1 \qquad \text{A - 15}$$

The same equation can be also expressed by the definition of Shamsundar et al. [14] as:

$$\frac{F}{F_0} = \frac{T_m - T_F}{T_m - T_i} \qquad \text{A - 16}$$

Equation A.9 can be written also as follows:

$$\partial\,\tau = \left(\frac{1}{4}\ln(\mathrm{F}+1) + \frac{1}{\alpha_{PCM}} + \frac{1}{2\alpha_w\alpha_{PCM}}\ln(R)\right)\partial\,F \qquad \text{A - 17}$$

$$\tau = \int_0^F \left(\frac{1}{4}\ln(\mathrm{F}+1) + \frac{1}{\alpha_{PCM}} + \frac{1}{2\alpha_w\alpha_{PCM}}\ln(R)\right)\partial\,F \qquad \text{A - 18}$$

And finally the result is:

$$\tau = \frac{1}{4}\left((1+F)\ln(1+F) - F\right) + \frac{\mathrm{F}}{\alpha_{PCM}} + \frac{F}{2\alpha_w\alpha_{PCM}}\ln(R) \qquad \text{A - 19}$$

Appendix C

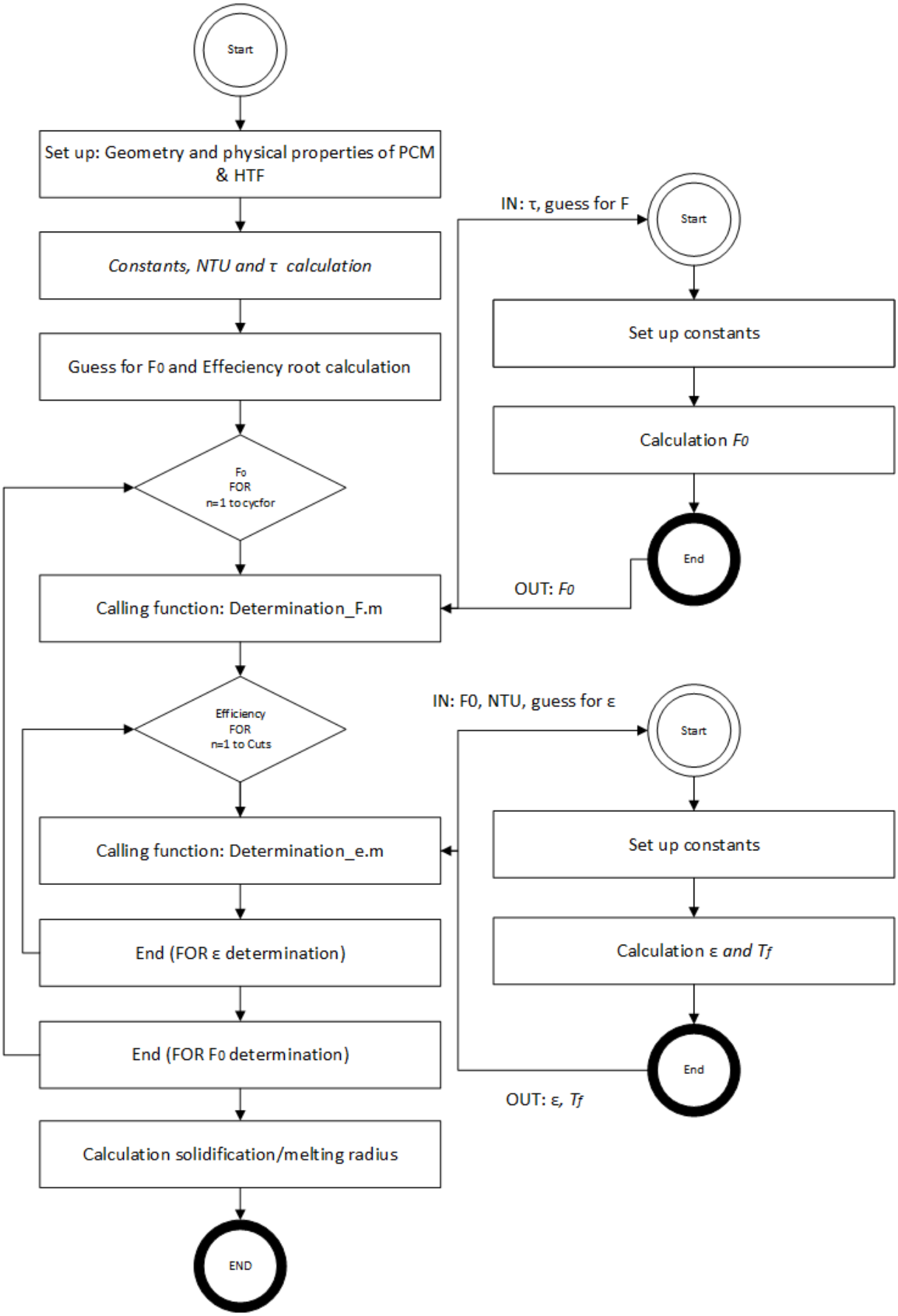
Start
Set up: Geometry and physical properties of PCM & HTF
Constants, NTU and τ calculation
Guess for F0 and Effeciency root calculation
F0 FOR n=1 to cycfor
Calling function: Determination_F.m
Efficiency FOR n=1 to Cuts
Calling function: Determination_e.m
End (FOR ε determination)
End (FOR F0 determination)
Calculation solidification/melting radius
END
IN: τ, guess for F
Start
Set up constants
Calculation F0
End
OUT: F0
IN: F0, NTU, guess for ε
Start
Set up constants
Calculation ε and Tf
End
OUT: ε, Tf

Appendix D

```
%% Program which calculates NTU method

clc
clear all
close all

global mf Ti kw Ri Ro Tm H cp km ro Hwall k R alfa U endtime
time cycfor...
    Length Cuts Lenght4NTU NTU timeH tau TfC Root_Emin Tf F rm
rmMM alfaPCM alfaW

%% Physical properties of HTF

mf=0.5;                  % Mass flow rate HTF (kg/s)
Ti=190+273.15;           % Inlet temperature of HTF [K]

%% Physical properties of Tube - Steel, Carbon 1%

kw = 43 ;              % conductivity tube [W/(m.K)]
Ri = 0.017;            % Outer radius of the tube [m]
Ro = 0.02;             % Innet radius of the tube [m]
Length=2;        % Length of the Tube [m]
Cuts=16 ;         % Number of the Tube cuts

%% Physical properties of PCM (KNO3 - NaNO3)

Tm= 220+273.15;          % Melting point of PCM [K]220 210 230
H= 100700;               % Latent heat of fusion of PCM [J/kg]
cp= 1350;                % Specific heat of PCM [J/(kg.K)]
km = 0.56;               % conductivity PCM [W/(m.K)]
ro= 1867 ;               % density of the PCM [kg/m3]

%% Time management

endtime=12;       % Number of hours to calculation +1 (zero
time)
time=0:1:endtime;
cycfor=endtime+1;
timeH = time*3600;
tau= (km*timeH*abs(Tm-Ti))/(H*ro*Ro*Ro);

%% Constants, Vatiables calculation

Hwall=(kw)/(Ri*log(Ro/Ri)); % convention heat transfer
coeficient of pipe [K]
k =  km / kw ;  % Conductivity ratio
R = Ro/Ri;       % Radius (Inner / Outer )
alfa = km/(2*Ri*Hwall);
alfaPCM = km/(2*Ri*Hwall/100);
```

```
alfaW = kw/(2*Ri*Hwall/100);
U=1/((Ri)/(Hwall*Ro)+(Ri*log(Ro/Ri))/(kw)); % Overall heat
transfer coefficient
Lenght4NTU = 0 : Length/(Cuts-1) : Length ;
NTU=(2*pi*Ri*Lenght4NTU*U)/(mf*cp); % NTU


%% Estimate roots
%F0
% because of the root is changing and Matlab have to have good
guess (hit)
hit(1)=0;
for W=2:cycfor+1
     hit(W)=hit(W-1)+(0.1)/Cuts;
end

% Effeciency root
hitE(1)=0.3;
for Q=2:cycfor+1
     hitE(Q)=hitE(Q-1)+(0.15)/Cuts;
 end

%% Calculation of F0 and Effeciency
% Two cycluses FOR are filling two tables. 1st for Efficiency
root (Root_Emin)
% and 2nd temperature table (Tf). There are used also two
functions for
% determination F0 and effeciency. Cycluses are controlled by
variable R (time - rows)
% and T (cuts - column).

for R=1:cycfor
    Fzero(R)= NTU_Determination_F(tau(R),hit(R));
    Fzero(1)=0;
        for T=1:Cuts
            [Root_Emin(R,T), Tf(R,T)] =
NTU_Determination_e(Fzero(R),NTU(T),hitE(Q));
        end
end

TfC=Tf-273.15; %Temperature K -> °C

%% Calculation of Solidification/Melting radius

for W=1:cycfor
       for T=1:Cuts
        F(W,T)=Fzero(W)*(Tm-Tf(W,T))/(Tm-Ti);
        rm(W,T)=sqrt((F(W,T)+1)*Ro*Ro);
      end
end

rmMM=rm*100; % Solidification/Melting radius in [mm]
```

Appendix E

```
% Auxiliary function for NTU method to determine F0

function [F0] = NTU_Determination_F(tau,hit)

% INPUT     - Tau
%           - hit (estimate, where is F0 root expected)
% OUTPUT    - Inlet Frozen factor
% F0 - inlet sodification radius
% Tm - metling temperature of PCM
% Ti - inlet temperature of HTF

global kw Ri Ro Tm H cp km ro mf Ti Hwall R alfaPCM alfaW

syms x

%% Calculation of F0 root (F0 is inlet F at position X=0)

fxx = @(x) (0.25*((1+x)*log(1+x)-x) + x/alfaPCM + x/alfaPCM +
(x*log(R))/(2*alfaPCM*alfaW) -tau);
F0 = fzero(fxx,hit);
```

Appendix F

```
% Auxiliary function for NTU method to determine efficiency
and outflow temperature

function [Root_Emin, Tf] = Determination_e(F0,NTU,hitE)

% INPUT     - Inlet Frozen factor
%           - NTU (Number of transfer units)
% OUTPUT    - Effeciency root
%           - Temperature [K]
% F0 - inlet sodification radius
% Tm - metling temperature of PCM
% Ti - inlet temperature of HTF

global kw Ri Ro Tm H cp km ro mf Ti Hwall R alfaPCM alfaW

k1=17/450;
syms x

%% Calculation of Effeciency root

fEmin = @(x)-NTU -log(1-x)+ (log(R)*log(1-x))/(2*alfaW)+
(1/(4*alfaPCM))*(
((log(1+F0)*(1+k1*(log(1+F0))^2))/(1+0.01*(log(1+F0))^2)+0.25*
(log(1+F0))^2) - ((log(1+(F0-x*F0))*(1+k1*(log(1+(F0-
x*F0)))^2))/(1+0.01*(log(1+(F0-x*F0)))^2)+0.25*(log(1+(F0-
x*F0)))^2));
Root_Emin = fzero(fEmin,hitE);

%% Calcuulation of temperature

Tf=Root_Emin*(Tm-Ti)+Ti;
```

Apendix G

Numerical results of discharging mode:

		Length [m]	0,000	0,222	0,444	0,667	0,889	1,111	1,333	1,556	1,778	2,000
Time [hour]	Tau	F0 | NTU	0,000	0,296	0,592	0,888	1,183	1,479	1,775	2,071	2,367	2,663
0	0,000	0,000	190,000	197,901	203,721	208,008	211,166	213,493	215,207	216,469	217,399	218,084
1	1,072	0,017	190,000	197,344	202,988	207,284	210,529	212,965	214,786	216,141	217,148	217,894
2	2,145	0,035	190,000	196,856	202,311	206,587	209,896	212,428	214,349	215,796	216,880	217,689
3	3,217	0,052	190,000	196,427	201,689	205,921	209,271	211,884	213,898	215,434	216,596	217,470
4	4,289	0,070	190,000	196,047	201,117	205,288	208,659	211,338	213,436	215,057	216,297	217,237
5	5,362	0,087	190,000	195,710	200,593	204,690	208,065	210,794	212,966	214,667	215,983	216,990
6	6,434	0,104	190,000	195,410	200,112	204,126	207,490	210,256	212,491	214,266	215,655	216,729
7	7,506	0,122	190,000	195,140	199,670	203,596	206,937	209,727	212,014	213,856	215,315	216,454
8	8,578	0,139	190,000	194,897	199,264	203,098	206,406	209,209	211,538	213,440	214,964	216,168
9	9,651	0,156	190,000	194,677	198,891	202,632	205,900	208,704	211,066	213,019	214,605	215,870
10	10,723	0,174	190,000	194,478	198,547	202,195	205,417	208,214	210,600	212,597	214,238	215,562
11	11,795	0,191	190,000	194,296	198,229	201,785	204,957	207,740	210,142	212,175	213,865	215,245
12	12,868	0,209	190,000	194,129	197,934	201,402	204,520	207,284	209,693	211,755	213,489	214,920

Apendix H

Numerical results of charging mode:

		Length [m]	0,000	0,222	0,444	0,667	0,889	1,111	1,333	1,556	1,778	2,000
Time [hour]	Tau	F0 | NTU	0,000	0,296	0,592	0,888	1,183	1,479	1,775	2,071	2,367	2,663
0	0,000	0,000	250,000	242,099	236,279	231,992	228,834	226,507	224,793	223,531	222,601	221,916
1	0,804	0,013	250,000	242,656	237,012	232,716	229,471	227,035	225,214	223,859	222,852	222,106
2	1,608	0,026	250,000	243,144	237,689	233,413	230,104	227,572	225,651	224,204	223,120	222,311
3	2,413	0,039	250,000	243,573	238,311	234,079	230,729	228,116	226,102	224,566	223,404	222,530
4	3,217	0,052	250,000	243,953	238,883	234,712	231,341	228,662	226,564	224,943	223,703	222,763
5	4,021	0,065	250,000	244,290	239,407	235,310	231,935	229,206	227,034	225,333	224,017	223,010
6	4,825	0,078	250,000	244,590	239,888	235,874	232,510	229,744	227,509	225,734	224,345	223,271
7	5,630	0,091	250,000	244,860	240,330	236,404	233,063	230,273	227,986	226,144	224,685	223,546
8	6,434	0,104	250,000	245,103	240,736	236,902	233,594	230,791	228,462	226,560	225,036	223,832
9	7,238	0,117	250,000	245,323	241,109	237,368	234,100	231,296	228,934	226,981	225,395	224,130
10	8,042	0,130	250,000	245,522	241,453	237,805	234,583	231,786	229,400	227,403	225,762	224,438
11	8,846	0,143	250,000	245,704	241,771	238,215	235,043	232,260	229,858	227,825	226,135	224,755
12	9,651	0,156	250,000	245,871	242,066	238,598	235,480	232,716	230,307	228,245	226,511	225,080

Appendix I

```
%% Program which calculates Numerical method

clc
clear all
close all

%% PCM Storage
global L Ri Ro N_x N_r N_t rho_f mio_f Cp_f m_f k_f Np rho_s
rho_l...
    Cp_s Cp_l dH T_m dT_m k_s k_l dx dr dt U T R_PCM
f_PCM_t...
    Cp_PCM k_PCM rho_PCM Theta_PCM_t Theta_HTF_t  A B
time_h...
    step Tf_ini Tp_ini Re Pr dTheta


%% Geometry parameters
L  = 2;        %Length of cylinder tube (m)
Ri = 0.020;    %Inside radius of the tube (m)
Ro  = 0.022;   %Outside radius of the tube(m)
R_PCM=0.03;    %Radius of the PCM (m)

%% Grid parameters
N_x = 20;                %Number of points in x direction
N_r = 20;                %Number of points in r direction
time_h = 1;              %Time in seconds *3600
N_t = 1000;              %Number of time steps

%% Physical properties of HTF
Tf_ini = 190+273.15;  %Inlet temperature of HTF (K)
rho_f = 985;          %density (kg/m3)
mio_f = 4.92*10^-4;   %Dynamic viscosity of water (kg/m s)
Cp_f = 4178;          %Specific heat capacity (J/kg.K)
m_f = 0.12;           %Mass flow rate of HTF (kg/s)
k_f = 0.652;          %Thermal conductivity (W/m.K)
Np=1;                 %Number of pipes

%% Physical properties of PCM (KNO3 - NaNO3)
Tp_ini = 240+273.15;  %Initial temperature of PCM (K)
rho_s = 1867;        %Density of solid PCM (kg/m3)
rho_l = 2100;        %Density of liquid PCM (kg/m3)
Cp_s = 1350;         %Specific heat capacity of solid
PCM(J/kg.K)
Cp_l = 1450;         %Specific heat capacity of liquid PCM
(J/kg.K)
k_s = 0.8;           %Thermal conductivity of solid PCM (W/m.K)
k_l = 1.5;           %Thermal conductivity of liquid PCM
(W/m.K)
```

```
T_m = 223 + 273.15; %Melting point of the PCM (K)
dT_m = 15;          %Diference of melting point (K)
dH = 105000;        %Latent heat

%% Reynolds number and Prandtl number calculations
Re = 2*m_f/(pi*Np*Ri*mio_f); %Reynolds number
Pr = Cp_f*mio_f/k_f;         %Prandtl number

if Re<2200
    Nu = 3.66;
else
    if Re>5*10^6
        Nu = 0.023*Re^0.8*Pr^0.4;
    else
        if (Re >=2100)&& (Re<=5*10^6);
            f = ((0.79*log(Re))-1.64)^-2;
            Nu = ((f/8)*(Re-
1000)*Pr)/(1+(12.7*((f/8)^0.5)*((Pr^(2/3))-1)));
        end
    end
end

U =Nu*k_f/(2*Ri); %Convective heat transfer coefficient
(W/m2.K)

%% Constants
dx = L/(N_x-1);
dr = (R_PCM-Ri)/(N_r-1);
dt = ((( rho_s*Cp_s ) / ( 2*k_s ))*( ( dr^2 * dx^2) / ( dr^2 +
2*dx^2 ) ))/1;
dTheta=dx;
T_m1=T_m-dT_m/2;
T_m2=T_m+dT_m/2;
A= (m_f)/(rho_f*pi*Ri^2);
B= (2*U)/(rho_f*Cp_f*Ri);

%% Initial conditions
% Initial conditions for PCM
Theta_PCM_t = zeros(N_x,N_r,N_t);
for q=1:N_x
    for w=1:N_r
           Theta_PCM_t(q,w,1) =Tp_ini-T_m;
    end
end

% Initial conditions for HTF
Theta_HTF_t = zeros(N_x , N_t);
for q=1:N_x
       Theta_HTF_t(q,1) =Tf_ini-T_m;
end
```

```
% Filling PCM properties to matrix
% Initial state for Cp (_s =solid) - Specific heat

Cp_PCM= ones(N_x,N_r);
for q=1:N_x
    for w=1:N_r
        Cp_PCM(q,w)=Cp_s;
    end
end

% Initial state for rho_pcm (_s=solid) - Density
rho_PCM = ones(N_x,N_r);
for q=1:N_x
    for w=1:N_r
        rho_PCM(q,w)=rho_s;
    end
end

% Initial state for k (_s=solid) - Thermal conductivity
k_PCM= ones(N_x,N_r);
for q=1:N_x
    for w=1:N_r
        k_PCM(q,w)=k_s;
    end
end

% Initial state for f (f=0 for solid) - Liquid fraction
f_PCM_t = ones(N_x,N_r,N_t);
for q=1:N_x
    for w=1:N_r
        f_PCM_t(q,w,1)=0;
    end
end

%% Boundary conditions
 Theta_PCM_t(1:N_x,1,1)=(k_s/U)*((Theta_PCM_t(1:N_x,1,1) -
Theta_PCM_t(1:N_x,1,1))/(dr))+Theta_HTF_t(1:N_x,1,1); %downer

                    Theta_PCM_t(N_x,1:N_r,1)=0;     %Right
                    Theta_PCM_t(1,1:N_r,1)=0;       %Left
                    Theta_PCM_t(1:N_x,N_r,1)=0;     %Upper

%% Calculations
step=1;

for n=2:step:N_t

    if rem(n,100)==0;
        display([num2str(n) 'th time step of '
num2str(N_t/step)]);
```

```
    end

 % Re-calculation material's matrixes in each time step
    for e=1:N_x
        for r=1:N_r
            T=Theta_PCM_t(e,r,n)+T_m;

[Cp_PCM(e,r),k_PCM(e,r),rho_PCM(e,r),f_PCM_t(e,r,n)] =
Material_properties3(T);
        end
    end

 %% Calculation temperature PCM matrix

    for q=2:N_x-1

        for w=2:N_r-1

        % Calculation PCM
         Theta_PCM_t(q,w,n)=((k_PCM(q,w)*dt ) /
(rho_PCM(q,w)*(Cp_PCM(q,w) - dH * (f_PCM_t(q+1,w,n-1)-
f_PCM_t(q-1,w,n-1))/(2*dTheta)  )))*...
             (( Theta_PCM_t(q,w-1,n-1) -2 * Theta_PCM_t(q,w,n-
1) + Theta_PCM_t(q,w+1,n-1) ) / ( dr^2 ) +...
             (  Theta_PCM_t(q,w+1,n-1) - Theta_PCM_t(q,w-1,n-
1)) / (Ro*2*dr)+...
             (  Theta_PCM_t(q-1,w,n-1) -2 * Theta_PCM_t(q,w,n-
1) + Theta_PCM_t(q+1,w,n-1) ) / ( dx^2 ) +...
             (  Theta_PCM_t(q+1,w,n-1) - Theta_PCM_t(q-1,w,n-
1)) / (2*dx) )+...
             Theta_PCM_t(q,w,n-1);
        end

        Theta_PCM_t(q,1,n)=
(k_PCM(q,w)/U)*((Theta_PCM_t(q+1,w,n-1) - Theta_PCM_t(q-1,w,n-
1))/(2*dr))+Theta_HTF_t(q,n-1);

        %% Calculation for HTF
        Theta_HTF_t(1,n)=Tf_ini-T_m;
        Theta_HTF_t(q,n)=( (Theta_HTF_t(q-1,n))/(dt)-
(A*Theta_HTF_t(q-1,n))/(dx)+B*Theta_PCM_t(q,1,n) ) / ( B+
(1)/(dt)+(A)/(dx));

        if w==N_x-1
            Theta_HTF_t(N_x,n)=( (Theta_HTF_t(q-1,n))/(dt)-
(A*Theta_HTF_t(q-1,n))/(dx)+B*Theta_PCM_t(q,1,n) ) / ( B+
(1)/(dt)+(A)/(dx));
        end
    end
end
```

Appendix J

```
%% Auxiliary function for Numerical method to determine
material properties

function [Cp_p,k_p,rho_p,f_PCM] = Material_properties3(T)

% INPUT     - Temperature (K)
% OUTPUT    - Thermal capacity
%           - Thermal conductivity
%           - Density
global rho_s rho_l Cp_s Cp_l dH T_m dT_m k_s k_l D_T B_T
f_s=0;
f_l=1;

 %% D(T)
if T > (T_m + dT_m/2)
   D_T=0;
elseif T < (T_m - dT_m/2)
   D_T=0;
else
    D_T= (exp((-T*(T-T_m)^2)/(dT_m^2)))/((sqrt(pi*dT_m^2)));
end

%%  B(T)
if T < (T_m - dT_m)
    B_T=0;
elseif T > (T_m + dT_m)
    B_T=1;
else
    B_T= (T-T_m+dT_m)/(2*dT_m);
end

%% Calculation Cp_p,k_p,rho_p
if T > (T_m + dT_m/2)
    Cp_p=Cp_l;
    k_p=k_l;
    rho_p=rho_l;
    f_PCM=f_l;

elseif T < (T_m - dT_m/2)
    Cp_p=Cp_s;
    k_p=k_s;
    rho_p=rho_s;
    f_PCM=f_s;
else T < (T_m + dT_m/2) && T > (T_m - dT_m/2);
     Cp_p=Cp_s+(Cp_l-Cp_s)*B_T + dH*D_T;
     k_p=k_s+(k_l-k_s)*B_T;
     rho_p=rho_s+(rho_l-rho_s)*B_T;
     f_PCM=f_s+(f_l-f_s)*B_T;
end
```

Appendix K

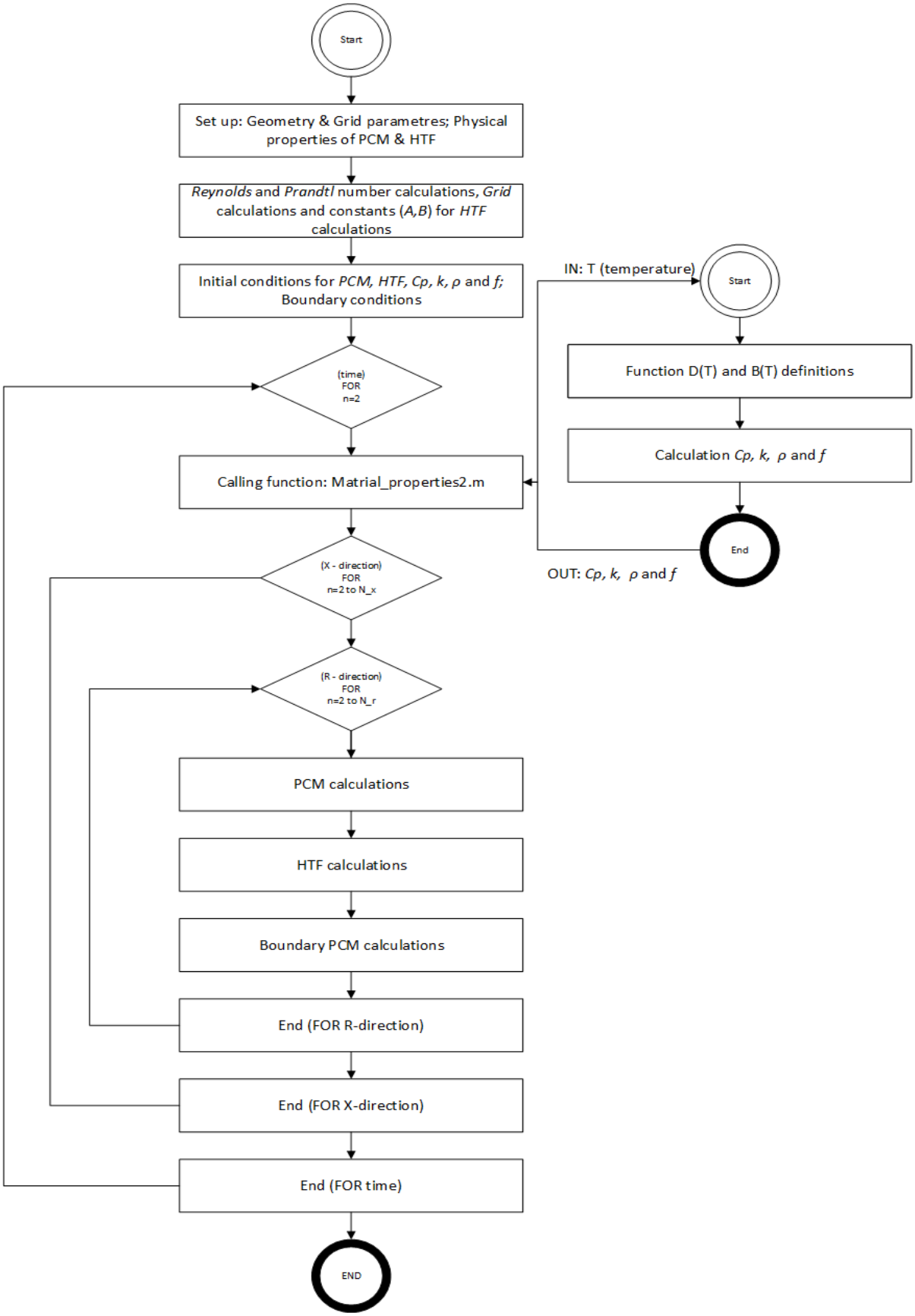
Start
Set up: Geometry & Grid parametres; Physical properties of PCM & HTF
Reynolds and Prandtl number calculations, Grid calculations and constants (A,B) for HTF calculations
Initial conditions for PCM, HTF, Cp, k, ρ and f; Boundary conditions
(time) FOR n=2
Calling function: Matrial_properties2.m
(X - direction) FOR n=2 to N_x
(R - direction) FOR n=2 to N_r
PCM calculations
HTF calculations
Boundary PCM calculations
End (FOR R-direction)
End (FOR X-direction)
End (FOR time)
END
IN: T (temperature)
Start
Function D(T) and B(T) definitions
Calculation Cp, k, ρ and f
End
OUT: Cp, k, ρ and f